

MICROFILMED 1991

U·M·I

8

9

5

0

1

1

6

INFORMATION TO USERS

The most advanced technology has been used to photograph and reproduce this manuscript from the microfilm master. UMI films the text directly from the original or copy submitted. Thus, some thesis and dissertation copies are in typewriter face, while others may be from any type of computer printer.

The quality of this reproduction is dependent upon the quality of the copy submitted. Broken or indistinct print, colored or poor quality illustrations and photographs, print bleedthrough, substandard margins, and improper alignment can adversely affect reproduction.

In the unlikely event that the author did not send UMI a complete manuscript and there are missing pages, these will be noted. Also, if unauthorized copyright material had to be removed, a note will indicate the deletion.

Oversize materials (e.g., maps, drawings, charts) are reproduced by sectioning the original, beginning at the upper left-hand corner and continuing from left to right in equal sections with small overlaps. Each original is also photographed in one exposure and is included in reduced form at the back of the book.

Photographs included in the original manuscript have been reproduced xerographically in this copy. Higher quality 6" x 9" black and white photographic prints are available for any photographs or illustrations appearing in this copy for an additional charge. Contact UMI directly to order.

U·M·I

University Microfilms International
A Bell & Howell Information Company
300 North Zeeb Road, Ann Arbor, MI 48106-1346 USA
313/761-4700 800/521-0600

Order Number 9110566

Reactions of the excited state of polypyridyl chromium(III) ions

Steffan, Carl R., Ph.D.

Iowa State University, 1990

U·M·I

**300 N. Zeeb Rd.
Ann Arbor, MI 48106**

**Reactions of the excited state of polypyridyl
chromium(III) ions**

by

Carl R. Steffan

**A Dissertation Submitted to the
Graduate Faculty in Partial Fulfillment of
The Requirements for the Degree of
DOCTOR OF PHILOSOPHY**

**Department: Chemistry
Major: Inorganic Chemistry**

Approved:

Signature was redacted for privacy.

In Charge of Major Work

Signature was redacted for privacy.

For the Major Department

Signature was redacted for privacy.

For the Graduate College

**Iowa State University
Ames, Iowa**

1990

TABLE OF CONTENTS

GENERAL INTRODUCTION	Page 1
PART I KINETICS AND MECHANISM OF THE QUENCHING OF $^*\text{CrL}_3^{3+}$ BY OXALATE	2
INTRODUCTION	3
EXPERIMENTAL	5
Reagents	5
Photochemical experiments	6
Kinetics	6
Spectra of the secondary transient and final product	7
Quantum yields	8
RESULTS	11
Kinetics of quenching by oxalate ions	11
Quantum yields	14
Spectra and kinetics of the secondary transient	17
DISCUSSION	19
Mechanism of the quenching of $^*\text{Cr}(\text{bpy})_3^{3+}$ by oxalate	19
Quenching of $^*\text{Cr}(\text{bpy})_3^{3+}$ at high initial ground state concentrations	24
Oxalate quenching of other $^*\text{CrL}_3^{3+}$	27
The intermediate	29
REFERENCES	51
APPENDIX	54

PART II KINETICS AND MECHANISM OF THE REACTIONS OF ORGANOCHROMIUM COMPLEXES WITH TRIS (2, 2'-BIPYRIDYL)RUTHENIUM(III) AND WITH THE EXCITED STATE OF TRIS(POLY- PYRIDYL)CHROMIUM(III) IONS	73
INTRODUCTION	74
EXPERIMENTAL	82
Materials	82
Preparation and characterization of previously unknown organochromium compounds	83
Stoichiometry of the reaction of $\text{Ru}(\text{bpy})_3^{3+}$ and organochromium	84
Kinetics	85
Spectrum of product and quantum yields	86
RESULTS	88
Kinetics of quenching of $^*\text{CrL}_3^{3+}$ by organochromiums	88
Products of quenching reactions	92
Stoichiometry of the reaction of $\text{Ru}(\text{bpy})_3^{3+}$ and $\text{L}'\text{CrR}^{2+}$	93
Kinetics of the reaction between $\text{Ru}(\text{bpy})_3^{3+}$ and $\text{L}'\text{CrR}^{2+}$	94
DISCUSSION	96
Kinetics of the quenching of $^*\text{CrL}_3^{3+}$ by $\text{L}'\text{CrR}^{2+}$	96
Quenching of $^*\text{CrL}_3^{3+}$ by the inorganic complex $\text{L}'\text{CrBr}^{2+}$	99

Quantum yields and the spectrum of the initial product	99
Reaction of $\text{Ru}(\text{bpy})_3^{3+}$ with $\text{L}'\text{CrR}^{2+}$	102
Effect of different quenchers	103
The reactivity trend	106
Lifetime of the oxidized organochromium intermediate, $\text{L}'\text{CrR}^{3+}$	109
REFERENCES	134
APPENDIX	142
GENERAL SUMMARY	175
ACKNOWLEDGEMENT	176

LIST OF FIGURES

	Page
Figure I-1. The plot of the observed rate constant versus the oxalate concentration for the quenching of $^*\text{Cr}(\text{bpy})_3^{3+}$ at non-constant ionic strength. Experiments done at high initial ground state concentration and at $(23 \pm 2)^\circ\text{C}$	39
Figure I-2. The plot of the observed rate constant versus the oxalate concentration for the quenching of $^*\text{Cr}(\text{bpy})_3^{3+}$ at ionic strengths of 1.0M(●) and 2.0M(+). Experiments were done at high initial ground state concentration and 23°C	40
Figure I-3. The plot of the observed rate constant for the quenching of $^*\text{Cr}(\text{bpy})_3^{3+}$ versus the ground state concentration at a constant oxalate concentration of 0.0522M and at $(23 \pm 2)^\circ\text{C}$	41
Figure I-4. The plot of the observed rate constant versus the oxalate concentration for the quenching of $^*\text{Cr}(\text{bpy})_3^{3+}$ at non-constant	

ionic strength. Experiments were done at low initial ground state concentration where the dots correspond to the data points while the line is that calculated using the data as well as the calculated ion-pairing constants and at $(23 \pm 2)^{\circ}\text{C}$

42

Figure I-5. The plot of the observed rate constant versus the oxalate concentration for the quenching of $^*\text{Cr}(\text{bpy})_3^{3+}$ at ionic strengths of 0.75M (●) and 2.00M (▲). Experiments were done at low initial ground state concentration and at $(23 \pm 2)^{\circ}\text{C}$

43

Figure I-6. The plot of the observed rate constant versus the oxalate concentration for the quenching of $^*\text{Cr}(\text{Clphen})_3^{3+}$ (x), $^*\text{Cr}(\text{bpy})_3^{3+}$ (●), $^*\text{Cr}(\text{phen})_3^{3+}$ (+), $^*\text{Cr}(\text{Mephen})_3^{3+}$ (*) and $^*\text{Cr}(\text{Me}_2\text{bpy})_3^{3+}$ (o) at an ionic strength of 0.75 M and $(23 \pm 2)^{\circ}\text{C}$

44

Figure I-7. Spectrum of the intermediate (+) and final product (●) formed after the quenching of $^*\text{Cr}(\text{Clphen})_3^{3+}$ by oxalate. The inter-

mediate absorbances were determined
8 μ sec after the flash and at $(23 \pm 2)^{\circ}\text{C}$ 45

Figure I-8. Spectrum of the intermediate(+) and final product(●) formed after the quenching of $^{*}\text{Cr}(\text{Clphen})_3^{3+}$ by EDTA^{2-} . The intermediate absorbances were determined 8 μ sec after the flash and at $(23 \pm 2)^{\circ}\text{C}$ 46

Figure I-9. The plot of the observed rate constant for the loss of the secondary transient produced after the quenching of $^{*}\text{Cr}(\text{Clphen})_3^{3+}$ by oxalate(▲) and EDTA^{2-} (●) versus the ground state concentration at $(23 \pm 2)^{\circ}\text{C}$ 47

Figure I-10. The plot of the observed rate constant for the loss of the secondary transient produced after the quenching of $^{*}\text{Cr}(\text{bpy})_3^{3+}$ by EDTA^{2-} versus the ground state concentration at 23°C 48

Figure I-11. The plot of the observed rate constant for the loss of the secondary transient produced after the quenching of $^{*}\text{Cr}(\text{phen})_3^{3+}$ by EDTA^{2-} (▲) and oxalate(●) versus the

ground state concentration at 23°C 49

Figure I-12. The plot of the logarithm of k_B versus the excited state potentials($E^{\circ}_{*3+/2+}$) 50

Figure II-1. Quenching of $^{*}\text{Cr}(\text{bpy})_3^{3+}$ by the organochromiums $\text{L}'\text{Cr}(\text{1-Pr})^{2+}$ (+), $\text{L}'\text{Cr}(\text{CH}_2\text{C}_6\text{H}_4\text{Br})^{2+}$ (o), $\text{L}'\text{Cr}(\text{CH}_2\text{C}_6\text{H}_5)^{2+}$ (●), and $\text{L}'\text{Cr}(\text{2-Bu})^{2+}$ (*) at $(23 \pm 2)^{\circ}\text{C}$ 122

Figure II-2. Quenching of $^{*}\text{CrL}_3^{3+}$ by $\text{L}'\text{CrEt}^{2+}$, where L is Clphen (●), bpy (o), Mephen (+) and Me_2bpy (*) at $(23 \pm 2)^{\circ}\text{C}$ 123

Figure II-3. Quenching of $^{*}\text{CrL}_3^{3+}$ by $\text{L}'\text{Cr}(\text{2-Pr})^{2+}$, where L is Clphen (●), bpy (+), Mephen (o) and Me_2phen (*) at $(23 \pm 2)^{\circ}\text{C}$ 124

Figure II-4. Final product spectrum for the quenching of $^{*}\text{Cr}(\text{bpy})_3^{3+}$ by $\text{L}'\text{Cr}(\text{2-Bu})^{2+}$ 125

Figure II-5. Plot of the absorbance at 450 nm versus the ratio of reactants for the titration of $\text{Ru}(\text{bpy})_3^{3+}$ by $[\text{15}] \text{aneN}_4\text{Cr}(\text{CH}_2\text{C}_6\text{H}_4\text{Br})^{2+}$ 126

- Figure II-6. Plot of the absorbance at 450 nm versus the ratio of reactants for the titration of [15]aneN₄Cr(CH₂C₆H₄Br)²⁺ by Ru(bpy)₃³⁺ 127
- Figure II-7. Plot of k_{obs} versus the organochromium concentration for the reaction of Ru(bpy)₃³⁺ with the organochromiums, L'Cr(Et)²⁺ (●), L'Cr(2-Bu)²⁺ (*), L'Cr(c-Hex)²⁺ (+) at (23 ± 2)°C 128
- Figure II-8. Plot of log(k_q) versus E°*_{3+/2+} for the reaction of *CrL₃³⁺ with L'Cr(Ethyl)²⁺ (+) and with L'Cr(2-Propyl)²⁺ (●) 129
- Figure II-9. Plot of log(k_q) for the reaction of *Cr(bpy)₃³⁺ with L'CrR²⁺ versus log(k_q) for the reaction of *CrL₃³⁺ with (H₂O)₅CrR²⁺ 130
- Figure II-10. Plot of log(k_q) for the reaction of *Cr(bpy)₃³⁺ with L'CrR²⁺ versus log(k) for the reaction of Ru(bpy)₃³⁺ with (H₂O)₅CrR²⁺ 131

Figure II-11. Plot of the logarithm of the rate constants for the reaction of $\text{Ru}(\text{bpy})_3^{3+}$ (●) and $^*\text{Cr}(\text{bpy})_3^{3+}$ (⊙) with the organochromiums versus the ionization potential of the radicals (I_p) 132

Figure II-12. Plot of the logarithm of the rate constants for the reaction of $\text{Ru}(\text{bpy})_3^{3+}$ with the organochromiums versus the Hammett σ values 133

LIST OF TABLES

	Page
Table I-1. Extinction Coefficients for $^*\text{Cr}(\text{Clphen})_3^{3+}$ Determined Using Different Quenchers	32
Table I-2. Summary of Rate Constants for the Quenching of $^*\text{CrL}_3^{3+}$ by Oxalate Ions	33
Table I-3. Experimental and Simulated Quantum Yields for the Formation of $\text{Cr}(\text{bpy})_3^{2+}$ as a Function of the Ground State Concentration	34
Table I-4. Quantum Yields for the Formation of $\text{Cr}(\text{Clphen})_3^{2+}$ as a Function of the Ground State Concentration	35
Table I-5. Quantum Yields for the Formation of $\text{Cr}(\text{Me}_2\text{bpy})_3^{2+}$ as a Function of the Ground State Concentration	36
Table I-6. Rate Constants for the Loss of the Secondary Transient Produced in Oxalate and EDTA^{2-} Quenching Reactions of $^*\text{CrL}_3^{3+}$	37

Table I-7.	Rate Constants for the Decay of the Secondary Transient Produced in the Quenching of the Excited State of $\text{Cr}(\text{Clphen})_3^{3+}$ by Oxalate as a Function of the Monitoring Wavelength	38
Table A-1.	Rate Constants for the Quenching of the Excited State of $\text{Cr}(\text{bpy})_3^{3+}$ by Oxalate	54
Table A-2.	Rate Constants for the Quenching of the Excited State of $\text{Cr}(\text{bpy})_3^{3+}$ by Oxalate	55
Table A-3.	Rate Constants for the Quenching of the Excited State of $\text{Cr}(\text{bpy})_3^{3+}$ by Oxalate	56
Table A-4.	Rate Constants for the Quenching of the Excited State of $\text{Cr}(\text{bpy})_3^{3+}$ by Oxalate	57
Table A-5.	Rate Constants and Calculated Ion-Pairing Constants for the Quenching of the Excited State of $\text{Cr}(\text{bpy})_3^{3+}$ by Oxalate	58
Table A-6.	Rate Constants for the Quenching of the Excited State of $\text{Cr}(\text{bpy})_3^{3+}$ by Oxalate	59

Table A-7.	Rate Constants for the Quenching of the Excited State of $\text{Cr}(\text{bpy})_3^{3+}$ by Oxalate	60
Table A-8.	Rate Constants for the Quenching of the Excited State of $\text{Cr}(\text{phen})_3^{3+}$ by Oxalate	61
Table A-9.	Rate Constants for the Quenching of the Excited State of $\text{Cr}(\text{Mephen})_3^{3+}$ by Oxalate	62
Table A-10.	Rate Constants for the Quenching of the Excited State of $\text{Cr}(\text{Me}_2\text{bpy})_3^{3+}$ by Oxalate	63
Table A-11.	Rate Constants for the Quenching of the Excited State of $\text{Cr}(\text{Clphen})_3^{3+}$ by Oxalate	64
Table A-12.	Quantum Yields for the Formation of $\text{Cr}(\text{bpy})_3^{2+}$ by Quenching of the Excited State of $\text{Cr}(\text{bpy})_3^{3+}$ by Oxalate	65
Table A-13.	Quantum Yields for Oxalate Quenching of $^*\text{Cr}(\text{Clphen})_3^{3+}$	66

Table A-14.	Quantum Yields for Oxalate Quenching of $^*\text{Cr}(\text{Me}_2\text{bpy})_3^{3+}$	67
Table A-15.	Rate Constants for the Loss of the Secondary Transient Produced by the Quenching of the Excited State of $\text{Cr}(\text{Clphen})_3^{3+}$ by Oxalate	68
Table A-16.	Rate Constants for the Loss of the Secondary Transient Produced by the Quenching of the Excited State of $\text{Cr}(\text{Clphen})_3^{3+}$ by EDTA^{2-}	69
Table A-17.	Rate Constants for the Loss of the Secondary Transient Produced by the Quenching of the Excited State of $\text{Cr}(\text{phen})_3^{3+}$ by Oxalate	70
Table A-18.	Rate Constants for the Loss of the Secondary Transient Produced by the Quenching of the Excited State of $\text{Cr}(\text{phen})_3^{3+}$ by EDTA^{2-}	71

Table A-19.	Rate Constants for the Loss of the Secondary Transient Produced by the Quenching of the Excited State of $\text{Cr}(\text{bpy})_3^{3+}$ by EDTA^{2-}	72
Table II-1.	Spectral Parameters for the Various $[\text{15}] \text{aneN}_4\text{Cr}(\text{CH}_2\text{C}_6\text{H}_4\text{X})^{2+}$ Complexes	114
Table II-2.	Observed Rate Constants for the Reaction of $^*\text{Cr}(\text{bpy})_3^{3+}$ and $\text{L}'\text{Cr}(\text{2-Pr})^{2+}$	115
Table II-3.	Rate Constants for the Quenching of $^*\text{CrL}_3^{3+}$ by $\text{L}'\text{CrR}^{2+}$	116
Table II-4.	Observed Rate Constants for the Quenching of $^*\text{Cr}(\text{bpy})_3^{3+}$ by $\text{L}'\text{CrBr}^{2+}$	117
Table II-5.	Observed Rate Constants for the Quenching of $^*\text{Cr}(\text{Clphen})_3^{3+}$ by $\text{L}'\text{CrBr}^{2+}$	118
Table II-6.	Quantum Yields of Formation of $\text{Cr}(\text{bpy})_3^{2+}$	119

Table II-7.	Second Order Rate Constants for the Reaction of $\text{Ru}(\text{bpy})_3^{3+}$ with $\text{L}'\text{CrR}^{2+}$	120
Table II-8.	Rate Constants for the Organochromium Independent Loss of Excited State (k_0)	121
Table A-1.	Rate Constants for the Quenching of the Excited State of $\text{Cr}(\text{bpy})_3^{3+}$ by the $\text{L}'\text{CrCH}_3^{2+}$ Ion	142
Table A-2.	Rate Constants for the Quenching of the Excited State of $\text{Cr}(\text{bpy})_3^{3+}$ by the $\text{L}'\text{Cr}(\text{CH}_2\text{CH}_3)^{2+}$ Ion	143
Table A-3.	Rate Constants for the Quenching of the Excited State of $\text{Cr}(\text{bpy})_3^{3+}$ by the $\text{L}'\text{Cr}(1\text{-Propyl})^{2+}$ Ion	144
Table A-4.	Rate Constants for the Quenching of the Excited State of $\text{Cr}(\text{bpy})_3^{3+}$ by the $\text{L}'\text{Cr}(1\text{-Butyl})^{2+}$ Ion	145
Table A-5.	Rate Constants for the Quenching of the Excited State of $\text{Cr}(\text{bpy})_3^{3+}$ by the $\text{L}'\text{Cr}(2\text{-Propyl})^{2+}$ Ion	146

Table A-6.	Rate Constants for the Quenching of the Excited State of $\text{Cr}(\text{bpy})_3^{3+}$ by the $\text{L}'\text{Cr}(\text{2-Butyl})^{2+}$ Ion	147
Table A-7.	Rate Constants for the Quenching of the Excited State of $\text{Cr}(\text{bpy})_3^{3+}$ by the $\text{L}'\text{Cr}(\text{C}_6\text{H}_{11})^{2+}$ Ion	148
Table A-8.	Rate Constants for the Quenching of the Excited State of $\text{Cr}(\text{bpy})_3^{3+}$ by the $\text{L}'\text{Cr}(\text{CH}_2\text{C}_6\text{H}_5)^{2+}$ Ion	149
Table A-9.	Rate Constants for the Quenching of the Excited State of $\text{Cr}(\text{bpy})_3^{3+}$ by the $\text{L}'\text{Cr}(\text{CH}_2\text{C}_6\text{H}_4\text{CH}_3)^{2+}$ Ion	150
Table A-10.	Rate Constants for the Quenching of the Excited State of $\text{Cr}(\text{bpy})_3^{3+}$ by the $\text{L}'\text{Cr}(\text{CH}_2\text{C}_6\text{H}_4\text{Br})^{2+}$ Ion	151
Table A-11.	Rate Constants for the Quenching of the Excited State of $\text{Cr}(\text{5-Clphen})_3^{3+}$ by the $\text{L}'\text{Cr}(\text{2-Propyl})^{2+}$ Ion	152

Table A-12.	Rate Constants for the Quenching of the Excited State of $\text{Cr}(4,7\text{-diMephen})_3^{3+}$ by the $\text{L}'\text{Cr}(2\text{-Propyl})^{2+}$ Ion	153
Table A-13.	Rate Constants for the Quenching of the Excited State of $\text{Cr}(5\text{-Mephen})_3^{3+}$ by the $\text{L}'\text{Cr}(2\text{-Propyl})^{2+}$ Ion	154
Table A-14.	Rate Constants for the Quenching of the Excited State of $\text{Cr}(4,4'\text{-diMebpy})_3^{3+}$ by the $\text{L}'\text{Cr}(\text{CH}_2\text{CH}_3)^{2+}$ Ion	155
Table A-15.	Rate Constants for the Quenching of the Excited State of $\text{Cr}(5\text{-Mephen})_3^{3+}$ by the $\text{L}'\text{Cr}(\text{CH}_2\text{CH}_3)^{2+}$ Ion	156
Table A-16.	Rate Constants for the Quenching of the Excited State of $\text{Cr}(5\text{-Clphen})_3^{3+}$ by the $\text{L}'\text{Cr}(\text{CH}_2\text{CH}_3)^{2+}$ Ion	157
Table A-17.	Rate Constants for the Reaction of $\text{Ru}(\text{bpy})_3^{3+}$ with $\text{L}'\text{Cr}(\text{CH}_3)^{2+}$	158

Table A-18.	Rate Constants for the Reaction of $\text{Ru}(\text{bpy})_3^{3+}$ with $\text{L}'\text{Cr}(\text{Ethyl})^{2+}$	159
Table A-19.	Rate Constants for the Reaction of $\text{Ru}(\text{bpy})_3^{3+}$ with $\text{L}'\text{Cr}(1\text{-Propyl})^{2+}$	160
Table A-20.	Rate Constants for the Reaction of $\text{Ru}(\text{bpy})_3^{3+}$ with $\text{L}'\text{Cr}(1\text{-Butyl})^{2+}$	160
Table A-21.	Rate Constants for the Reaction of $\text{Ru}(\text{bpy})_3^{3+}$ with $\text{L}'\text{Cr}(2\text{-Propyl})^{2+}$	161
Table A-22.	Rate Constants for the Reaction of $\text{Ru}(\text{bpy})_3^{3+}$ with $\text{L}'\text{Cr}(2\text{-Butyl})^{2+}$	162
Table A-23.	Rate Constants for the Reaction of $\text{Ru}(\text{bpy})_3^{3+}$ with $\text{L}'\text{Cr}(\text{c-Hex})^{2+}$	163
Table A-24.	Rate Constants for the Reaction of $\text{Ru}(\text{bpy})_3^{3+}$ with $\text{L}'\text{Cr}(\text{CH}_2\text{C}_6\text{H}_5)^{2+}$	164
Table A-25.	Rate Constants for the Reaction of $\text{Ru}(\text{bpy})_3^{3+}$ with $\text{L}'\text{Cr}(\text{CH}_2\text{C}_6\text{H}_4\text{Br})^{2+}$	165

Table A-26.	Rate Constants for the Reaction of $\text{Ru}(\text{bpy})_3^{3+}$ with $\text{L}'\text{Cr}(\text{CH}_2\text{C}_6\text{H}_4\text{CH}_3)^{2+}$	166
Table A-27.	Rate Constants for the Reaction of $\text{Ru}(\text{bpy})_3^{3+}$ with $\text{L}'\text{Cr}(\text{Ethyl})^{2+}$	167
Table A-28.	Rate Constants for the Reaction of $\text{Ru}(\text{bpy})_3^{3+}$ with $\text{L}'\text{Cr}(1\text{-Propyl})^{2+}$	168
Table A-29.	Rate Constants for the Reaction of $\text{Ru}(\text{bpy})_3^{3+}$ with $\text{L}'\text{Cr}(\text{Ethyl})^{2+}$	169
Table A-30.	Rate Constants for the Reaction of $\text{Ru}(\text{bpy})_3^{3+}$ with $\text{L}'\text{Cr}(\text{CH}_2\text{C}_6\text{H}_4\text{F})^{2+}$	170
Table A-31.	Rate Constants for the Reaction of $\text{Ru}(\text{bpy})_3^{3+}$ with $\text{L}'\text{Cr}(\text{CH}_2\text{C}_6\text{H}_4\text{Cl})^{2+}$	171
Table A-32.	Rate Constants for the Reaction of $\text{Ru}(\text{bpy})_3^{3+}$ with $\text{L}'\text{Cr}(\text{CH}_2\text{C}_6\text{H}_4\text{CF}_3)^{2+}$	172
Table A-33.	Rate Constants for the Reaction of $\text{Ru}(\text{bpy})_3^{3+}$ with $\text{L}'\text{Cr}(\text{CH}_2\text{C}_6\text{H}_4\text{OCH}_3)^{2+}$	173

Table A-34. Rate Constants for the Reaction of
 $\text{Ru}(\text{bpy})_3^{3+}$ with $\text{L}'\text{Cr}(\text{CH}_2\text{C}_6\text{H}_4\text{Br})_2^{2+}$

GENERAL INTRODUCTION

Recently the photochemistry of chromium polypyridyl complexes has been of much interest. The excited states of these species are both good energy transfer agents and good oxidizing agents.

In Part I the kinetics and mechanism of the quenching of the excited state of chromium polypyridyl complexes is discussed. Quantum yields for the formation of the reduced chromium polypyridyl complexes are used as well to assist in the determination of the mechanism of the reaction.

Part II concerns the reaction of the excited state of the chromium polypyridyl complexes with the organochromium complexes, $[15]aneN_4CrR^{2+}$ and attempts to answer the question of the type of quenching process occurring--energy or electron transfer. As a comparison, the rate constants for the electron transfer reaction of $Ru(bpy)_3^{3+}$ with the organochromiums are also presented.

**PART I KINETICS AND MECHANISM OF THE
QUENCHING OF $*CrL_3^{3+}$ BY OXALATE**

INTRODUCTION

There has been much recent interest in the photochemistry and photophysics of transition metal polypyridine complexes due to the possibility of their use in solar energy conversion systems. The excited state of these compounds are known to undergo useful electron transfer and energy transfer reactions.¹

The doublet excited state (2E) of CrL_3^{3+} complexes have been shown to possess relatively high reduction potentials.² This coupled with the fact that the excited states are somewhat long lived makes it possible to study the electron and energy transfer reactions of the excited state. The lifetime of $^*Cr(bpy)_3^{3+}$ was measured to be 0.11 msec³ while that of $^*Cr(phen)_3^{3+}$ was measured to be between 0.25 msec and 0.42 msec under various conditions.^{3,4,5}

Quenching of the excited state of CrL_3^{3+} complexes via an electron transfer pathway creates the possibility of conveniently studying the subsequent reactions of CrL_3^{2+} . Recently, it was found that oxalate ions and the disodium salt of ethylenediaminetetraacetic acid quench the excited state to produce CrL_3^{2+} .⁶ The quenching does not occur in acidic media implying that the doubly deprotonated species are the quenchers in the reaction.

This work attempts to elucidate the mechanism of the quenching of $^*CrL_3^{3+}$ (where L = 2,2'-bipyridine, 4,4'-dimethyl-2,2'-bipyridine, 1,10-phenanthroline, 5-chloro-

1,10-phenanthroline, 5-methyl-1,10-phenanthroline) by oxalate ions in neutral pH. Evidence suggests an ion-pairing pre-equilibrium followed by rate limiting electron transfer to produce CrL_3^{2+} and CO_2^- . The CO_2^- can then react with ground state chromium(III) species to produce another mole of the reduced product or it can produce a secondary transient as in the case of phenanthroline and substituted phenanthroline complexes. The secondary transient reacts to produce CrL_3^{2+} in a subsequent reaction.

EXPERIMENTAL

Reagents

$[\text{Cr}(2,2'\text{-bpy})_3][\text{ClO}_4]_3 \cdot 1/2\text{H}_2\text{O}$ was made by a modification of the literature procedure². $\text{Cr}(\text{ClO}_4)_3 \cdot x\text{H}_2\text{O}$ was dissolved in 0.1 M HClO_4 . This was reduced to Cr^{2+} electrolytically at -1.77 V versus a calomel electrode. The Cr^{2+} solution was transferred air-free to a suspension of 2,2'-bipyridine in 0.1 M HClO_4 instantly producing a purplish-black solution. A small amount of saturated aqueous Br_2 was added until the color changed to yellow. The product was precipitated by addition of saturated LiClO_4 . After collecting the precipitate, the solid was redissolved in water and extracted with chloroform to remove any free bipyridine. The final solid product was obtained by precipitation using saturated NaClO_4 . The purity of the compound was checked spectroscopically ($\epsilon^{400} = 980 \text{ M}^{-1}\text{cm}^{-1}$ ⁷; exp. $\epsilon^{400} = 930 \text{ M}^{-1}\text{cm}^{-1}$) and by measurement of the excited state lifetime.⁸

The chromium complexes of 1,10-phenanthroline, 5-chloro-1,10-phenanthroline, 5-methyl-1,10-phenanthroline and 4,4'-dimethyl-2,2'-bipyridine were gifts from C. Simmons and K. Zahir. These complexes will later be referred to as $\text{Cr}(\text{phen})_3^{3+}$, $\text{Cr}(\text{Clphen})_3^{3+}$, $\text{Cr}(\text{Mephen})_3^{3+}$ and $\text{Cr}(\text{Me}_2\text{bpy})_3^{3+}$, respectively.

A stock solution of Ti^{3+} was made in the standard manner.⁹ Titanium sponge was dissolved in 3.3 M HCl under anaerobic

conditions. The concentration of Ti^{3+} was determined spectroscopically ($\lambda_{\text{max}} = 502 \text{ nm}$; $\epsilon = 3.9 \text{ M}^{-1}\text{cm}^{-1}$).

The Fe^{2+} stock solution was made by dissolving ferrous ammonium sulfate in 1 M H_2SO_4 and treating with zinc amalgam to remove any trace Fe^{3+} which may have been present.

All other materials, such as Na_2SO_4 , Na_2EDTA and $\text{Na}_2\text{C}_2\text{O}_4$ were reagent grade obtained from Fischer and used as purchased without prior purification. In some cases sodium oxalate was recrystallized from water prior to use; however, this made no difference in the results.

Photochemical experiments

The laser system used for all flash photolysis experiments was that described previously.^{10,11} The excitation source was a Phase-R model DL-1100 pulsed dye laser. Two dyes were used in this work. Coumarin 460 ($1.5 \times 10^{-4} \text{ M}$ in methanol) emitting at 461 nm (range 448 nm to 489 nm) and LD423 ($2 \times 10^{-4} \text{ M}$ in methanol) emitting at 426 nm (range 415 nm to 447 nm) were used.

Kinetics

The kinetics of all the reactions were performed using a Phase-R DL-1100 dye laser system with a Nicolet oscilloscope interfaced to an Apple II-e computer.

The kinetics of the quenching of the excited state was followed by monitoring the decay in emission at 727 nm for the 2,2'-bipyridine complex or 728 nm for the other polypyridine

complexes. All quenching reactions were done under pseudo first order conditions in which the quencher concentration was in a large excess over the excited state concentration and the kinetics showed first order decays.

The kinetics of the decay of the secondary transient was followed by monitoring the decay in absorbance at 605 nm from the point at which quenching was almost complete (7 to 12 microseconds depending on the complex). In these experiments a high quencher concentration was employed in order to facilitate the quenching process. The rate of decay of the secondary intermediate produced in the quenching of the bipyridine complex by EDTA^{2-} was determined as well as for those produced by the quenching of the 5-chloro-1,10-phenanthroline and the 1,10-phenanthroline complex by oxalate and EDTA^{2-} .

Spectra of the secondary transient and final product

The spectra of the secondary transient and final product were determined for the case where the excited state of the 5-chloro-1,10-phenanthroline complex was quenched by oxalate and EDTA^{2-} . The absorbance of the secondary intermediate was taken to be that observed 8 μsec into the absorbance-time profile (the point at which the quenching was complete according to emission measurements) and the final product absorbance was that residual absorbance found after the reaction was completed.

Quantum yields

The quantum yield for the formation of the chromium(II) product was determined as a function of the ground state concentration for the 2,2'-bipyridine, 5-chloro-1,10-phenanthroline and 4,4'-dimethyl-2,2'-bipyridine complexes.

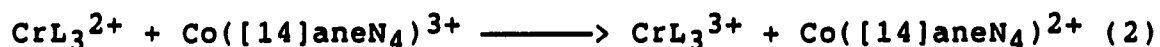
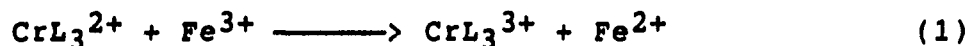
In the case of the 2,2'-bipyridine complex the amount of excited state formed in the flash was determined by monitoring the absorbance at 445 nm ($\epsilon = 3.0 \times 10^3 \text{ M}^{-1}\text{cm}^{-1}$ ¹²) in the absence of quencher (oxalate) since the chromium(II) product formed in the quench has an extinction coefficient of $3.42 \times 10^3 \text{ M}^{-1}\text{cm}^{-1}$ at 445 nm¹³. The concentration of the chromium(II) produced was determined from the absorbance at 560 nm ($\epsilon = 4.81 \times 10^3 \text{ M}^{-1}\text{cm}^{-1}$ ¹³).

A similar procedure was used to determine the quantum yields for formation of the chromium(II) complex produced in the quenching of the excited states of the 5-chloro-1,10-phenanthroline and the 4,4'-dimethyl-2,2'-bipyridine complexes by oxalate. Although the spectra of the excited state of these two complexes have appeared in the literature, no values have been determined for their extinction coefficients⁸, thus before determining the quantum yields, the extinction coefficients for the excited state complexes were determined. In the determination of the quantum yields and extinction coefficients of the excited state complexes, the following values of the extinction coefficients for the chromium(II) products

were used: $\text{Cr}(\text{Clphen})_3^{2+}$, $3.0 \times 10^3 \text{ M}^{-1}\text{cm}^{-1}(\lambda_{\text{max}} 480 \text{ nm})$, $\text{Cr}(\text{Me}_2\text{bpy})_3^{2+}$, $4.5 \times 10^3 \text{ M}^{-1}\text{cm}^{-1}(\lambda_{\text{max}} 560 \text{ nm})^{13}$.

The extinction coefficient for $^*\text{Cr}(\text{Clphen})_3^{3+}$ was determined in the following manner. The absorbance of the excited state was determined at three wavelengths (490 nm, 510 nm, and 545 nm). The amount of $\text{Cr}(\text{Clphen})_3^{2+}$ formed by the quenching of the excited state by Fe^{2+} , Ti^{3+} and $\text{Co}([\text{14}] \text{aneN}_4)^{2+}$ was determined at 480 nm. These reagents are believed to quench the excited state by a single electron transfer mechanism.^{6,14,15} If the quenching is quantitative, one can determine the extinction coefficients for the excited state. These values are listed in Table I-1.

The extinction coefficient determined for $^*\text{Cr}(\text{Me}_2\text{bpy})_3^{3+}$ is not as well defined as that for $^*\text{Cr}(\text{Clphen})_3^{3+}$. There is a return electron transfer reaction after the initial quenching reaction in both the Fe^{2+} and $\text{Co}([\text{14}] \text{aneN}_4)^{2+}$ cases:



These return electron transfer reactions are moderately slow in the case of other chromium polypyridine complexes such as the $\text{Cr}(\text{Clphen})_3^{2+}$. The quenching reactions also are faster for chromium polypyridine complexes other than $^*\text{Cr}(\text{Me}_2\text{bpy})_3^{3+}$. These two facts coupled together thus prevent the use of Fe^{2+} and $\text{Co}([\text{14}] \text{aneN}_4)^{2+}$ in the determination of the extinction coefficients of the excited state of $\text{Cr}(\text{Me}_2\text{bpy})_3^{3+}$. However, the Ti^{3+} quenching reaction was used to determine the

extinction coefficient of the excited state of the 4,4'-dimethyl-2,2'-bipyridine complex at 445 nm ($4.72 \times 10^3 \text{ M}^{-1}\text{cm}^{-1}$).

RESULTS

Kinetics of quenching by oxalate ions

Concentrations and observed rate constants for all reactions studied will not be displayed here, but rather are collected in the tables of the Appendix.

As mentioned earlier, the rates of quenching were determined by monitoring the decrease in the emission signal of the excited state of the chromium complex with time. The rate of quenching as a function of the oxalate ion concentration for trials in which the ionic strength was due only to the amount of oxalate and those in which the ionic strength was maintained with sodium sulfate at 1.0 M or 2.0 M are shown in Figures I-1 and I-2. For these sets of the data, the initial concentration of $\text{Cr}(\text{bpy})_3^{3+}$ was 3.29×10^{-4} M. At non-constant ionic strength the characteristic curvature of a pre-equilibrium, in this case an ion-pairing equilibrium is observed. At the constant ionic strength trials, slight curvature is also visible. This may be due to quenching of $\text{*Cr}(\text{bpy})_3^{3+}$ by $\text{Cr}(\text{bpy})_3^{2+}$. An upper limit for the quenching of the excited state by the reduced chromium species was found to be $5 \times 10^9 \text{ M}^{-1}\text{s}^{-1.6}$

As further confirmation that quenching by $\text{Cr}(\text{bpy})_3^{2+}$ is occurring, the quenching by oxalate was studied as a function of the initial ground state concentration at constant oxalate concentration. A plot of the data is shown in Figure I-3 and

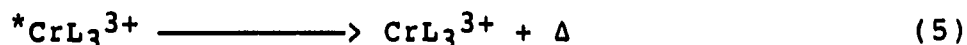
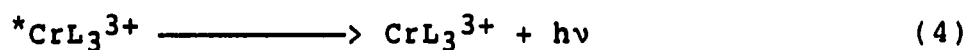
as can be seen the observed rate constants increase with increasing amount of the chromium complex.

The observed rate constants as a function of the oxalate concentration were determined at low levels of the $\text{Cr}(\text{bpy})_3^{3+}$ concentration. This was done in an attempt to minimize the quenching by $\text{Cr}(\text{bpy})_3^{2+}$. Again the rate constants were determined at non-constant and constant ionic strength ($\mu = 0.75$ M and 2.00 M). The plots of the data are shown in Figures I-4 and I-5 respectively and the k_{obs} values at each concentration are presented in Table A-5 to A-7. In the case of non-constant ionic strength curvature is again observed; however, the constant ionic strength plots of k_{obs} versus the oxalate concentration are now linear.

In the plot for the non-constant ionic strength trials data were fitted using a non-linear least squares analysis assuming an ion-pairing mechanism, such that:

$$k_{\text{obs}} = \frac{k_o + k_c K_1 [\text{C}_2\text{O}_4^{2-}]}{1 + K_1 [\text{C}_2\text{O}_4^{2-}]} \quad (3)$$

where K_1 is the ion-pairing constant and k_c is the rate constant for quenching the ion-pair and k_o is the sum of the rate constants for oxalate independent loss of the excited state:



The ion-pairing constant is a function of the ionic strength and at each oxalate concentration its value was calculated using the Fuoss equation 16,17:

$$K = \frac{4\pi N\sigma^3}{3000} \exp\left(\frac{-w(\sigma)}{kT}\right) \quad (6)$$

where:

$$w(\sigma) = \frac{z_1 z_2 e^2}{D_s \sigma (1 + \beta \sigma \sqrt{\mu})} \quad (7)$$

and:

$$\beta = \left(\frac{8\pi N e^2}{1000 D_s kT} \right)^{1/2} \quad (8)$$

In the above equations, D_s is the dielectric constant of the solvent, μ is the ionic strength, z_1 and z_2 are the charges of the ions involved and σ is the distance of closest approach in cm. All other symbols have the standard meaning. The distance of closest approach was taken to be the sum of the radii of $\text{Cr}(\text{bpy})_3^{3+}$ and oxalate. The radius of $\text{Cr}(\text{bpy})_3^{3+}$ was taken to be similar to that of $\text{Ru}(\text{bpy})_3^{2+}$ or $\text{Co}(\text{bpy})_3^{3+}$ which are estimated to be about $6.8 \text{ \AA}^{17,18}$, and oxalate was taken to be about 2.0 \AA^{19} . Using these calculated ion-pairing constants as well as the data and a non-linear least squares program, the curve shown in Figure I-4 was obtained. Non-linear least squares analysis yielded the following results: $k_C = (1.46 \pm 0.03) \times 10^5 \text{ M}^{-1}\text{s}^{-1}$, $k_O = (2.13 \pm 0.12) \times 10^4 \text{ s}^{-1}$.

In the case of the constant ionic strength trials, the rate law for the quenching of the excited state has the form:

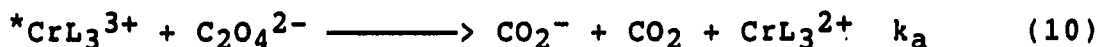
$$\text{Rate} = (k_A + k_B[\text{C}_2\text{O}_4^{2-}])[*\text{Cr}(\text{bpy})_3^{3+}] \quad (9)$$

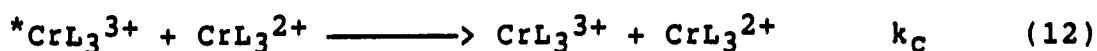
This is valid as well for the quenching of the excited states of the other polypyridine chromium complexes by oxalate. Rate constants for the quenching of the excited states of $\text{Cr}(\text{Clphen})_3^{3+}$, $\text{Cr}(\text{Mephen})_3^{3+}$, $\text{Cr}(\text{phen})_3^{3+}$ and $\text{Cr}(\text{Me}_2\text{bpy})_3^{3+}$ were also determined as a function of the oxalate concentration at constant ionic strength ($\mu = 0.75\text{M}$). The data are plotted in Figure I-6. Table I-2 summarizes the second order rate constants (k_B) obtained from the slopes of the lines in the above mentioned plots. Also listed are the fitted values of the intercept (k_A) as well as the experimental values determined in the absence of oxalate.

Quantum yields

The quantum yields for the formation of CrL_3^{2+} were determined for the bipyridine complex, the 5-chloro-1,10-phenanthroline complex and the 4,4'-dimethyl-2,2'-bipyridine complex. The data, including the amounts of CrL_3^{2+} formed as well as the concentration of $*\text{CrL}_3^{3+}$, are presented in the Appendix in Table A-12.

The quantum yield was determined as a function of the initial (prior to the flash) ground state concentration. The results for the bipyridine complex are presented in Table I-3. Also listed in Table I-3 are quantum yields determined from kinetic simulations using the experimental concentrations and the following approximate scheme:





The values for the rate constants used in the simulation were as follows. The value for the quenching by oxalate (k_a) was taken to be equal to Kk_B where k_B is an experimental quantity and K was calculated as before taking into account the ionic strength at which the quantum yields were determined ($k_B K = 1.61 \times 10^6 \text{s}^{-1}$). The rate constant for the quenching by CrL_3^{2+} was taken to be $5 \times 10^9 \text{M}^{-1} \text{s}^{-1}$ which is that determined previously⁷. The rate constant for the reaction of CO_2^- with CrL_3^{3+} was taken to be $2 \times 10^{10} \text{M}^{-1} \text{s}^{-1}$. This last value was used since in the quenching by oxalate there is no apparent buildup of CO_2^- . Also such large rate constants are not unheard of for CO_2^- reactions. For example, CO_2^- reacts with $\text{Co}(\text{bpy})_3^{3+}$ with a rate constant of $7.6\text{--}7.8 \times 10^9$ ^{20,21} and with $\text{Rh}(\text{bpy})_3^{3+}$ with a rate constant of 6.2×10^9 ²². Lastly, the value for the deactivation of the excited state (k_d) was taken to be $2 \times 10^4 \text{s}^{-1}$ and that for ground state quenching (k_e) of the excited state was estimated to be $1 \times 10^6 \text{M}^{-1} \text{s}^{-1}$. Although the ground state quenching rate constant is not known for the oxalate- $\text{Cr}(\text{bpy})_3^{3+}$ system, it appears that in other systems the ground state quenching rate constant is approximately this order of magnitude ($^*\text{Cr}(\text{bpy})_3^{3+}$ in 1 M NaCl is 1.6×10^6 ³ and in 5 M HCl it is 1.3×10^6 ⁵). The ground

state quenching term may not really be of significance in this system; however, it is included for completeness. In the absence of quenching by CrL_3^{2+} a quantum yield of 2 would be anticipated. However, due to the fact that CrL_3^{2+} quenches the excited state a decline in quantum yield below 2 is experimentally observed as the concentration of the ground state is increased. Quantum yields calculated using kinetic simulations also show a decrease as the concentration of the ground state is increased.

The values for the quantum yields for the formation of the $\text{Cr}(\text{Clphen})_3^{2+}$ are shown in Table I-4. The quenching of the excited state of the 5-chloro-1,10-phenanthroline complex by oxalate is approximately a factor of twenty greater than that for the bipyridine complex and thus the CrL_3^{2+} quenching reaction should be of less importance. Since the rate of quenching by $\text{Cr}(\text{bpy})_3^{2+}$ is near diffusion control the rate constant for the quenching by $\text{Cr}(\text{Clphen})_3^{2+}$ cannot be much larger. Over the range of ground state concentrations studied the quantum yields are steady at a value of 2.1. The quenching of this complex is complicated by the presence of an intermediate; however, as will be shown later this should not effect the quantum yields.

The quantum yields determined for the 4,4'-dimethyl-2,2'-bipyridine complex are presented in Table I-5. The rate constant for the quenching of this complex is the lowest of those studied in this work. The quenching of the excited

state by the chromium(II) species would be predicted to be most important here. The quantum yield for formation of $\text{Cr}(\text{Me}_2\text{bpy})_3^{2+}$ over the range of ground state concentrations studied is significantly less than two.

Spectrum and kinetics of the secondary transient

Quenching of the excited state of the 1,10-phenanthroline and substituted phenanthroline complexes by oxalate ions and EDTA^{2-} and of the 2,2'-bipyridine complex and its substituted analogs by EDTA^{2-} produce a secondary transient which has a broad absorption spectrum in the region 520nm to 660nm. A transient was not observed in the case of the quenching of the 2,2'-bipyridine complex or 4,4'-dimethyl-2,2'-bipyridine by oxalate ions. The EDTA^{2-} reactions were studied in an attempt to elucidate the mechanism in the oxalate case and to possibly shed some light on the structure of the intermediate since previously it was found that oxalate quenching was similar in several respects to quenching by EDTA^{2-} .

The spectrum of the secondary intermediate as well as the final product of the reaction was determined for the quenching of the excited state of the 5-chloro-1,10-phenanthroline complex by oxalate and EDTA^{2-} and are shown in Figures I-7 and I-8 respectively. The secondary transient in both cases look quite similar. The final product in both cases appears to be $\text{Cr}(\text{Clphen})_3^{2+}$ as their spectra are very similar to that observed previously in which the $\text{Cr}(\text{Clphen})_3^{2+}$ was prepared pulse radiolytically.¹³

The secondary transient decays by a process whose rate is dependent on the ground state concentration. The observed rate constants for the loss of the secondary intermediate at various ground state concentrations was determined at 605 nm for the 5-chloro-1,10-phenanthroline complex with EDTA^{2-} and oxalate, for the 2,2'-bipyridine complex with EDTA^{2-} and for the 1,10-phenanthroline complex with EDTA^{2-} and oxalate. The tables of rate constants are contained in the Appendix. Figures I-9, I-10 and I-11 are plots of the observed rate constants versus the ground state concentration. A tabulation of the second order rate constants (k_{2i}) obtained from the slopes of these plots is presented in Table I-6. Also listed in the table are the intercepts (k_{1i}).

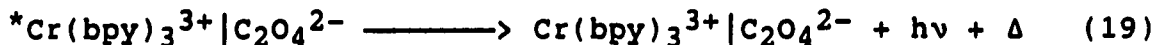
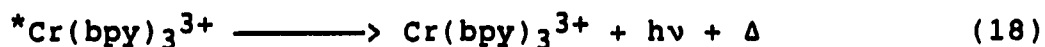
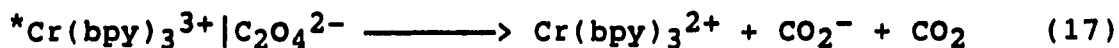
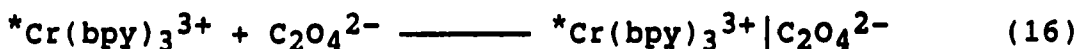
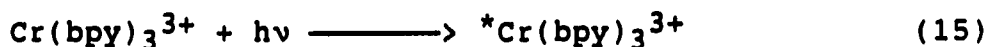
Whether one or more intermediates are produced in the reaction is shown in Table I-7. This is a listing of observed rate constants determined at several wavelengths in which the secondary transient for the reaction of $^*\text{Cr}(\text{Clphen})_3^{3+}$ with oxalate has a significant absorption. The rate constants are the same within the experimental error at each of the wavelengths studied. The wavelengths chosen were chosen such as to encompass most of the broad absorbance range of the intermediate. Owing to the constancy of the rate constants over the range it can be concluded that there is only one intermediate in the reaction of the 5-chloro-1,10-phenanthroline complex with oxalate.

DISCUSSION

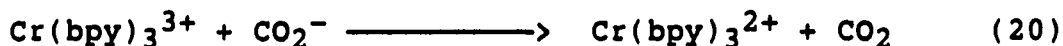
Mechanism for the quenching of $^*\text{Cr}(\text{bpy})_3^{3+}$ by oxalate

The mechanism for the quenching of the excited state of $\text{Cr}(\text{bpy})_3^{3+}$ will first be discussed for the cases in which the initial ground state concentration was low ($\sim 10^{-5}$ M).

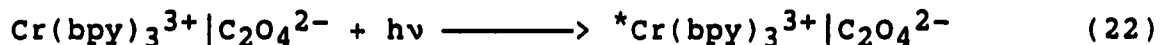
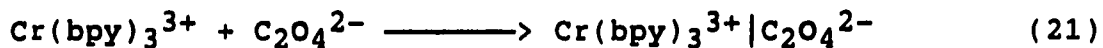
The shape of the plot of k_{obs} versus the oxalate concentration at non-constant ionic strength suggests a pre-equilibrium followed by electron transfer to produce $\text{Cr}(\text{bpy})_3^{2+}$ and CO_2^- .



The CO_2^- produced in the quench now reacts with another mole of $\text{Cr}(\text{bpy})_3^{3+}$:



It is also possible to include other steps for completeness; one may include for example ion-pairing prior to excitation and excitation of the ion-pair:



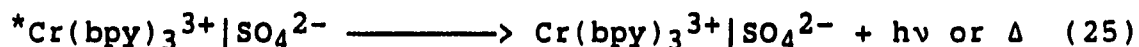
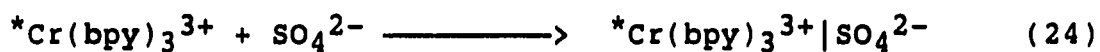
However, these are relatively inconsequential to the mechanism. The ion-pairing constant for the excited state and ground state should be similar since structurally the excited state (^2E) and ground state should be similar.²³

If one considers the mechanism for the quenching of the excited state then to consist of the steps 14 through 17 then the rate law becomes:

$$\frac{-d[C_{Exc}]}{dt} = \frac{k_o + (k_o' + k_{ox})K_1[C_2O_4^{2-}]}{1 + K_1[C_2O_4^{2-}]} C_{Exc} \quad (23)$$

In the above equation K_1 is the ion-pairing constant, k_{ox} is the rate constant for the electron transfer quenching and k_o and k_o' are the rate constants for the thermal or photochemical deactivation of the excited state and the excited state ion-pair, respectively, and C_{Exc} is the total excited state concentration. Although individual ion-pairing constants cannot be evaluated for the oxalate- $Cr(bpy)_3^{3+}$ system they can be calculated using the Fuoss equation. The validity of the above equation is shown by how well the data (k_{obs}) are fit to a function of K_1 and the oxalate concentration (Figure I-4).

The rate constant was also determined as a function of the oxalate concentration under conditions of constant ionic strength (either 0.75 M or 2.00 M). In these trials sodium sulfate was added to maintain the ionic strength. This now introduces the following into the mechanism:



The observed rate constant for the quenching of the excited state by oxalate can now be written:

$$k_{\text{obs}} = \frac{k_o + (k'_o + k_{\text{ox}})K_1[\text{C}_2\text{O}_4^{2-}] + k''_o K_2[\text{SO}_4^{2-}]}{1 + K_1[\text{C}_2\text{O}_4^{2-}] + K_2[\text{SO}_4^{2-}]} \quad (26)$$

Here K_2 is the ion-pairing constant for the sulfate- $^*\text{Cr}(\text{bpy})_3^{3+}$ ion-pair and k''_o is the rate constant for the photochemical or thermal deactivation of this second excited state ion-pair. The above can be simplified somewhat. Since oxalate and sulfate are doubly negative ions:

$$[\text{C}_2\text{O}_4^{2-}] + [\text{SO}_4^{2-}] = C \quad (27)$$

where C is a constant for a particular ionic strength.

Substitution of the above into the expression for k_{obs} yields the following result:

$$k_{\text{obs}} = \frac{(k_o + k''_o K_2 C) + ((k_{\text{ox}} + k'_o)K_1 - k''_o K_2)[\text{C}_2\text{O}_4^{2-}]}{(K_1 - K_2)[\text{C}_2\text{O}_4^{2-}] + (1 + K_2 C)} \quad (28)$$

Since the radius of sulfate²⁴ is very nearly the same as oxalate, the ion-pairing constants K_1 and K_2 should be nearly the same. Also C is always greater than or equal to the oxalate concentration so:

$$(K_1 - K_2)[\text{C}_2\text{O}_4^{2-}] < 1 + K_2 C$$

So at constant ionic strength, the observed rate constant should be a linear function of the oxalate concentration:

$$k_{\text{obs}} = \frac{k_o + k_o''K_2C + ((k_{\text{ox}} + k_o')K_1 - k_o''K_2)[C_2O_4^{2-}]}{1 + K_2C} \quad (29)$$

A plot of k_{obs} versus the oxalate concentration should be linear with a slope and intercept corresponding to:

$$\text{slope} = \frac{(k_o' + k_{\text{ox}})K_1 - k_o''K_2}{1 + K_2C} \quad (30)$$

$$\text{intercept} = \frac{k_o + k_o'K_2C}{1 + K_2C} \quad (31)$$

The difference in the slopes of the two constant ionic strength series can be shown to be due to the dependence of the ion-pairing constant on ionic strength. If one assumes that $K_1 = K_2$ and that the unimolecular rate constants k_o , k_o' , k_o'' and k_{ox} are ionic strength independent one obtains:

$$\text{slope} = ((k_o' + k_{\text{ox}}) - k_o'')K/(1 + KC) \quad (32)$$

If the Fuoss equation is used to calculate ion-pairing constants at the two ionic strengths, one obtains $K = 6.7 \text{ M}^{-1}$ ($\mu = 0.75 \text{ M}$) and $K = 4.3 \text{ M}^{-1}$ ($\mu = 2.00 \text{ M}$). The theoretical ratio of the slope at $\mu = 2.00 \text{ M}$ to that at $\mu = 0.75 \text{ M}$ is then 0.444. The experimental ratio is $1.57 \times 10^5 / 3.59 \times 10^5 = 0.431$. This agreement appears to confirm the validity of the mechanism and treatment.

The quantum yields for the formation of $\text{Cr}(\text{bpy})_3^{2+}$ also confirm the mechanism. If the quenching by oxalate is fast such that it exceeds the thermal and photochemical relaxation of the excited state and/or excited ion-pairs, a quantum yield

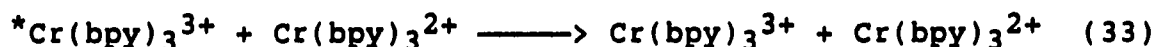
of 2 would be expected. The first mole of the reduced product is formed in the electron transfer quenching step, while the second is formed in the reaction of CO_2^- with another mole of $\text{Cr}(\text{bpy})_3^{3+}$. Theoretically CO_2^- could react either the ground state or the excited state complex; however, under the conditions employed here only ~10% of the initial amount of the chromium complex is excited in the flash and so it is >90% likely that the CO_2^- formed in the quench will attack a ground state species. It was found experimentally that the quantum yield for the formation of the $\text{Cr}(\text{bpy})_3^{2+}$ is nearly 2 in the limit of low initial $[\text{Cr}(\text{bpy})_3^{3+}]$. The quantum yields do however, decrease as the initial chromium concentration is increased and this shall be explained shortly.

Lastly, it proved impossible to directly detect the CO_2^- intermediate. Spectroscopically this was unlikely due to the fact that CO_2^- does not build up in the reaction and second the absorbance of the chromium complexes would obscure the CO_2^- absorption spectrum.²⁵ Scavenging of CO_2^- by other species such as methyl viologen (MV^{2+}) or $(\text{H}_3\text{N})_5\text{CoCl}^{2+}$ were attempted. MV^{2+} is known to react with CO_2^- with a rate constant of $1 \times 10^{10} \text{ M}^{-1}\text{s}^{-1}$ ^{26,27} while $(\text{H}_3\text{N})_5\text{CoCl}^{2+}$ reacts with a rate constant of $1.5 \times 10^8 \text{ M}^{-1}\text{s}^{-1}$.²¹ However, there were complications in these competition studies. First the product of the MV^{2+} and CO_2^- reaction is MV^+ . This species is quite capable of reacting with $\text{Cr}(\text{bpy})_3^{3+}$ to produce MV^{2+} and $\text{Cr}(\text{bpy})_3^{2+}$.²⁸ Second the reaction of CO_2^- and $\text{Cr}(\text{bpy})_3^{3+}$ is

extremely fast while the quenching of the excited state by oxalate is only moderately so thus making it difficult to perform competition studies. An attempt was made to detect CO_2^- using MV^{2+} in the $^*\text{Cr}(\text{Clphen})_3^{3+}$ and oxalate reaction. This quenching reaction is over an order of magnitude faster than that for the $^*\text{Cr}(\text{bpy})_3^{3+}$; however, as will be shown later, this reaction is complicated by the presence of a secondary transient. The spectrum of this secondary transient overlaps considerably with that of the MV^+ .

Quenching of $^*\text{Cr}(\text{bpy})_3^{3+}$ at high initial ground state concentrations

At high initial chromium complex concentrations the quenching of the excited state is complicated by the following process:



This reaction has been observed previously and an upper limit for its rate constant was found to be $5 \times 10^9 \text{ M}^{-1}\text{s}^{-1,6}$.

The effect of the $\text{Cr}(\text{bpy})_3^{2+}$ quenching is shown in the plot of the observed rate constant versus the ground state concentration at constant oxalate concentration (Figure I-3). Although in all cases the pseudo-first order conditions should have prevailed the observed rate constant increased as the ground state concentration increased. As the initial ground state concentration increases the amount of the excited state produced in the flash also increases and consequently the amount of $\text{Cr}(\text{bpy})_3^{2+}$ that can be made increases. Also for

each electron transfer quenching step by oxalate ions, two $\text{Cr}(\text{bpy})_3^{2+}$ can potentially be produced. Thus at high initial ground state concentrations the quenching of the excited state by $\text{Cr}(\text{bpy})_3^{2+}$ may become important. At low concentrations of $\text{Cr}(\text{bpy})_3^{3+}$ the $\text{Cr}(\text{bpy})_3^{2+}$ quenching becomes less important. If one uses a rate constant of $5 \times 10^9 \text{ M}^{-1}\text{s}^{-1}$ for the quenching by $\text{Cr}(\text{bpy})_3^{2+}$ and assumes an average value of the $[\text{Cr}(\text{bpy})_3^{2+}]$ of $1.6 \times 10^{-6} \text{ M}$ (for $[\text{Cr}(\text{bpy})_3^{3+}] = 1.6 \times 10^{-5} \text{ M}$) and $3.2 \times 10^{-5} \text{ M}$ (for $[\text{Cr}(\text{bpy})_3^{3+}] = 3.2 \times 10^{-4} \text{ M}$) one obtains observed rate constants of $8 \times 10^3 \text{ s}^{-1}$ and $1.6 \times 10^5 \text{ s}^{-1}$ respectively. Although this is not an exact calculation, as the $[\text{Cr}(\text{bpy})_3^{2+}]$ varies throughout a run it does show how the $\text{Cr}(\text{bpy})_3^{2+}$ quenching can become important. As a comparison to the above, the measured rate constants for the oxalate quenching are $7.6 \times 10^4 \text{ s}^{-1}$ and $1.57 \times 10^5 \text{ s}^{-1}$ at low and high initial ground state concentrations, respectively.

This interference, the quenching by $\text{Cr}(\text{bpy})_3^{2+}$, is also observed in the plots of k_{obs} versus the oxalate concentration at high initial ground state concentrations and constant ionic strength. As was shown earlier, these same plots done for runs in which the initial ground state concentration was low were linear. At high $[\text{Cr}(\text{bpy})_3^{3+}]$ the plots show curvature. Such curvature is predicted by kinetic simulations if one considers the mechanism postulated previously for low $[\text{Cr}(\text{bpy})_3^{3+}]$ and includes the $\text{Cr}(\text{bpy})_3^{2+}$ quenching process.

Lastly, quenching of the excited state by $\text{Cr}(\text{bpy})_3^{2+}$ affects the quantum yields for formation of the reduced product. It is obvious that as this secondary pathway becomes important the quantum yields should decrease from the theoretical value of 2 observed at low $[\text{Cr}(\text{bpy})_3^{3+}]$. This is indeed observed. The yields of $\text{Cr}(\text{bpy})_3^{2+}$ decrease from ~1.7 at low $[\text{Cr}(\text{bpy})_3^{3+}]$ to ~0.9 at the highest $[\text{Cr}(\text{bpy})_3^{3+}]$ studied. Similar although not identical values are obtained from kinetic simulations. Identical values are not obtained due to the fact that the rate for the CO_2^- reaction is not known, as well as the fact that the $\text{Cr}(\text{bpy})_3^{2+}$ quenching rate constant is only a limiting value.

This point is further proved by the quantum yields for formation of $\text{Cr}(\text{Clphen})_3^{2+}$ and $\text{Cr}(\text{Me}_2\text{bpy})_3^{2+}$ in the quenching by oxalate of $^*\text{Cr}(\text{Clphen})_3^{3+}$ and $^*\text{Cr}(\text{Me}_2\text{bpy})_3^{3+}$ respectively. The rate for quenching for the former is more than an order of magnitude larger than for the bipyridine complex and the latter an order of magnitude less. Thus one would predict quantum yields of nearly 2 for the 5-chloro-1,10-phenanthroline complex and significantly less than 2 for the 4,4'-dimethyl-2,2'-bipyridine complex. Experiment bears this out. Over the concentration range studied the quantum yield for formation of $\text{Cr}(\text{Clphen})_3^{2+}$ is 2 while for formation of $\text{Cr}(\text{Me}_2\text{bpy})_3^{2+}$ it is ~0.5. In the latter case it should be mentioned that such low quantum yields may be due as well to

ground state relaxation terms (k_0 , k_0' , k_0'') which may now become important.

Oxalate quenching of other $*CrL_3^{3+}$

The four other complexes, $Cr(Clphen)_3^{3+}$, $Cr(phen)_3^{3+}$, $Cr(Me_2bpy)_3^{3+}$ and $Cr(Mephen)_3^{3+}$ have a similar rate law at constant ionic strength, and all k_{obs} versus oxalate plots were linear. The slopes (k_B) are dependent on the $CrL_3^{*3+/2+}$ potential as is shown in Figure I-12 implying an outer sphere electron transfer quenching step is operative for all these species.

The phenanthroline and substituted phenanthroline complexes mechanistically behaved differently from the bipyridine and substituted bipyridine complexes. After the initial quenching step an intermediate was formed; however, this shall be discussed more fully in the next section.

Mention should be made concerning the values of the intercepts of the plots of k_{obs} versus the oxalate concentration. The values obtained are for the phenanthroline and substituted phenanthroline complexes larger than the experimental value obtained from trials in which the loss of the emission signal was monitored in which only sulfate (no oxalate) was present.

It is known that anions promote loss of the excited state by causing ground state quenching via the formation of an "ion-paired exciplex".²³ The rate constant of this ground state quenching is designated by 2k_g . This ground state

quenching has been studied most for $\text{Cr}(\text{phen})_3^{3+}$ where values of 2k_g such as 2.3×10^6 , 4.7×10^6 , 6.1×10^6 and 2.9×10^6 have been determined for 1 M HCl ⁵, 1 M HClO_4 ³, 1 M NaCl (pH 9.5)⁵, 1 M Na_2SO_4 ³ respectively. The lifetime at infinite dilution of CrL_3^{3+} (τ_0) is also affected by the anion used; however, τ_0 is in general longer due to anion effects.²³ The possibility may exist that the 2k_g in the presence of oxalate may be different from that of the sulfate. Thus as the $[\text{SO}_4^{2-}]/[\text{C}_2\text{O}_4^{2-}]$ ratio is varied (keeping the ionic strength constant) more or less ground state quenching can occur. However, one would expect slight curvature in the k_{obs} versus the oxalate concentration plots as well and this is not observed. If oxalate had a higher 2k_g than sulfate one would expect curvature upwards with an intercept lower than the actual value and if sulfate were the higher of the two one would expect downwards curvature and a higher intercept.

One point does seem to support the idea of ground state quenching and that is what is observed for the bipyridine and 4,4'-dimethyl-2,2'-bipyridine complexes. It is known that the phenomena of anion assisted ground state quenching is more pronounced for phenanthroline complexes.^{23,29} Indeed while an effect is seen for $^*\text{Cr}(\text{phen})_3^{3+}$ in 1 M HCl , the 2,2'-bipyridine analog shows the effect only in 5 M HCl ⁵. Also the 2k_g values tend to be smaller for the bipyridine and substituted bipyridines than for phenanthrolines. In the present set of experiments neither 2,2'-bipyridine nor 4,4'-

dimethyl-2,2'-bipyridine show much of a deviation between experimental and fitted intercept values at an ionic strength of 0.75 M. Only the phenanthroline and substituted phenanthrolines have relatively high intercepts at 0.75 M ionic strength. However, such effects are difficult to sort out owing to the fact that both the oxalate and sulfate concentrations are varying over the series of experiments.

It should also be mentioned that if CrL_3^{2+} quenching were important a higher intercept as well as downwards curvature would be expected as in the high $\text{Cr}(\text{bpy})_3^{3+}$ concentration runs.

Also it should be apparent that a 2k_g term for oxalate cannot be determined since oxalate quenches the excited state in an irreversible electron transfer step.

The intermediate

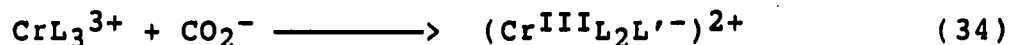
After the quenching step in the case of the 1,10-phenanthroline, 5-chloro-1,10-phenanthroline and 5-methyl-1,10-phenanthroline complexes an intermediate is formed. The CO_2^- apparently does not transfer an electron to directly produce CrL_3^{2+} and CO_2 as it does in the 2,2'-bipyridine and 4,4'-dimethyl-2,2'-bipyridine cases. The intermediate formed has a broad absorption in the visible as is shown by the spectra for the intermediate formed in the quenching of $^*\text{Cr}(\text{Clphen})_3^{3+}$ by oxalate and EDTA^{2-} (Figures I-7 and I-8, respectively).

There appear to be two possibilities for the identity of the intermediate. In the first case CO_2^- transfers an elec-

tron to the phenanthroline ligand to produce a ligand radical species $((\text{Cr}^{\text{III}}\text{L}_2\text{L}^-)^{2+})$. In the second case CO_2^- directly attacks the ligand producing a substituted ligand radical $((\text{Cr}^{\text{III}}\text{L}_2\text{L}'^-)^{2+})$. Although the former is not known, a ligand radical species was proposed in the pulse radiolysis of $\text{Ru}(\text{bpy})_3^{3+}$ ³⁰ and a Libpy compound is known.³¹ Venturi, et al recently observed a broadly absorbing intermediate in the reaction of $\text{Cr}(\text{phen})_3^{3+}$ with $\cdot\text{CH}_2\text{OH}$.³² They also noted that in the reaction of $\text{Cr}(\text{bpy})_3^{3+}$ with $\cdot\text{CH}_2\text{OH}$, the $\text{Cr}(\text{bpy})_3^{2+}$ was exclusively generated.

This last observation was also found here. An intermediate was observed for oxalate quenching only for the phenanthroline and substituted phenanthroline complexes. Neither the 2,2'-bipyridine nor the 4,4'-dimethyl-2,2'-bipyridine complexes quenched by oxalate showed the presence of an intermediate. However, in the case of quenching by EDTA^{2-} all the compounds showed intermediates.

Further, the intermediate decayed via first order kinetics showing a dependence on the ground state concentration and produced what appeared spectroscopically to be CrL_3^{2+} , thus:



The rate constant for the latter reaction (k_{21}) was determined as a function of the ground state chromium concentration for both oxalate and for EDTA^{2-} quenching of

$^*\text{Cr}(\text{Clphen})_3^{3+}$ and $^*\text{Cr}(\text{phen})_3^{3+}$ and for EDTA^{2-} quenching of $^*\text{Cr}(\text{bpy})_3^{3+}$. Although the rate constants for oxalate and EDTA^{2-} with $\text{Cr}(\text{Clphen})_3^{3+}$ are similar, those for $\text{Cr}(\text{phen})_3^{3+}$ were different. This seems to imply that the intermediate formed in the EDTA^{2-} system is different from that formed in the oxalate system, thus pointing to a ligand addition radical species. However, the fact that there is an intermediate in the $\text{Cr}(\text{bpy})_3^{3+}$ - EDTA^{2-} system and not one in the oxalate system implies that a common mechanism may not be operative.

The spectrum of the intermediate formed in the $\text{Cr}(\text{Clphen})_3^{3+}$ - EDTA^{2-} reaction is similar to that of the oxalate system. Both are broad and relatively featureless. Although bpy^- is known to have a broad absorption in a similar wavelength range^{33,34}, Venturi, et al attributed their absorption to a ligand addition species.³²

Table I-1. Extinction Coefficients^a for $^*\text{Cr}(\text{Clphen})_3^{3+}$
Determined Using Different Quenchers

$\lambda(\text{nm})$	$\text{Co}([\text{14}] \text{aneN}_4)^{2+}, \text{b}$	Fe^{2+}	Ti^{3+}	Average
490	2310	2690	2320	2440 ± 216
510	--	2710	2430	2570 ± 200
545	--	2620	2430	2530 ± 130

^aExtinction coefficients have units of $\text{M}^{-1}\text{cm}^{-1}$ and have an uncertainty of $\pm 10\%$.

^bWork done by C. A. Simmons at Ames Lab, Ames, IA.

Table I-2. Summary of Rate Constants for the Quenching of
 $^*CrL_3^{3+}$ by Oxalate Ions^a

L	$E^{\circ}_{*3+/2+}$	$10^{-3}xk_o \text{ exp/s}^{-1}$	$10^{-3}xk_A \text{ fit/s}^{-1}$	$10^{-5}k_B/M^{-1}s^{-1}$
Clphen ^b	1.53	10.8	43.8	85.4
bpy ^b	1.44	29.7	30.8	3.59
bpy ^c	1.44	27.5	22.1	1.57
phen ^b	1.42	5.05	7.93	4.14
Mephen ^b	1.39	4.18	8.87	3.18
Me ₂ bpy ^b	1.25	7.41	7.88	.210

^aPotentials from Ref. 2.

^bIonic strength = 0.75 M and at $(23 \pm 2)^{\circ}C$.

^cIonic strength = 2.00 M and at $(23 \pm 2)^{\circ}C$.

Table I-3. Experimental and Simulated Quantum Yields^a for the Formation of $\text{Cr}(\text{bpy})_3^{2+}$ as a Function of the Ground State Concentration

$10^5 \times [\text{Cr}(\text{bpy})_3^{3+}]/\text{M}$	ϕ_{exp}	ϕ_{sim}^b
1.64	1.72	1.71
4.91	1.38	1.59
8.18	1.31	1.50
11.4	1.20	1.41
16.4	1.22	1.36
22.9	1.22	1.27
32.7	1.02	1.15
42.5	0.91	1.08
55.5	0.85	1.03
65.3	0.87	1.00
81.7	0.89	0.99
98.0	0.89	0.96

^aQuantum yield is defined as the ratio $[\text{CrL}_3^{2+}]/[*\text{CrL}_3^{3+}]$. $[\text{C}_2\text{O}_4^{2-}] = 0.100 \text{ M}$ and $(23 \pm 2)^\circ\text{C}$.

^bThe values of the rate constants used in the simulations are given in the text.

Table I-4. Quantum Yields for the Formation of $\text{Cr}(\text{Clphen})_3^{2+}$ as a Function of the Ground State Concentration^a

$10^5 \times [\text{Cr}(\text{Clphen})_3^{3+}]/\text{M}$	ϕ_{exp}
2.40	2.1
4.80	2.0
7.20	2.1
9.61	2.05
12.0	2.1
14.4	2.1

^a $[\text{C}_2\text{O}_4^{2-}] = 0.104 \text{ M}$ and at $(23 \pm 2)^\circ\text{C}$.

Table I-5. Quantum Yields for the Formation of $\text{Cr}(\text{Me}_2\text{bpy})_3^{2+}$ as a Function of the Ground State Concentration^a

$10^5 \times [\text{Cr}(\text{Me}_2\text{bpy})_3^{3+}]/\text{M}$	ϕ_{exp}
2.56	0.41
5.13	0.65
7.69	0.59
10.3	0.49
12.8	0.49

^a $[\text{C}_2\text{O}_4^{2-}] = 0.159 \text{ M}$ and at $(23 \pm 2)^\circ\text{C}$.

Table I-6. Rate Constants for the Loss of the Secondary Transient Produced in Oxalate and EDTA²⁻ Quenching Reactions of *CrL₃³⁺ a

L	Quencher	$10^{-4} \times k_{1i}/s^{-1}$	$10^{-9} \times k_{2i}/M^{-1}s^{-1}$
bpy	EDTA ²⁻	$1.02 \pm .30$	$1.41 \pm .07$
phen	C ₂ O ₄ ²⁻	$2.06 \pm .30$	$0.82 \pm .04$
phen	EDTA ²⁻	$1.14 \pm .46$	$1.68 \pm .07$
Clphen	C ₂ O ₄ ²⁻	$0.96 \pm .27$	$1.10 \pm .08$
Clphen	EDTA ²⁻	$2.06 \pm .21$	$1.35 \pm .05$

^aDone at $(23 \pm 2)^{\circ}C$.

Table I-7. Rate Constants for the Decay of the Secondary Transient Produced in the Quenching of the Excited State of $\text{Cr}(\text{Clphen})_3^{3+}$ by Oxalate as a Function of the Monitoring Wavelength^a

$\lambda(\text{nm})$	$10^{-4} \times k_{\text{obs}}/\text{s}^{-1}$
530	$3.65 \pm .22$
550	$3.15 \pm .13$
570	$3.47 \pm .37$
605	$3.41 \pm .40$
640	$3.29 \pm .32$

^a $[\text{Cr}(\text{Clphen})_3^{3+}] = 4.49 \times 10^{-5} \text{ M}$; $[\text{C}_2\text{O}_4^{2-}] = 0.156 \text{ M}$ and $(23 \pm 2)^\circ\text{C}$.

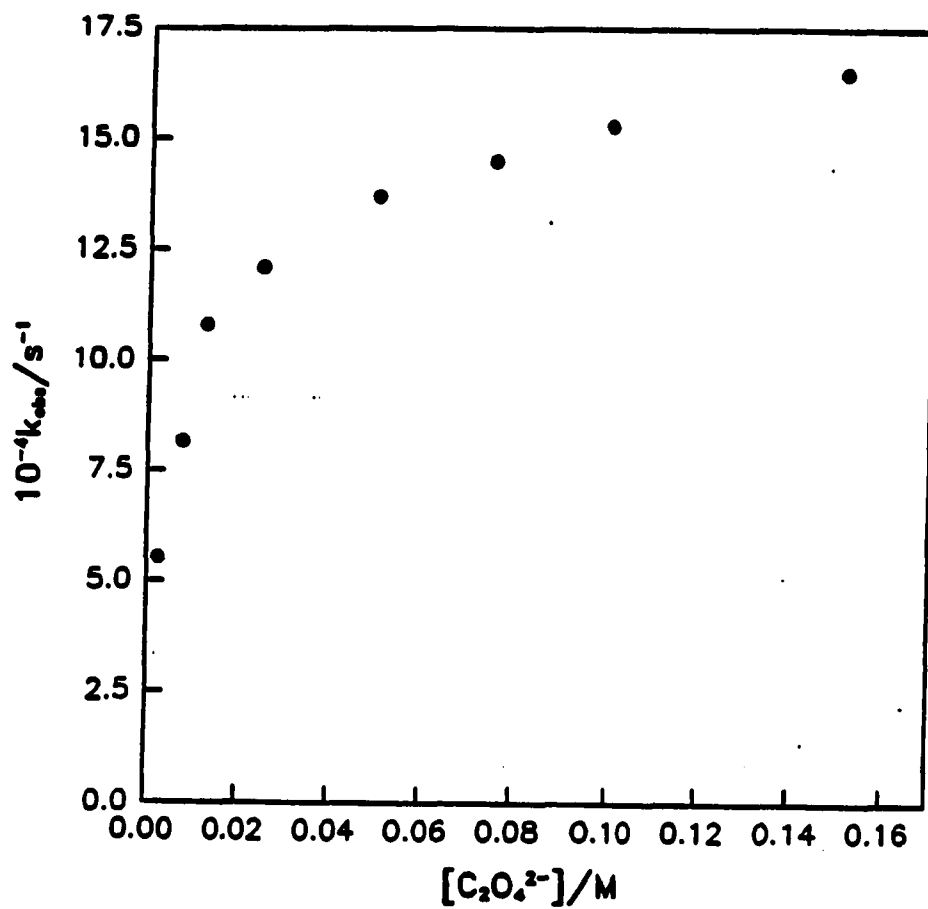


Figure I-1. The plot of the observed rate constant versus the oxalate concentration for the quenching of $^*Cr(bpy)_3^{3+}$ at non-constant ionic strength. Experiments done at high initial ground state concentration and at $(23 \pm 2)^\circ C$

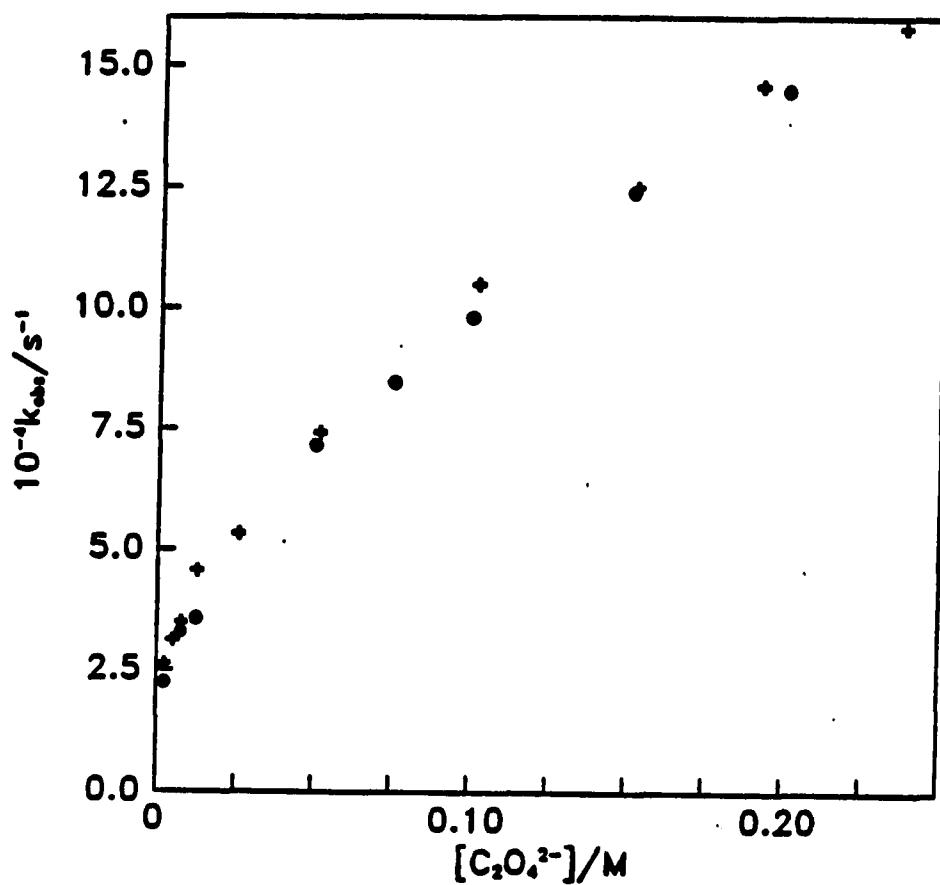


Figure I-2. The plot of the observed rate constant versus the oxalate concentration for the quenching of $^*Cr(bpy)_3^{3+}$ at ionic strengths of 1.0M(●) and 2.0M(+). Experiments were done at high initial ground state concentration and 23°C

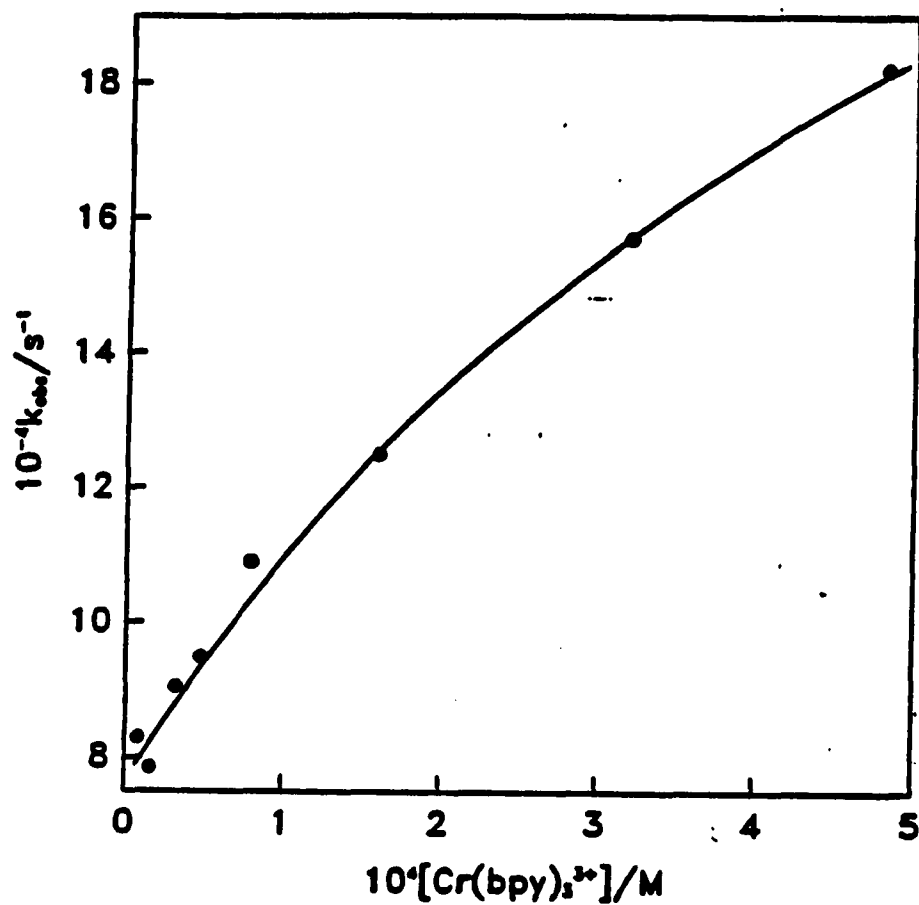


Figure I-3. The plot of the observed rate constant for the quenching of $^*\text{Cr}(\text{bpy})_3^{3+}$ versus the ground state concentration at a constant oxalate concentration of 0.0522 M and at $(23 \pm 2)^\circ\text{C}$

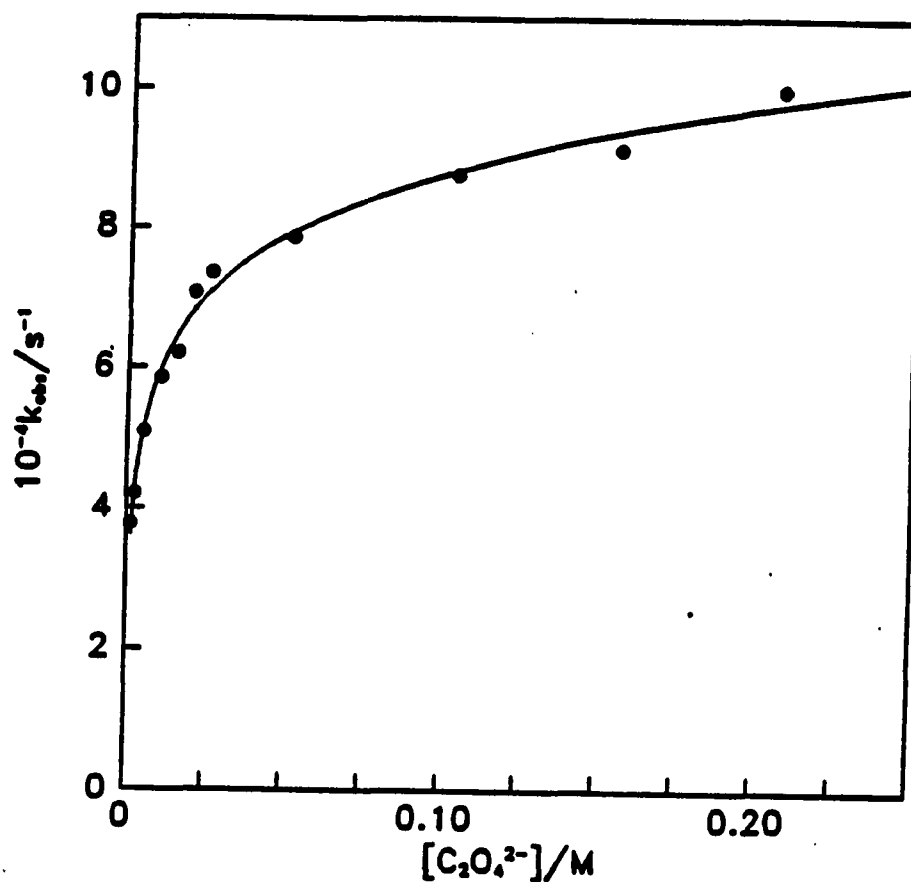


Figure I-4. The plot of the observed rate constant versus the oxalate concentration for the quenching of $^*Cr(bpy)_3^{3+}$ at non-constant ionic strength. Experiments were done at low initial ground state concentration where the dots correspond to the data points while the line is that calculated using the data as well as the calculated ion-pairing constants and at $(23 \pm 2)^\circ C$

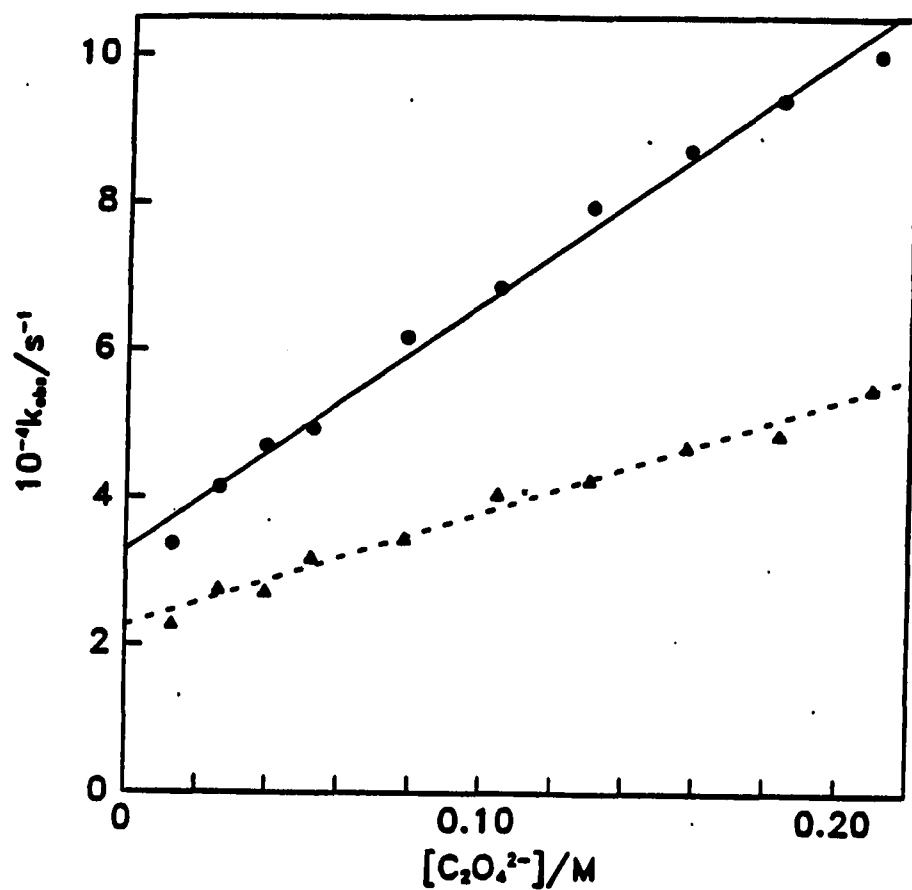


Figure I-5. The plot of the observed rate constant versus the oxalate concentration for the quenching of $^*Cr(bpy)_3^{3+}$ at ionic strengths of 0.75M (●) and 2.00M (▲). Experiments were done at low initial ground state concentration and at $(23 \pm 2)^\circ C$

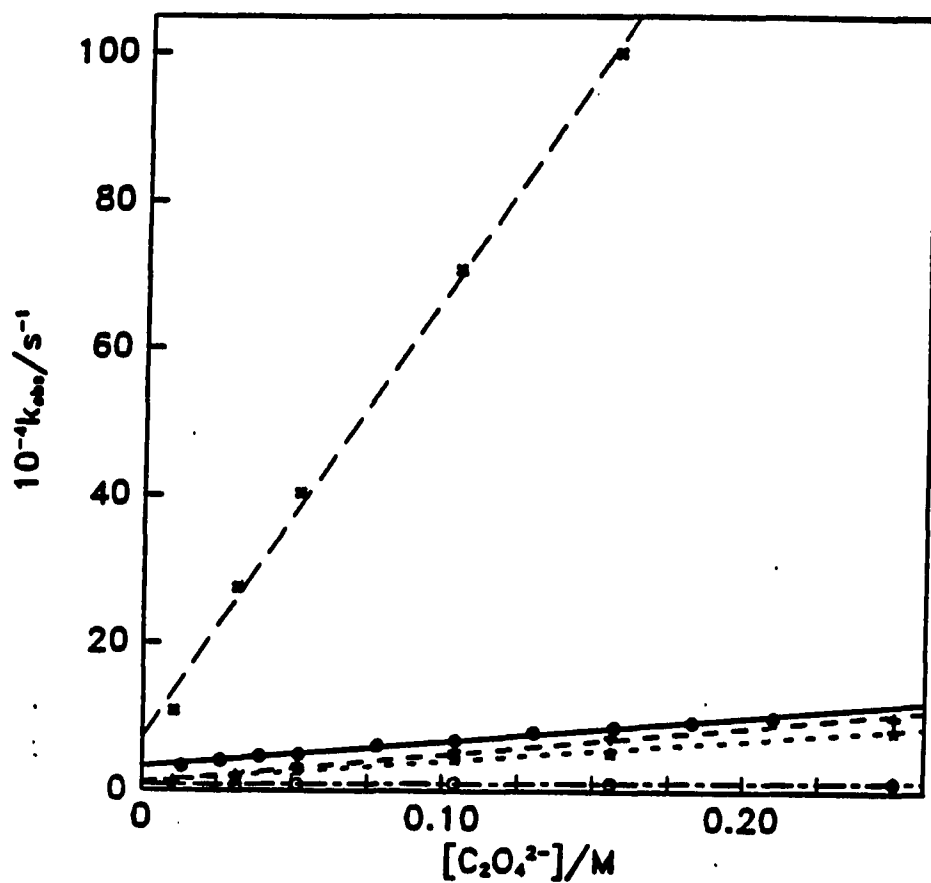


Figure I-6. The plot of the observed rate constant versus the oxalate concentration for the quenching of $^*\text{Cr}(\text{Clphen})_3^{3+}(\text{x})$, $^*\text{Cr}(\text{bpy})_3^{3+}(\bullet)$, $^*\text{Cr}(\text{phen})_3^{3+}(+)$, $^*\text{Cr}(\text{Mephen})_3^{3+}(\ast)$ and $^*\text{Cr}(\text{Me}_2\text{bpy})_3^{3+}(\text{o})$ at an ionic strength of 0.75 M and $(23 \pm 2)^\circ\text{C}$

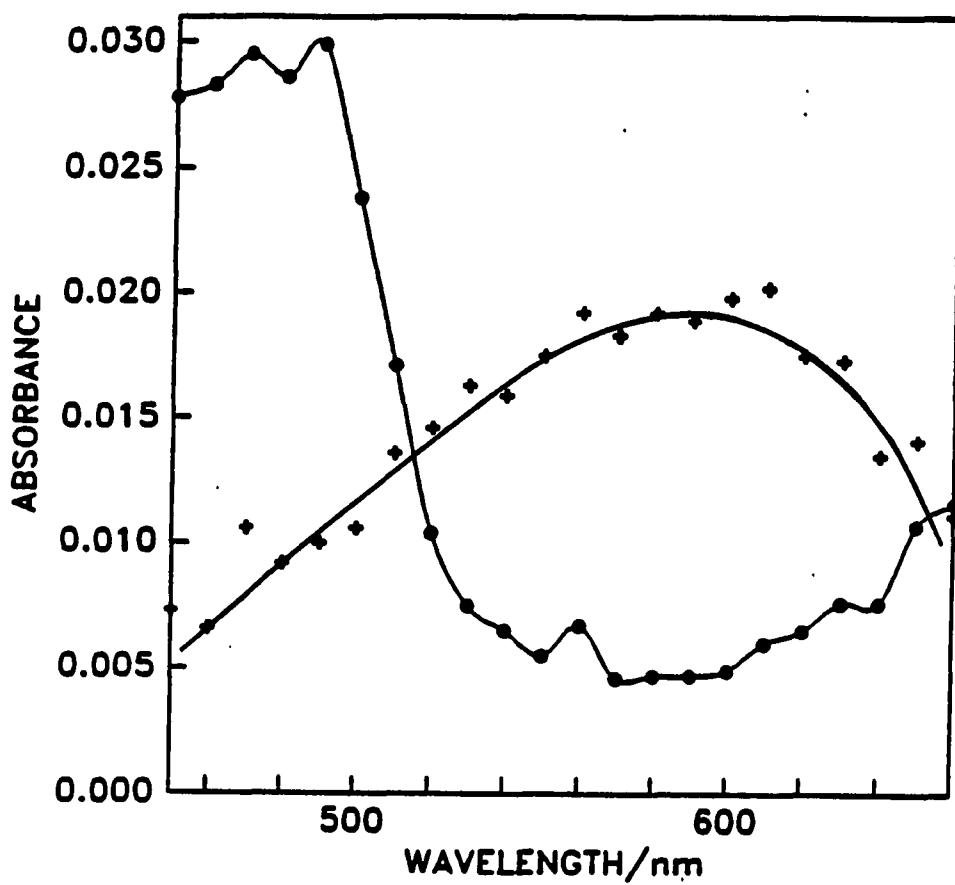


Figure I-7. Spectrum of the intermediate(+) and final product(●) formed after the quenching of $^*\text{Cr}(\text{Clphen})_3^{3+}$ by oxalate. The intermediate absorbances were determined 8 μs after the flash and at $(23 \pm 2)^\circ\text{C}$

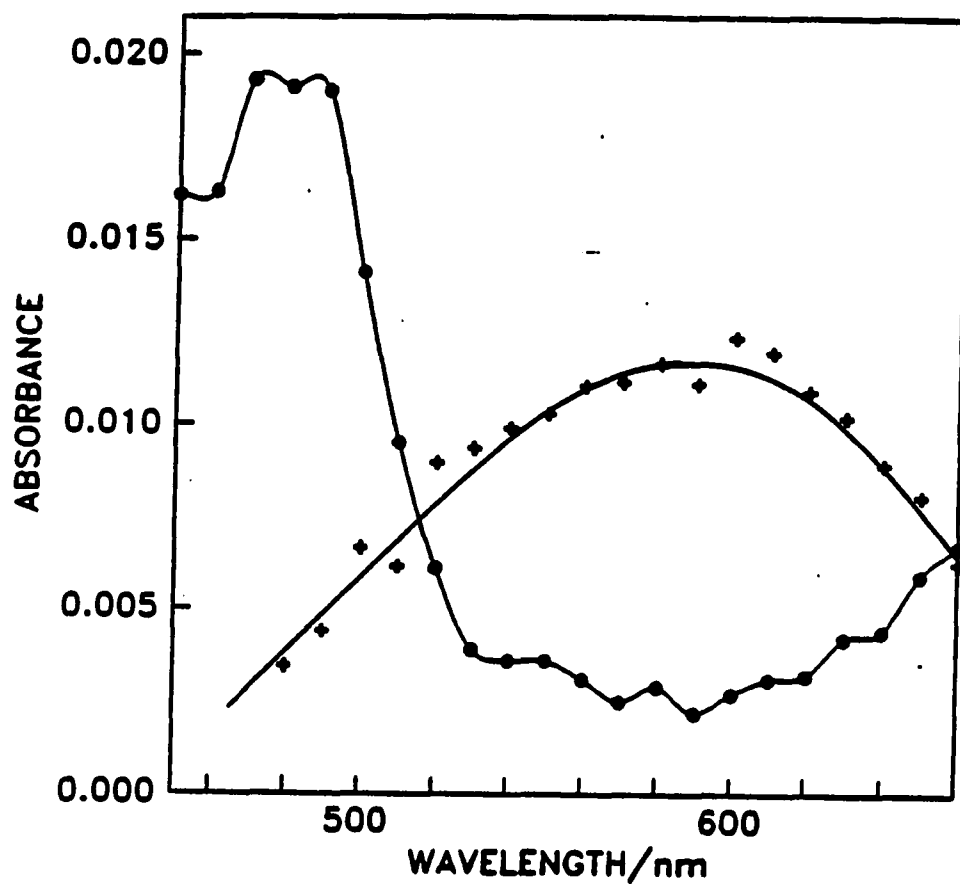


Figure I-8. Spectrum of the intermediate(+) and final product(●) formed after the quenching of $^*\text{Cr}(\text{Clphen})_3^{3+}$ by EDTA^{2-} . The intermediate absorbances were determined 8 μs after the flash and at $(23 \pm 2)^\circ\text{C}$

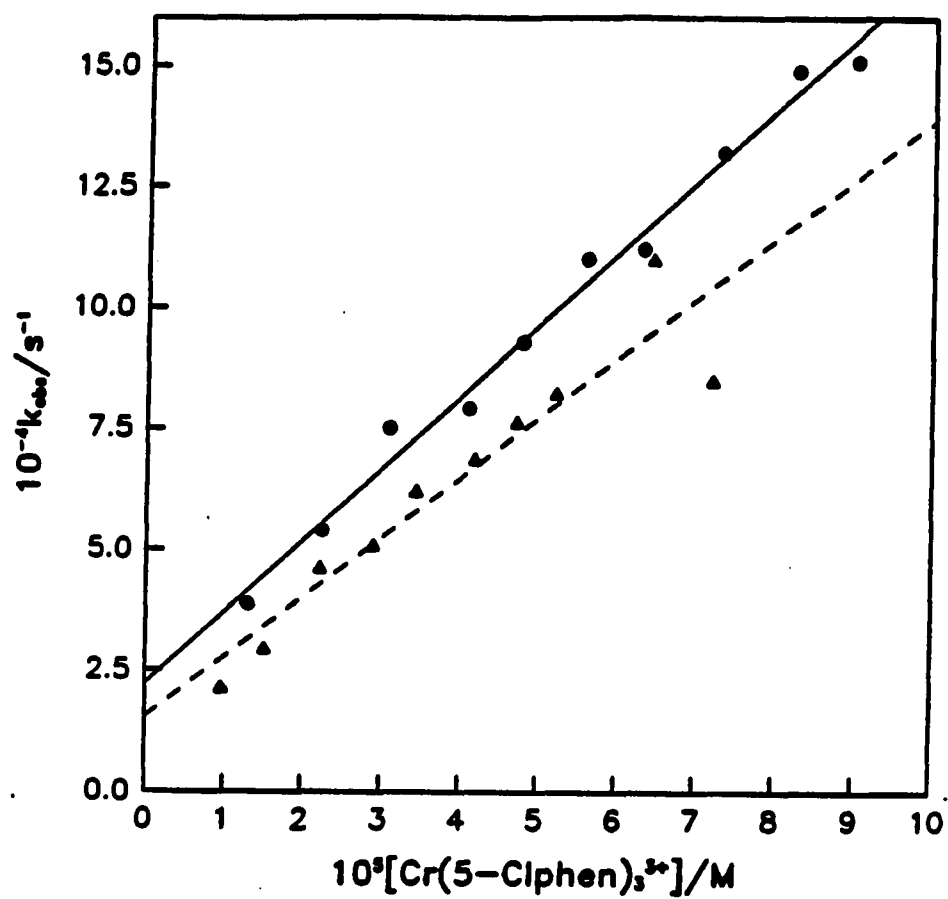


Figure I-9. The plot of the observed rate constant for the loss of the secondary transient produced after the quenching of $^*Cr(Clphen)_3^{3+}$ by oxalate(▲) and $EDTA^{2-}$ (●) versus the ground state concentration at $(23 \pm 2)^{\circ}C$

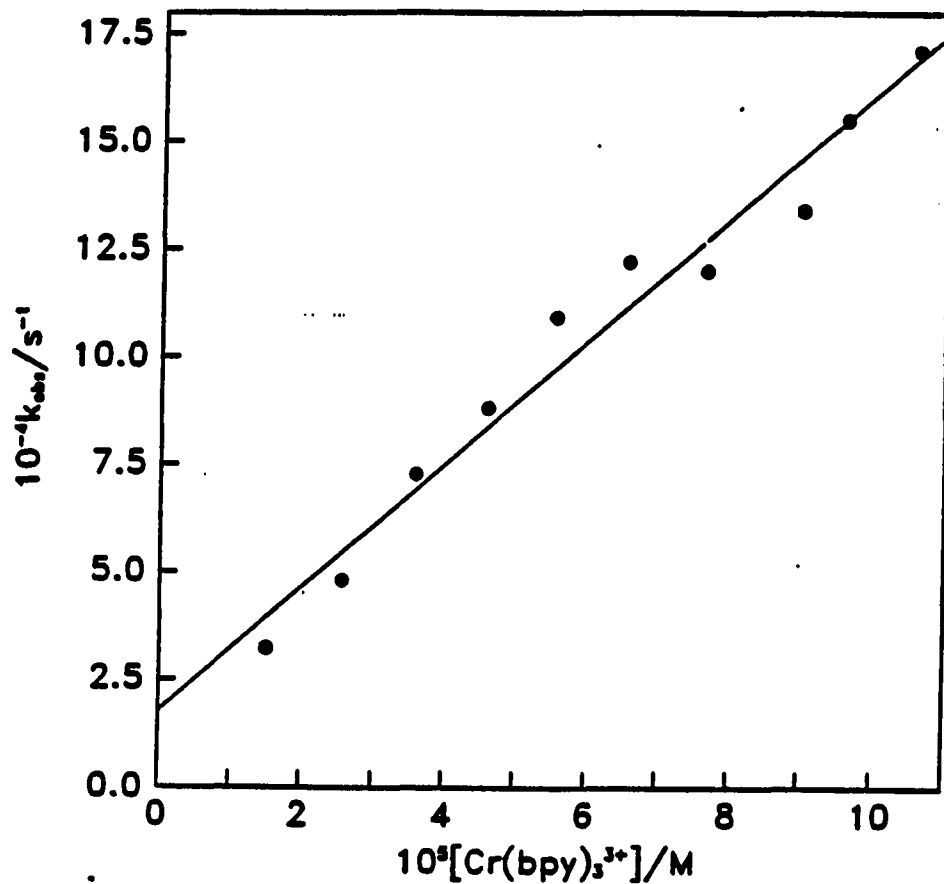


Figure I-10. The plot of the observed rate constant for the loss of the secondary transient produced after the quenching of $^*\text{Cr}(\text{bpy})_3^{3+}$ by EDTA^{2-} versus the ground state concentration at 23°C

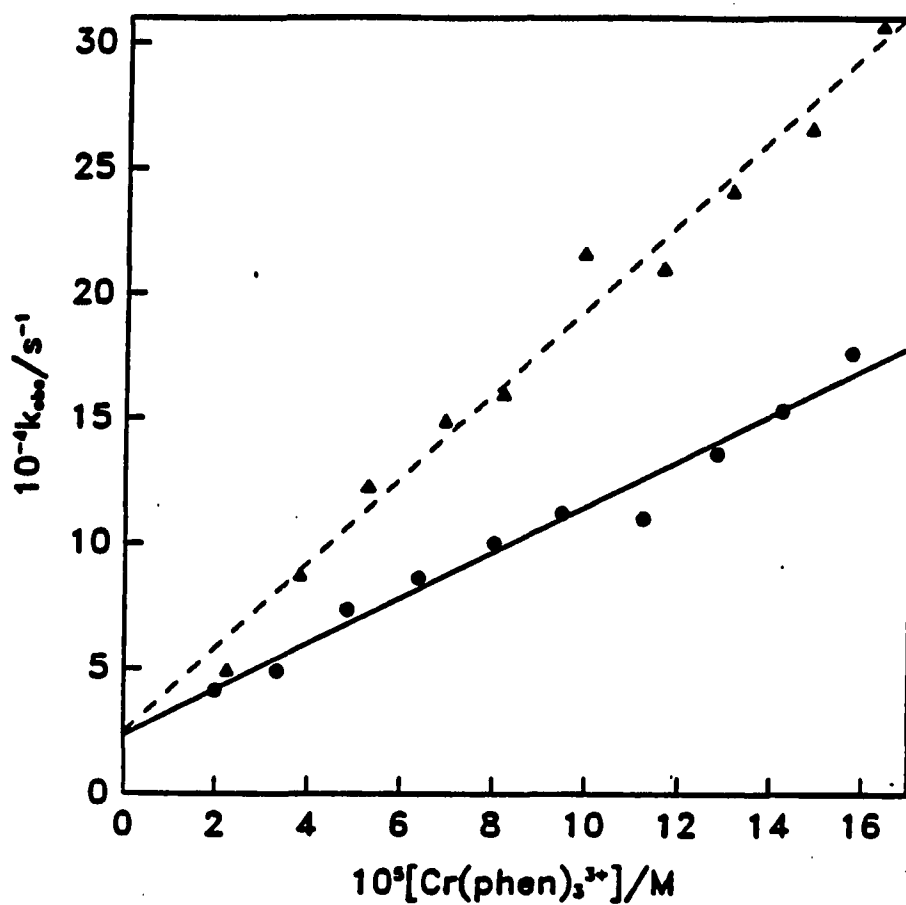


Figure I-11. The plot of the observed rate constant for the loss of the secondary transient produced after the quenching of $^*Cr(phen)_3^{3+}$ by $EDTA^{2-}$ (Δ) and oxalate (\bullet) versus the ground state concentration at $23^\circ C$

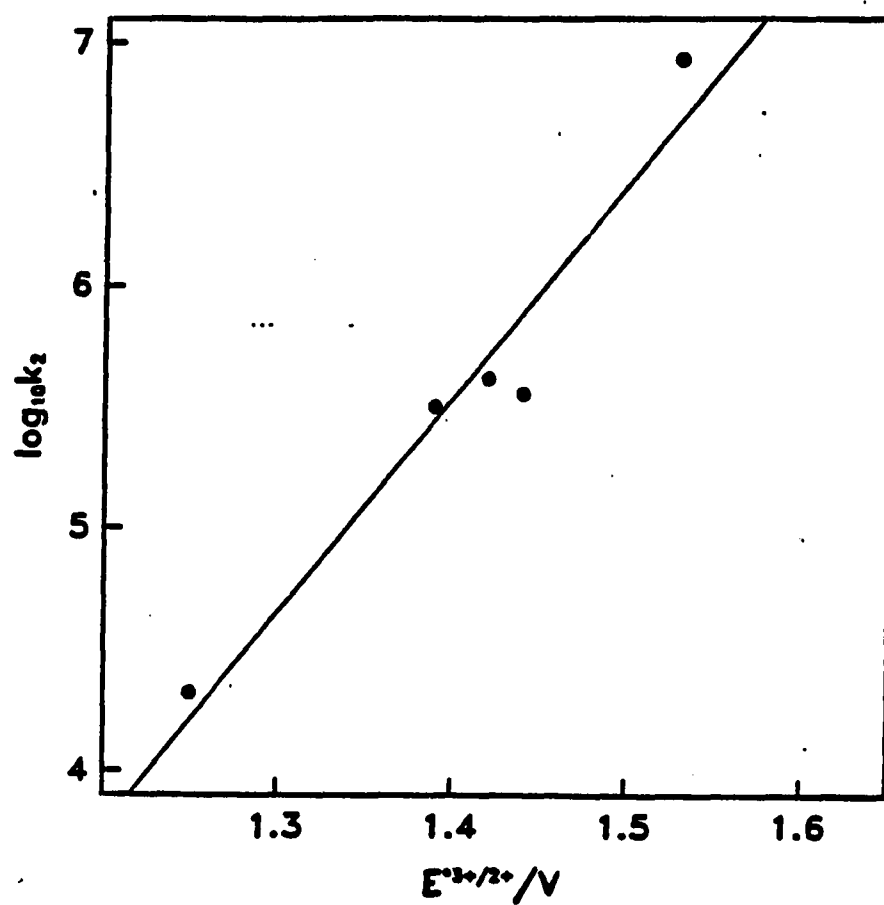


Figure I-12. The plot of the logarithm of k_B versus the excited state potentials ($E^{*3+/2+}$)

REFERENCES

- 1 (a) Balzani, V.; Moggo, L.; Manfrin, M. F.; Bolletta, F.; Lawrence, G. S. Coord. Chem. Rev. 1975, 15, 321;
(b) Balzani, V.; Bolletta, F.; Gandolfi, M. T.; Maestri, M. Top. Curr. Chem. 1978, 75, 1.
- 2 Brunschwig, B.; Sutin, N. J. Am. Chem. Soc. 1978, 100 7568.
- 3 Jamieson, M. A.; Serpone, N.; Hoffman, M. Z.; Bolletta, F. Inorg. Chim. Acta 1983, 72, 247.
- 4 Bolletta, F.; Maestri, M.; Moggi, L.; Jamieson, M. A.; Serpone, N.; Henry, M. S.; Hoffman, M. Z. Inorg. Chem. 1981, 22, 2502.
- 5 Serpone, N.; Jamieson, M. A.; Sriram, R.; Hoffman, M. Z. Inorg. Chem. 1981, 20, 3983.
- 6 (a) Bakac, A.; Zahir, K.; Espenson, J. H. J. Am. Chem. Soc. 1988, 110, 5059; (b) Simmons, C. A.; Bakac, A.; Espenson, J. H., submitted for publication.
- 7 Konig, E.; Herzog, S. J. Inorg. Nucl. Chem. 1970, 32, 585.
- 8 Serpone, N.; Jamieson, M. A.; Henry, M. S.; Hoffman, M. Z.; Bolletta, F.; Maestri, M. J. Am. Chem. Soc. 1979, 101, 2907.
- 9 Bakac, A.; Espenson, J. H.; Lovric, J.; Orhanovic, M.; Inorg. Chem. 1987, 26, 4096.
- 10 Melton, J. D.; Espenson, J. H.; Bakac, A. Inorg. Chem. 1986, 25, 4104.

- 11 Hoselton, M. A.; Lin, C.-T; Schwarz, H. A.; Sutin, N.
J. Am. Chem. Soc. 1978, 100, 2383.
- 12 Maestri, M.; Bolletta, F.; Moggi, L.; Balzani, V.;
Henry, M. S.; Hoffman, M. Z. J. Am. Chem. Soc. 1978,
100, 2694.
- 13 Serpone, N.; Jamieson, M. A.; Emmi, S. S.; Fuochi,
P. G.; Mulazzani, Q. G.; Hoffman, M. Z. J. Am. Chem.
Soc. 1981, 103, 1091.
- 14 Bakac, A.; Zahir, K.; Espenson, J. H. Inorg. Chem.
1988, 27, 315.
- 15 (a) Simmons, C. A.; Bakac, A.; Espenson, J. H. Inorg.
Chem. (submitted); (b) Huston, P. L.; research in
progress at Ames Lab, Ames, IA.
- 16 Sutin, N. Acc. Chem. Res. 1982, 15, 275.
- 17 Sutin, N. Prog. Inorg. Chem. 1983, 30, 441.
- 18 Endicott, J. F.; Heeg, M. J.; Gaswick, D. G.; Pyke, S.
C. J. Phys. Chem. 1981, 85, 1777.
- 19 Pederson, B. F.; Pederson, B. Acta Chim. Scand. 1964,
18, 1454.
- 20 Simic, M. G.; Hoffman, M. Z.; Cheney, R. R.; Mulazzani,
Q. G. J. Phys. Chem. 1979, 83, 439.
- 21 Hoffman, M. Z.; Simic, M. G. Inorg. Chem. 1973, 12,
2471.
- 22 Mulazzani, Q. G.; Emmi, S.; Roffi, G.; Hoffman, M. Z.
Vol. 5, Lab di Fotochimica e Radiazioni d'Alta Energia,
Rapporto annuale 1973, Bologna Consiglio Nazionale della

- Ricerche, 1974, 111.
- 23 Jamieson, M. A.; Serpone, N. Coord. Chem. Rev. 1981, 39, 121.
 - 24 Pringle, G. E.; Broadbent, T. A. Acta Crystallogr. 1965, 19, 426.
 - 25 Neta, P.; Simic, M.; Hayon, E. J. Phys. Chem. 1969, 73, 4207.
 - 26 Farrington, J. A.; Ebert, M.; Land, E. J.; Fletcher, K. Biochim. Biophys. Acta 1973, 314, 372.
 - 27 Mulazzani, Q. G.; D'Angelantonio, M.; Venturi, M.; Hoffman, M. Z.; Rogers, M. A. J. J. Phys. Chem. 1986, 90, 5347.
 - 28 Howes, K. R.; Pippin, C. G.; Sullivan, J. C.; Meisel, D.; Espenson, J. H.; Bakac, A. Inorg. Chem. 1988, 27, 2932.
 - 29 Sriram, R.; Hoffman, M. Z.; Jamieson, M. A.; Serpone, N. J. Amer. Chem. Soc. 1980, 102, 1754.
 - 30 Jonah, C. D.; Matheson, M. S.; Meisel, D. J. Am. Chem. Soc. 1978, 100, 1449.
 - 31 McWhinnie, W. R.; Miller, J. D.; Adv. Inorg. Chem. Radiochem. 1969, 12, 135.
 - 32 Venturi, M.; Emmi, S.; Fuochi, P. G.; Mulazzani, Q. P. J. Phys. Chem. 1980, 84, 135.
 - 33 Konig, E.; Kremer, S. Chem. Phys. Lett. 1970, 5, 87.
 - 34 Creutz, C. Commun. Inorg. Chem., 1982, 1, 293.

APPENDIX

Table A-1. Rate Constants for the Quenching of the
Excited State of $\text{Cr}(\text{bpy})_3^{3+}$ by Oxalate^a.

$[\text{C}_2\text{O}_4^{2-}]/\text{M}$	$10^{-4} \times k_{\text{obs}}/\text{s}^{-1}$
0.0025	5.53
0.0075	8.16
0.0125	10.8
0.0251	12.1
0.0502	13.7
0.0753	14.5
0.100	15.3
0.151	16.5

^a $[\text{Cr}(\text{bpy})_3^{3+}] = 3.29 \times 10^{-4} \text{ M}$. Ionic strength is not constant.

Table A-2. Rate Constants for the Quenching of the
Excited State of $\text{Cr}(\text{bpy})_3^{3+}$ by Oxalate^a.

$[\text{C}_2\text{O}_4^{2-}]/\text{M}$	$10^{-4} \times k_{\text{obs}}/\text{s}^{-1}$
0.0025	2.26
0.0075	3.30
0.0125	3.58
0.0502	7.16
0.0753	8.46
0.100	9.81
0.151	12.4
0.200	14.5

^a $[\text{Cr}(\text{bpy})_3^{3+}] = 3.29 \times 10^{-4} \text{ M}$. Ionic strength = 1.0 M.

Table A-3. Rate Constants for the Quenching of the
Excited State of $\text{Cr}(\text{bpy})_3^{3+}$ by Oxalate^a.

$[\text{C}_2\text{O}_4^{2-}]/\text{M}$	$10^{-4} \times k_{\text{obs}}/\text{s}^{-1}$
0.0026	2.63
0.0052	3.13
0.0078	3.49
0.0129	4.57
0.0259	5.33
0.0517	7.42
0.102	10.5
0.152	12.5
0.192	14.6
0.237	15.8

^a $[\text{Cr}(\text{bpy})_3^{3+}] = 3.29 \times 10^{-4} \text{ M}$. Ionic strength = 2.0 M.

Table A-4. Rate Constants for the Quenching of the
Excited State of $\text{Cr}(\text{bpy})_3^{3+}$ by Oxalate^a.

$10^4 \times [\text{Cr}(\text{bpy})_3^{3+}]/\text{M}$	$10^{-4} \times k_{\text{obs}}/\text{s}^{-1}$
4.81	18.2
3.20	15.7
1.60	12.5
0.80	10.9
0.48	9.49
0.32	9.05
0.16	7.86
0.08	8.30

^a $[\text{C}_2\text{O}_4^{2-}] = 0.0522 \text{ M}.$

Table A-5. Rate Constants and Calculated Ion-Pairing
 Constants for the Quenching of the Excited
 State of $\text{Cr}(\text{bpy})_3^{3+}$ by Oxalate^a.

$[\text{C}_2\text{O}_4^{2-}]/\text{M}$	$10^{-4} \times k_{\text{obs}}/\text{s}^{-1}$	K_1
0.00	1.96	221.8
0.0013	3.78	105.5
0.0026	4.21	82.6
0.0052	5.09	61.1
0.0104	5.86	42.9
0.0156	6.21	34.2
0.0208	7.07	28.9
0.0260	7.36	25.3
0.0521	7.86	16.6
0.104	8.75	11.0
0.156	9.12	8.8
0.208	9.97	7.5
0.255	10.3	6.8

^a $[\text{Cr}(\text{bpy})_3^{3+}] = 1.60 \times 10^{-5} \text{ M}$. Variable ionic strength.

Table A-6. Rate Constants for the Quenching of the
Excited State of $\text{Cr}(\text{bpy})_3^{3+}$ by Oxalate^a.

$[\text{C}_2\text{O}_4^{2-}]/\text{M}$	$10^{-4} \times k_{\text{obs}}/\text{s}^{-1}$
0.00	2.97
0.0131	3.37
0.0261	4.14
0.0392	4.70
0.0522	4.94
0.0782	6.17
0.104	6.85
0.130	7.94
0.157	8.70
0.183	9.39
0.210	10.0

^a $[\text{Cr}(\text{bpy})_3^{3+}] = 1.60 \times 10^{-5} \text{ M}$. Ionic strength = 0.75 M.

Table A-7. Rate Constants for the Quenching of the
Excited State of $\text{Cr}(\text{bpy})_3^{3+}$ by Oxalate^a.

$[\text{C}_2\text{O}_4^{2-}]/\text{M}$	$10^{-4} \times k_{\text{obs}}/\text{s}^{-1}$
0.00	2.75
0.0131	2.29
0.0261	2.77
0.0392	2.73
0.0522	3.19
0.0782	3.45
0.104	4.06
0.130	4.25
0.157	4.70
0.183	4.87
0.209	5.50

^a $[\text{Cr}(\text{bpy})_3^{3+}] = 1.60 \times 10^{-5} \text{ M}$. Ionic strength = 2.00 M.

Table A-8. Rate Constants for the Quenching of the
Excited State of $\text{Cr}(\text{phen})_3^{3+}$ by Oxalate^a.

$[\text{C}_2\text{O}_4^{2-}]/\text{M}$	$10^{-4} \times k_{\text{obs}}/\text{s}^{-1}$
0.00	0.506
0.0104	1.20
0.0312	1.97
0.0519	3.43
0.104	5.44
0.156	7.35
0.250	10.1

^a $[\text{Cr}(\text{phen})_3^{3+}] = 1.47 \times 10^{-5} \text{ M}$. Ionic strength = 0.75 M.

Table A-9. Rate Constants for the Quenching of the
Excited State of $\text{Cr}(\text{Mephen})_3^{3+}$ by Oxalate^a.

$[\text{C}_2\text{O}_4^{2-}]/\text{M}$	$10^{-4} \times k_{\text{obs}}/\text{s}^{-1}$
0.00	0.417
0.0102	1.12
0.0312	2.17
0.0519	2.82
0.104	4.47
0.156	5.38
0.250	8.37

^a $[\text{Cr}(\text{Mephen})_3^{3+}] = 1.45 \times 10^{-5} \text{ M}$. Ionic strength =
0.75 M.

Table A-10. Rate Constants for the Quenching of the
Excited State of $\text{Cr}(\text{Me}_2\text{bpy})_3^{3+}$ by Oxalate^a.

$[\text{C}_2\text{O}_4^{2-}]/\text{M}$	$10^{-4} \times k_{\text{obs}}/\text{s}^{-1}$
0.00	0.759
0.0312	0.839
0.0519	0.891
0.104	1.08
0.156	1.09
0.250	1.31

^a $[\text{Cr}(\text{Me}_2\text{bpy})_3^{3+}] = 1.45 \times 10^{-5} \text{ M}$. Ionic strength =
0.75 M.

Table A-11. Rate Constants for the Quenching of the
Excited State of $\text{Cr}(\text{Clphen})_3^{3+}$ by Oxalate^a.

$[\text{C}_2\text{O}_4^{2-}]/\text{M}$	$10^{-1} \times k_{\text{obs}}/\text{s}^{-1}$
0.00	1.08
0.0104	10.8
0.0312	27.5
0.0519	40.3
0.104	70.7
0.156	100.
0.250	--

^a $[\text{Cr}(\text{Clphen})_3^{3+}] = 1.49 \times 10^{-5} \text{ M}$. Ionic strength =
0.75 M.

Table A-12. Quantum Yield for the Formation of $\text{Cr}(\text{bpy})_3^{2+}$ by Quenching of the Excited State of $\text{Cr}(\text{bpy})_3^{3+}$ by Oxalate^a.

$10^5 \times [\text{CrL}_3^{3+}] / \text{M}$	$10^6 \times [\text{CrL}_3^{2+}] / \text{M}$	$10^6 \times [^*\text{CrL}_3^{3+}] / \text{M}$	Φ
1.64	3.27	1.90	1.72
4.91	8.05	5.82	1.38
8.18	12.5	9.52	1.31
11.4	16.7	13.9	1.20
16.4	20.7	17.0	1.22
22.9	28.1	23.0	1.22
32.7	33.5	32.7	1.02
42.5	39.5	43.4	0.91
55.5	42.5	49.8	0.85
65.3	49.1	56.3	0.87
81.7	50.1	56.2	0.89
98.0	56.5	63.3	0.89

^a $[\text{C}_2\text{O}_4^{2-}] = 0.100 \text{ M}.$

Table A-13. Quantum Yields for Oxalate Quenching of
 $^*\text{Cr}(\text{Clphen})_3^{3+}, \text{a.}$

$10^5 \times [\text{CrL}_3^{3+}] / \text{M}$	$10^5 \times [\text{CrL}_3^{2+}] / \text{M}$	$10^5 \times [^*\text{CrL}_3^{3+}] / \text{M}$	Φ
2.40	1.10	0.515	2.1
4.80	2.29	1.08	2.1
7.20	3.57	1.74	2.05
9.61	4.80	2.28	2.1
12.0	5.67	2.81	2.0
14.4	7.22	3.46	2.1

$\text{a}[\text{C}_2\text{O}_4^{2-}] = 0.104 \text{ M.}$

Table A-14. Quantum Yields for Oxalate Quenching of
 $^*\text{Cr}(\text{Me}_2\text{bpy})_3^{3+}$, a.

$10^5 \times [\text{CrL}_3^{3+}]/\text{M}$	$10^6 \times [\text{CrL}_3^{2+}]/\text{M}$	$10^6 \times [^*\text{CrL}_3^{3+}]/\text{M}$	Φ
2.56	0.73	1.77	0.41
5.13	1.96	3.01	0.65
7.69	2.54	4.30	0.59
10.3	3.14	6.40	0.49
12.8	4.08	8.22	0.49

a[$\text{C}_2\text{O}_4^{2-}$] = 0.159 M.

Table A-15. Rate Constants for the Loss of the Secondary Transient Produced by the Quenching of the Excited State of $\text{Cr}(\text{Clphen})_3^{3+}$ by Oxalate^a.

$10^5 \times [\text{Cr}(\text{Clphen})_3^{3+}]/\text{M}$	$10^{-4} \times k_{\text{obs}}/\text{s}^{-1}$
0.97	2.16
1.52	2.96
2.22	4.64
2.89	5.10
3.43	6.21
4.18	6.87
4.72	7.63
5.22	8.22
6.44	11.0
7.21	8.50

^a $[\text{C}_2\text{O}_4^{2-}] = 0.156 \text{ M}$.

Table A-16. Rate Constants for the Loss of the Secondary Transient Produced by the Quenching of the Excited State of $\text{Cr}(\text{Clphen})_3^{3+}$ by EDTA^{2-} , a .

$10^5 \times [\text{Cr}(\text{Clphen})_3^{3+}]/\text{M}$	$10^{-4} \times k_{\text{obs}}/\text{s}^{-1}$
1.30	3.88
2.24	5.40
3.09	7.51
4.10	7.91
4.79	9.27
5.60	11.0
6.31	11.2
7.32	13.2
8.26	14.9
9.00	15.1

$a[\text{EDTA}^{2-}] = 0.0515 \text{ M.}$

Table A-17. Rate Constants for the Loss of the Secondary Transient Produced by the Quenching of the Excited State of $\text{Cr}(\text{phen})_3^{3+}$ by Oxalate^a.

$10^5 \times [\text{Cr}(\text{phen})_3^{3+}]/\text{M}$	$10^{-4} \times k_{\text{obs}}/\text{s}^{-1}$
1.99	4.13
3.33	4.90
4.84	7.34
6.37	8.61
8.00	10.0
9.46	11.2
11.2	11.0
12.8	13.6
14.2	15.3
15.7	17.6

^a $[\text{C}_2\text{O}_4^{2-}] = 0.156 \text{ M}.$

Table A-18. Rate Constants for the Loss of the Secondary Transient Produced by the Quenching of the Excited State of $\text{Cr}(\text{phen})_3^{3+}$ by EDTA^{2-} , ^a.

$10^5 \times [\text{Cr}(\text{phen})_3^{3+}]/\text{M}$	$10^{-4} \times k_{\text{obs}}/\text{s}^{-1}$
2.25	4.95
3.81	8.76
5.27	12.3
6.93	14.9
8.17	16.0
9.91	21.6
11.6	21.0
13.1	24.1
14.8	26.6
16.3	30.7

^a $[\text{EDTA}^{2-}] = 0.0515 \text{ M}.$

Table A-19. Rate Constants for the Loss of the Secondary Transient Produced by the Quenching of the Excited State of $\text{Cr}(\text{bpy})_3^{3+}$ by EDTA^{2-} , ^a.

$10^5 \times [\text{Cr}(\text{bpy})_3^{3+}]/\text{M}$	$10^{-4} \times k_{\text{obs}}/\text{s}^{-1}$
1.52	3.23
2.58	4.81
3.59	7.28
4.61	8.80
5.55	10.9
6.56	12.2
7.66	12.0
9.01	13.4
9.59	15.5
10.6	17.1

^a $[\text{EDTA}^{2-}] = 0.0515 \text{ M.}$

**PART II KINETICS AND MECHANISM OF THE REACTIONS
OF ORGANOCHROMIUM COMPLEXES WITH TRIS
(2, 2'-BIPYRIDYL)RUTHENIUM(III) AND
WITH THE EXCITED STATE OF TRIS(POLY-
PYRIDYL)CHROMIUM(III) IONS**

INTRODUCTION

There has been much recent interest in the photochemistry and photophysics of transition metal polypyridine complexes due to the possibility of their use in solar energy conversion systems. The excited state of these compounds are known to undergo useful electron transfer and energy transfer reactions.¹

The doublet excited state (2E) of CrL_3^{3+} complexes have been shown to possess relatively high reduction potentials.² This coupled with the fact that the excited states are somewhat long lived makes it possible to study the electron and energy transfer reactions of the excited state. The lifetime of $^*Cr(bpy)_3^{3+}$ was measured to be 0.11 msec³ while that of $^*Cr(phen)_3^{3+}$ was measured to be between 0.24 msec and 0.42 msec under various conditions.^{3,4,5}

Recently, the quenching of the excited state of chromium polypyridyl complexes by $(H_2O)_5CrR^{2+}$ and $(H_2O)([14]aneN_4)CoR^{2+}$ was studied.⁶ Based on the trend in rate constants for different R groups (primary alkyl < secondary alkyl) and comparison to the rate constants for the reaction of $Ru(bpy)_3^{3+}$ with $(H_2O)_5CrR^{2+}$ it was concluded that quenching occurred via an electron transfer process. However, in the case of the organocobalt complexes, it was postulated that an energy transfer process was operating. This was deduced based on the fact that no correlation was observed between the rate constants for quenching of $^*CrL_3^{3+}$ by $(H_2O)_5CoR^{2+}$ and the rate

constants for the one electron reduction of $\text{Ru}(\text{bpy})_3^{3+}$ by the organocobalt complexes as well as the previous observation that inorganic cobalt complexes $((\text{H}_2\text{O})_5[\text{Co}(\text{N}_4)\text{CoX}]^{2+}; \text{X} = \text{Cl}, \text{Br})$ react efficiently as energy transfer agents.

One possible way of differentiating between electron and energy transfer processes is by determining whether electron transfer products are produced. For example the quenching of $^*\text{Cr}(\text{bpy})_3^{3+}$ by Ti^{3+} 7, Fe^{2+} 8 and $\text{Co}([\text{14}] \text{aneN}_4)^{2+}$ 9 all produce $\text{Cr}(\text{bpy})_3^{2+}$ directly in the quench. The situation is more complicated however with quenching by organotransition metal complexes. It is still true that an electron transfer quench may produce electron transfer products. The possibility now also exists that electron transfer products will be observed even though the mechanism of quenching is energy transfer. For example, in the situation present for the previously mentioned quenching by organocobalt complexes, energy transfer to the organocobalt from the $^*\text{Cr}(\text{bpy})_3^{3+}$ could cause homolysis of the organocobalt. The homolysis products $(\text{Co}([\text{14}] \text{aneN}_4)^{2+}$ and R) could then react with the excited or ground state of $\text{Cr}(\text{bpy})_3^{3+}$ to produce some $\text{Cr}(\text{bpy})_3^{2+}$.

Outer sphere oxidations of organochromium complexes have generally been postulated to produce initially CrR^{3+} which then decomposes resulting in Cr^{3+} and R . Thus in the oxidation of $(\text{H}_2\text{O})_5\text{CrR}^{2+}$ by $\text{Ni}([\text{14}] \text{aneN}_4)^{3+}$ and $\text{Ni}([\text{9}] \text{aneN}_3)^{3+}$ 10, $\text{Ru}(\text{bpy})_3^{3+}$ 11, NO^+ 12 and $^*\text{Cr}(\text{bpy})_3^{3+}$ 6, $(\text{H}_2\text{O})_5\text{CrR}^{3+}$ has been invoked. In a like manner, oxidation of $([\text{15}] \text{aneN}_4)\text{CrR}^{2+}$

by Ce^{4+} , IrCl_6^{2-} and ABTS^- ($\text{ABTS}^{2-} = 2,2'$ -azinobis-(3-ethylbenzthiazoline-6-sulphonate)) is believed to occur via formation of $([\text{15}] \text{aneN}_4) \text{CrR}^{3+}$.¹³ Oxidation is then followed rapidly by homolysis of the oxidized form of the organochromium. Indeed, the homolysis step is so rapid that in the reaction of the pentaquaorganochromium the $(\text{H}_2\text{O})_5\text{CrR}^{3+}$ is not observed and also that kinetic factors originating in the reactions of R are seen.

Oxidation of organometallics has not only been observed for organochromium compounds. Oxidation of tetraalkyl lead, tetraalkyl tin, organocobaloximes, organomercury, iron and nickel organic compounds have all been studied.

The reaction of tetraalkyl lead (methyl and ethyl) compounds with IrCl_6^{2-} was found to proceed via oxidative homolysis.^{14,15} The initial step was postulated to produce R_4Pb^+ and IrCl_6^{3-} and the unstable R_4Pb^+ then underwent homolysis to yield R_3Pb^+ and R. Radicals then reacted with excess IrCl_6^{2-} via a halogen abstraction pathway. That oxidation was a major component of the mechanism was shown by the linearity of the plot of the logarithm of the rate constants obtained for the different tetraalkyl leads studied versus the oxidation potentials of the organolead compounds. That radicals are produced was determined by observation of the esr spectrum of the adduct of the ethyl radical with nitrosoisobutane which was made by reaction of R_4Pb with IrCl_6^{2-} in the presence of nitrosoisobutane. The

decomposition of R_4Pb^+ was noted to be fast as the oxidized organolead species was not observed in the esr.

A similar scheme has been invoked for the reaction of organomercurials with hexachloroiridate(IV).¹⁶ The rate determining electron transfer produces R_2Hg^+ which is followed by homolysis of a mercury-carbon bond. A rate determining electron transfer was proposed based on the similarity of the reactivity trend (methyl < ethyl < 2-propyl < t-butyl) with the trend in the vertical ionization potential and the trend in the frequency of the charge transfer bands produced when tetracyanoethylene was in the presence of the organomercury compounds. The homolysis product (RHg^+) was identified by its NMR spectrum. Esr trapping experiments with tert-butylnitron showed the presence of alkyl radicals. The initial product expected R_2Hg^+ was not observed and no incorporation of bromide in the organic product was found when bromide was added as a potential nucleophilic trapping agent.

Dialkyliron(II)bis(bipyridine) complexes are known to undergo coupling of the organic moieties when induced by the oxidation by such species as Br_2 , $Ce(IV)$, and $IrCl_6^{2-}$.¹⁷ Transient electrochemical techniques were utilized to study the oxidation to the dialkyiron(III) species as well as to the dialkyliron(IV).¹⁸ It was found that the dialkyiron(III) decomposes via homolytic fragmentation yielding products originating from alkyl radicals. The dialkyiron(IV) decomposes to yield coupled dialkyls chiefly.

Square planar nickel complexes (Et_2Nibpy) undergo similar reactions. Biaryls are formed when trans aryl nickel complexes ($\text{Ar}_2\text{Ni}(\text{PEt}_3)_2$) are oxidized by any of several agents.¹⁷ Monoarylnickel(II) complexes ($\text{ArNi}(\text{X})(\text{PEt}_3)_2$) can be treated with such agents as well and produce the coupled arylphosphonium (ArPEt_3^+). The initial nickel product formed when the monoarylnickel is reacted with hexachloroiridate(IV) was postulated to be a Ni(III) species ($\text{ArNiBr}(\text{PEt}_3)_2^+$) based on esr spectral evidence. This intermediate then eliminates the coupled arylphosphonium product.

Oxidation of the tetraalkyl tin species (R_4Sn) via a photochemical reaction with analogues of flavins (3-methyl-10-phenylisoalloxazine or 3-methyl-10-phenyl-5-deaza-isoalloxazine) produced R_4Sn^+ .¹⁹ The R_4Sn^+ then decomposes by a homolysis path to yield the radical R and R_3Sn^+ . Similar (in that R_4Sn^+ is initially produced) is the reaction of R_4Sn with the bipyridine and phenanthroline complexes of iron(III) or with hexachloroiridate(IV).^{20,21}

Oxidation of dialkyl platinum compounds by IrCl_6^{2-} to yield formally the Pt(III), R_2PtL_2^+ ($\text{L} = \text{PMe}_2\phi, \text{P}\phi_3$) has also been studied.²² Whether the final products are Pt(II) or Pt(IV) containing species was found to depend on the alkyl group and the coordinated phosphine. The rate of reaction depends on the donor properties of both R and L ($\text{Et} > \text{Me}$ and $\text{PMe}_2\phi > \text{P}\phi_3$).

Studies on the oxidation of organocobalt complexes by far surpass in number the other organometallic compounds. Even though oxidized forms of organocobalt complexes have been characterized, to date the tetrakis(1-norbornyl)cobalt complex is the only isolable Co(IV) species known.²³ It is prepared from $\text{CoCl}_2 \cdot 1.5\text{THF}$ and 1-norbornyllithium in pentane.²⁴ It has been characterized and appears to be a low spin tetrahedral complex.²⁵ The compound exhibits two reversible electrochemical waves at -0.65 V and -2.02 V (versus ferrocenium/ferrocene) which correspond to $\text{Co}(\text{nor})_4^+/\text{Co}(\text{nor})_4$ and $\text{Co}(\text{nor})_4/\text{Co}(\text{nor})_4^-$.

Many other oxidized forms of organocobalt have been prepared and studied including $\text{RCo}(\text{dmgH})_2^+$ (dmgH₂ is dimethylglyoxime), $\text{RCo}(\text{dpgH})_2^+$ (dpgH₂ is diphenylglyoxime), $\text{RCo}(\text{salen})^+$ (salen is bis(salicylidene)ethylenediamine), $\text{RCo}(\text{acacen})^+$ (acacen is bis(acetylaceton)ethylenediamine) and others.²⁶

The potentials for oxidation of organocobaloximes were determined and the trend in $E_{1/2}$ was found to be in the direction expected of increasing ease of oxidation of the organocobaloximes which is due to the increasing electron donor power of the organic ligand, R.^{27,28} The lifetimes of the oxidized forms decrease in the order: primary alkyl > secondary alkyl > benzyl. Kinetic measurements on the reaction of $\text{RCo}(\text{dmgH})_2$ and IrCl_6^{2-} indicate an equilibrium step between reactants and the initial products, $\text{RCo}(\text{dmgH})_2^+$

and IrCl_6^{3-} which is followed by decomposition of the oxidized organocobalt.^{29,30} Decomposition may occur via nucleophilic attack or in the case of primary alkyls by a pathway including disproportionation of the oxidized organocobalt to yield formally a $\text{RCo}(\text{dmgH})_2^{2+}$ and a $\text{RCo}(\text{dmgH})_2$.

The electrochemical potentials for oxidation of methyl, ethyl, 1-propyl, 1-butyl and 2-propyl cobalt salen complexes as well as some rhodium analogues have been determined.³¹ Addition of nucleophiles (Cl^- or pyridine) was found to result in heterolysis of the metal(IV)-carbon bond.

Esr studies have confirmed the nature of the oxidized organocobalt.^{32,33,34} The oxidized complexes although unstable at room temperature are stable at or below -50°C allowing determination of esr spectra. The results imply the oxidized organocobalt to be an organocobalt(IV) complex rather than a carbonium ion-cobalt(III) complex.

Alkylcobalt(IV) dioximato complexes have also been found to undergo nucleophilic attack by halides as mentioned above. This displacement of cobalt occurs with inversion of configuration at the α -carbon of the alkyl group.^{35,36} The mechanism of nucleophilic displacement has been postulated to proceed via an $\text{S}_{\text{N}}2$ mechanism for dioximato complexes and S_{Ni} for Schiff base compounds.³⁷

Other studies of organocobalt(IV) have been concerned with their preparation and intermediacy in reactions of benzyl cobaloximes with manganese(III) acetate,³⁸ the oxidative

dealkylation of benzyl cobaloximes by thiocyanogen,³⁹ iodine chloride,⁴⁰ Cl_2 or Br_2 ,^{41,42,43} I_2 ,⁴⁴ solvent effects on oxidation⁴⁵ and steric effects.⁴⁶

This study was performed in order to determine the mechanism of quenching of the excited state of chromium polypyridyl complexes by $([\text{15}] \text{aneN}_4) \text{CrR}^{2+}$. An attempt is made to discern whether the process involves energy or electron transfer. Also, an attempt to observe the elusive oxidized organochromium species is made.

EXPERIMENTAL

Materials

Solutions of CrCl_2 and $\text{Cr}(\text{ClO}_4)_2$ were prepared by the method of Samuels⁴⁷ which is a modification of another method reported previously.⁴⁸

The organochromium complexes $\text{L}'\text{CrR}^{2+}$ (where L' is $[\text{15}] \text{aneN}_4$ and $\text{R} = \text{CH}_3, \text{CH}_2\text{CH}_3, \text{CH}_2\text{CH}_2\text{CH}_3, \text{CH}_2(\text{CH}_2)_2\text{CH}_3, \text{CH}(\text{CH}_3)_2, \text{CH}(\text{CH}_3)(\text{CH}_2\text{CH}_3), \text{cyclohexyl}, \text{CH}_2\text{C}_6\text{H}_5, \text{CH}_2\text{C}_6\text{H}_4\text{Br}, \text{CH}_2\text{C}_6\text{H}_4\text{CH}_3$) were prepared using a modification of that previously reported.⁴⁹ Only slight excesses of alkyl halide were added to the $\text{L}'\text{Cr}^{2+}$ solution thus eliminating the need to extract repeatedly with CCl_4 to remove unreacted alkyl halide. The $\text{L}'\text{Cr}\{\text{CH}(\text{CH}_3)(\text{CH}_2\text{CH}_3)\}^{2+}$, $\text{L}'\text{Cr}\{\text{CH}_2\text{C}_6\text{H}_4\text{Br}\}^{2+}$ and $\text{L}'\text{Cr}\{\text{CH}_2\text{C}_6\text{H}_4\text{CH}_3\}^{2+}$ were identified by their UV/Vis absorption spectra.¹³ The other complexes as well as $\text{L}'\text{CrBr}^{2+}$ were likewise characterized.⁴⁹

Chromium metal was obtained from Alfa and the ligand $[\text{15}] \text{aneN}_4$ was purchased from Strem. All alkyl halides except methyl iodide were obtained from Aldrich. The methyl iodide was available from Fischer. All alkyl halides used were the iodides except for 2-butyl bromide and the arylalkyls which were also bromides.

Other chemicals used in this study were obtained from the following sources: $\text{Ru}(\text{bpy})_3\text{Cl}_2 \cdot 6\text{H}_2\text{O}$ (Aldrich), NaClO_4 (Fischer), pyridine (Fischer), N,N -dimethylformamide (Fischer), $\text{FeCl}_3 \cdot 6\text{H}_2\text{O}$ (Fischer).

The polypyridyl chromium complexes were either available from a previous study or made in a manner similar to that before.⁵⁰ The $[\text{Co}(\text{NH}_3)_5\text{Br}](\text{ClO}_4)_2$ was prepared from $[\text{Co}(\text{NH}_3)_5\text{Br}]\text{Br}_2$. The $[\text{Co}(\text{NH}_3)_5\text{py}](\text{ClO}_4)_3$ was prepared by using known methods and characterized by its UV/Vis spectrum.⁵¹ The $[\text{Co}(\text{NH}_3)_5\text{OH}_2](\text{ClO}_4)_3$ was prepared in the standard way.

Preparation and characterization of previously unknown organochromium compounds

The $[\text{15}] \text{aneN}_4\text{Cr}(\text{CH}_2\text{C}_6\text{H}_4\text{CF}_3)^{2+}$, $[\text{15}] \text{aneN}_4\text{Cr}(\text{CH}_2\text{C}_6\text{H}_4\text{F})^{2+}$, $[\text{15}] \text{aneN}_4\text{Cr}(\text{CH}_2\text{C}_6\text{H}_4\text{Cl})^{2+}$, $[\text{15}] \text{aneN}_4\text{Cr}(\text{CH}_2\text{C}_6\text{H}_4\text{OCH}_3)^{2+}$ $[\text{15}] \text{aneN}_4\text{Cr}(\text{CH}_2\text{C}_6\text{H}_4\text{CN})^{2+}$ were prepared by the general method outlined above. They were prepared using the following arylalkyl halides obtained from Aldrich: α' -bromo- α, α, α -trifluoro-p-xylylene, α, p -dichloro-toluene, α -bromo-p-tolunitrile, 4-methoxybenzylchloride, 4-fluorobenzylbromide. An attempt was made to produce $[\text{15}] \text{aneN}_4\text{Cr}(\text{CH}_2\text{C}_6\text{H}_4\text{NO}_2)^{2+}$ using p-nitrobenzylbromide; however, the major products obtained were $[\text{15}] \text{aneN}_4\text{CrBr}^{2+}$ and $[\text{15}] \text{aneN}_4\text{Cr}^{3+}$ as determined from comparison of the spectra to the known spectra of these species.⁴⁹ The major products in the preparation of cyano derivative were also $[\text{15}] \text{aneN}_4\text{CrBr}^{2+}$ and $[\text{15}] \text{aneN}_4\text{Cr}^{3+}$; however, a small amount of the organochromium was also collected. All compounds are para substituted.

The extinction coefficients for the organochromium compounds were determined using the spectrum of each compound

as well as the results of chromium analyses. A portion of the compound was decomposed in base using hydrogen peroxide. The amount of chromate present was then determined at λ 372 nm (ϵ = 4830 M⁻¹cm⁻¹). The results are presented in Table II-1.

Stoichiometry of the reaction of Ru(bpy)₃³⁺ and organo-chromium

The stoichiometry of the reaction of the bromobenzyl chromium complex with Ru(bpy)₃³⁺ was determined under two conditions. A sample of Ru(bpy)₃³⁺ was titrated with [15]aneN₄Cr(CH₂C₆H₄Br)²⁺ and also a sample of the organo chromium was titrated with Ru(bpy)₃³⁺. These titrations essentially give conditions under which the Ru(bpy)₃³⁺ and the [15]aneN₄Cr(CH₂C₆H₄Br)²⁺ are initially in excess, respectively.

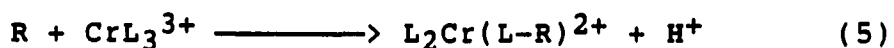
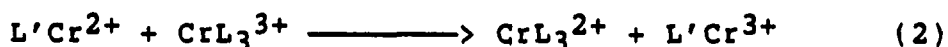
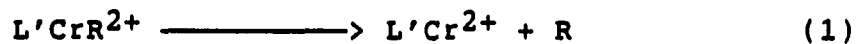
The Ru(bpy)₃³⁺ was produced by reacting Ru(bpy)₃²⁺ in 3 M H₂SO₄ with PbO₂.⁵² The resulting green solution was filtered several times to remove unreacted PbO₂ and PbSO₄. The concentration of Ru(bpy)₃³⁺ was determined spectrophotometrically (λ_{max} 676 nm; ϵ = 409 M⁻¹cm⁻¹).⁵³

The titrations were performed spectrophotometrically. The spectrum of the product Ru(bpy)₃³⁺ was observed and the absorbance at λ 450 nm used as an indication of the amount of Ru(bpy)₃²⁺ produced. Plots of absorbance versus the ratio of reactants yielded two straight line portions whose intersection point is the stoichiometry of the reaction.

A Cary 219 was used for all absorbance measurements.

Kinetics

The kinetics of the quenching of the excited states of the chromium polypyridyl complexes were performed by monitoring the decay of their emission signals (727nm for the bpy complex and 728 nm for all the others).^{2,54} In all cases excess quencher was used (organochromium complex) and solutions contained 0.2 M NaClO₄ and 10 mM HClO₄. The dye laser system used to produce and study the excited states has been described elsewhere.⁵⁵ In all cases Coumarin 460 (1.5×10^{-4} M in methanol) was used as the laser dye. In order to study the quenching of the excited states of CrL_3^{3+} (L = polypyridine) by secondary alkyl chromium complexes (namely cyclohexyl, 2-butyl, 2-propyl) a small amount of Fe^{3+} was added to eliminate the unwanted effects of the presence of any homolysis products formed prior to the flash. Thus the following may occur:



The kinetics of the reaction between RuL_3^{3+} and the organochromiums were performed by use of a photochemical method.¹¹ A solution containing RuL_3^{2+} , the organochromium and either $\text{Co}(\text{NH}_3)_5\text{Br}^{2+}$ or $\text{Co}(\text{NH}_3)_5\text{py}^{3+}$ (or $\text{Co}(\text{NH}_3)_5\text{OH}_2^{3+}$) was flashed at 460 nm (± 20 nm). The flash produced the excited

state of the ruthenium complex which was subsequently quenched by the $\text{Co}(\text{NH}_3)_5\text{Br}^{2+}$ or $\text{Co}(\text{NH}_3)_5\text{py}^{3+}$ via an electron transfer mechanism producing RuL_3^{3+} (and $\text{Co}^{2+} + \text{Br}^- + 5\text{NH}_4^+$ or $\text{Co}^{2+} + \text{pyH}^+ + 5\text{NH}_4^+$). These quenching reactions have been relatively well characterized and it has been determined that $\text{Co}(\text{NH}_3)_5\text{Br}^{2+}$ has a $k_q = 2.1 \times 10^9 \text{ M}^{-1}\text{s}^{-1}$ ⁵⁶ while $\text{Co}(\text{NH}_3)_5\text{py}^{3+}$ has $k_q = (1.7-2.1) \times 10^8 \text{ M}^{-1}\text{s}^{-1}$ ⁵⁷ and $\text{Co}(\text{NH}_3)_5\text{OH}_2^{3+}$ has $k_q = (7.5 - 15) \times 10^7 \text{ M}^{-1}\text{s}^{-1}$.⁵⁸ The reaction between RuL_3^{3+} and $\text{L}'\text{CrR}^{2+}$ was monitored at a wavelength of 450nm, the absorption maximum of RuL_3^{2+} .⁵⁹ The reactions were performed under the pseudo first order condition of excess $[\text{L}'\text{CrR}^{2+}]$. In all cases except the methyl chromium complex did this method prove fruitful. The reaction between $\text{L}'\text{CrMe}^{2+}$ and RuL_3^{3+} is much too sluggish to study by laser flash photolysis and so a conventional method (using a Cary 219 UV/Vis spectrophotometer) was employed to measure the rate of this reaction. The RuL_3^{3+} was produced by mixing an acidic solution of RuL_3^{2+} with PbO_2 .⁵² The resulting green solution was filtered, diluted and used to study the reaction. The amount of RuL_3^{3+} present was determined from its spectrum.⁵³

Spectrum of product and quantum yields

The point by point spectrum of the product of the quenching of the excited state of $\text{Cr}(\text{bpy})_3^{3+}$ by $\text{L}'\text{Cr}(2\text{-Bu})^{2+}$ was produced by determining the final absorbance shortly after the reaction was complete every 10 nm over the range 510 nm to 650 nm.

Quantum yields for the formation of CrL_3^{2+} as defined by the ratio $\phi = [\text{CrL}_3^{2+}]/[*\text{CrL}_3^{3+}]$ were determined for the quenching of the excited state of $\text{Cr}(\text{bpy})_3^{3+}$ by the following organochromium complexes: $\text{L}'\text{Cr}(\text{Et})^{2+}$, $\text{L}'\text{Cr}(1\text{-Pr})^{2+}$, $\text{L}'\text{Cr}(1\text{-Bu})^{2+}$, $\text{L}'\text{Cr}(2\text{-Pr})^{2+}$, $\text{L}'\text{Cr}(2\text{-Bu})^{2+}$. The amount of CrL_3^{2+} produced after the quench was determined from the absorbance at 560 nm ($\epsilon = 4.81 \times 10^3 \text{ M}^{-1}\text{cm}^{-1}$).⁶⁰ The concentration of the excited state was determined from the absorbance at 445 nm found shortly after the laser flash in the absence of quencher (λ 445 nm: $\epsilon = 3 \times 10^3 \text{ M}^{-1}\text{cm}^{-1}$).⁶¹

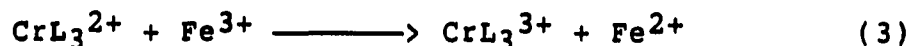
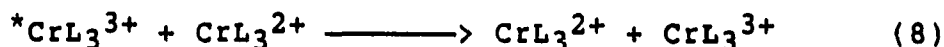
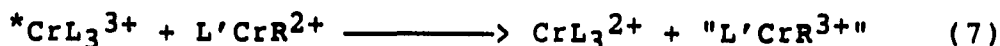
RESULTS

Kinetics of quenching of $^*\text{CrL}_3^{3+}$ by organochromiums

The quenching of the excited state of $\text{Cr}(\text{bpy})_3^{3+}$ by a wide range of organochromium complexes, $\text{L}'\text{CrR}^{2+}$ (where R = methyl, ethyl, 1-propyl, 1-butyl, 2-propyl, 2-butyl, cyclohexyl, benzyl, xylyl, bromobenzyl) were studied. Quenching by $\text{L}'\text{Cr}(\text{2-propyl})^{2+}$ of the excited states of such chromium polypyridyl complexes as $\text{Cr}(\text{Clphen})_3^{3+}$, $\text{Cr}(\text{Mephen})_3^{3+}$ and $\text{Cr}(\text{Me}_2\text{phen})_3^{3+}$ as well as quenching of the polypyridyls $\text{Cr}(\text{Clphen})_3^{3+}$, $\text{Cr}(\text{Mephen})_3^{3+}$, $\text{Cr}(\text{Me}_2\text{bpy})_3^{3+}$ by $\text{L}'\text{CrEt}^{2+}$ were studied. In all cases, the experiments were conducted using a large excess concentration of quencher, and the kinetics were found to obey the rate law:

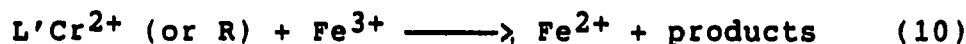
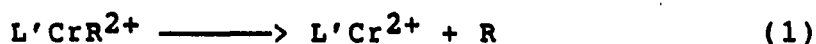
$$\text{Rate} = (a + b[\text{L}'\text{CrR}^{2+}])[^*\text{CrL}_3^{3+}] \quad (6)$$

In the quenching of the excited states of the chromium polypyridyl complexes by secondary organochromium complexes, Fe^{3+} was added to the solution prior to flashing the reaction mixture. The iron serves a two-fold purpose. First, Fe^{3+} eliminates the unwanted effect of CrL_3^{2+} quenching of the excited states. If quenching of $^*\text{CrL}_3^{3+}$ by organochromium occurs by an electron transfer mechanism, then CrL_3^{2+} would be a direct product:



The CrL_3^{2+} formed in the initial quenching may then go on to react with the remaining excited state. The second reaction is known and a lower limit on its rate was set at $5.0 \times 10^9 \text{ M}^{-1}\text{s}^{-1}$.⁸ This quenching manifests itself in terms of non-linear plots of k_{obs} versus $[\text{Q}]$.⁵⁰ However, Fe^{3+} has been shown to be an effective scavenger of CrL_3^{2+} and reacts with a rate constant of $7.3 \times 10^8 \text{ M}^{-1}\text{s}^{-1}$.⁶²

The second purpose of the Fe^{3+} is to eliminate any homolysis products present prior to reaction or to eliminate the effects of homolysis products. A reaction between solutions of $\text{L}'\text{CrR}^{2+}$ and CrL_3^{3+} was observed. This is probably due just to the reaction of the homolysis products $\text{L}'\text{Cr}^{2+}$ and R with CrL_3^{3+} . Adding Fe^{3+} to such solutions prevents the loss of CrL_3^{3+} . The possible scheme then for the effect of Fe^{3+} would consist of the following sequence:



Most of these reactions (or variants of these reactions) are known. The homolysis of organochromium complexes with the macrocyclic ligand [15]aneN₄ has been studied.¹³ It has been shown that homolysis for the secondary organochromiums is fast ($\text{R} = 2\text{-propyl}$, $k_{\text{H}} = 4.9 \times 10^{-4} \text{ s}^{-1}$) while for the primary complexes the rate constants are too slow to measure. This partially explains why Fe^{3+} is not needed when studying the

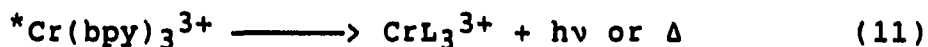
the quenching reactions of the primary complexes. Reactions of R with CrL_3^{3+} and Fe^{3+} are known and have been studied. Organic radicals such as CH_2OH , CH_2CHOH and $(\text{CH}_3)_2\text{COH}$ react with Fe^{3+} with rate constants of 1×10^8 , 3.8×10^8 and 4.5×10^8 respectively.^{63,64,65} Also such reactions occur with CrL_3^{3+} .⁶⁶

The effect of Fe^{3+} is shown in Table II-2. The table contains the results in terms of k_{obs} for the quenching of $^*\text{Cr}(\text{bpy})_3^{3+}$ by $\text{L}'\text{Cr}(2\text{-Propyl})_2^{2+}$ under various conditions. At constant $[\text{Fe}^{3+}]$, it can be seen that there is no variation in k_{obs} with the $[\text{Cr}(\text{bpy})_3^{3+}]$ over the range $(5.36 - 10.7) \times 10^{-5}\text{M}$. This is in accord with the fact that Fe^{3+} eliminates the CrL_3^{2+} quenching slowing the reaction. Apparently, 2.7 mM Fe^{3+} is the minimum of the concentrations studied for shutting off the reaction since any further increase in $[\text{Fe}^{3+}]$ has no effect.

Table II-3 summarizes the values of b (k_q) found in the quenching studies. The individual values of k_{obs} 's and concentrations are listed in the Appendix in Tables A-1 to A-16. Plots showing the trends with varying the chromium polypyridyl and also the organochromium are presented in Figures II-1 through II-3.

Observed rate constants for the quenching of $^*\text{Cr}(\text{bpy})_3^{3+}$ and $^*\text{Cr}(\text{Clphen})_3^{3+}$ by $\text{L}'\text{CrBr}_2^{2+}$ are presented in Tables II-4 and II-5, respectively. From the data shown in Table II-4, it appears $\text{L}'\text{CrBr}_2^{2+}$ is an ineffective quencher for $^*\text{Cr}(\text{bpy})_3^{3+}$.

A variation of $[L'CrBr^{2+}]$ of from 3.04×10^{-4} M to 9.12×10^{-4} M produces no effect on the k_{obs} and indeed the value of k_{obs} is that anticipated for k_0 , the thermal and photochemical unimolecular deactivation of $*Cr(bpy)_3^{3+}$:



This number has been measured previously to be $1.59 \times 10^4 \text{ s}^{-1}$ in 1 M HCl.⁶⁷ In the case of the Clphen complex there appears to be a slight inverse dependence on $[L'CrBr^{2+}]$; however, this may actually be due to the fact that in these runs the acid concentration varied slightly. How the acid would affect the quenching is not known, but it should be pointed out that the rate constants for quenching only vary by ~11% over the $[L'CrBr^{2+}]$ range of 3.04×10^{-4} M to 9.12×10^{-4} M and may reflect experimental error or a real trend due to changes in ionic strength or acidity. Most important to note is that like the $Cr(bpy)_3^{3+}$ case, $Cr(Clphen)_3^{3+}$ excited state is ineffectively quenched by $L'CrBr^{2+}$. One may expect the value of k_{obs} then to be nearly the same as the measured k_0 for $*Cr(Clphen)_3^{3+}$ of $8 \times 10^3 \text{ s}^{-1}$ ⁶⁷; however, as pointed out in Part 1, solvent effects have a more profound effect on the lifetimes of chromium phenanthroline complexes than bipyridine complexes and so although the k_{obs} measured for the bpy complex was nearly the same as the previously reported k_0 , it is not so unreasonable for the k_{obs} for the Clphen complex not to match that for k_0 .^{68,69}

Products of quenching reactions

A point by point spectrum was taken of the products formed after the quenching reaction for the system $^*\text{Cr}(\text{bpy})_3^{3+}$ - $\text{L}'\text{Cr}(2\text{-Butyl})^{2+}$. No intermediates were observed and the only product visible over the wavelength range 510 nm to 650 nm was $\text{Cr}(\text{bpy})_3^{2+}$. The spectrum favorably (Figure II-4) compares to that already known for authentic $\text{Cr}(\text{bpy})_3^{2+}$.⁶⁰

Quantum yields for the formation of CrL_3^{2+} were determined for quenching by several organochromiums, namely ethyl, 1-propyl, 1-butyl, 2-propyl, 2-butyl. These experiments of course were conducted in the absence of $[\text{Fe}^{3+}]$ even though two of the complexes studied were secondary alkyls. Thus for these two complexes one would have to assume the quantum yields are upper limits since there might be some small effects due to the previously mentioned homolysis products and their subsequent reactions. The quantum yields were determined using the ratio $\phi = [\text{CrL}_3^{2+}]/[^*\text{CrL}_3^{3+}]$ where the concentrations were calculated from the solution's absorbance after the flash for $[\text{CrL}_3^{3+}]$ (absence of quencher) ($\lambda_{\text{max}} = 445 \text{ nm}$; $\epsilon = 3 \times 10^3 \text{ M}^{-1}\text{cm}^{-1}$)⁶¹ and the absorbance after the quench for $[\text{CrL}_3^{2+}]$ ($\lambda_{\text{max}} = 560 \text{ nm}$; $\epsilon = 4.81 \times 10^3 \text{ M}^{-1}\text{cm}^{-1}$).⁶⁰ The results are presented in Table II-6 and show the qualitative trend: $\phi_{\text{prim}} < \phi_{\text{sec}}$. It should also be mentioned that in the case of quenching by $\text{L}'\text{Cr}(\text{CH}_2\text{C}_6\text{H}_5)^{2+}$ the amount of CrL_3^{2+} produced is very small.

Stoichiometry of the reaction of $\text{Ru}(\text{bpy})_3^{3+}$ and $\text{L}'\text{CrR}^{2+}$

Two titrations were performed in order to determine the stoichiometry of the reaction of organochromiums with $\text{Ru}(\text{bpy})_3^{3+}$. In the first titration $[\text{15}] \text{aneN}_4\text{Cr}(\text{CH}_2\text{C}_6\text{H}_4\text{Br})^{2+}$ was titrated with $\text{Ru}(\text{bpy})_3^{3+}$ and in the second titration $\text{Ru}(\text{bpy})_3^{3+}$ was titrated with $[\text{15}] \text{aneN}_4\text{Cr}(\text{CH}_2\text{C}_6\text{H}_4\text{Br})^{2+}$. These should nearly represent two limiting situations- one with the organochromium initially in excess, the other where $\text{Ru}(\text{bpy})_3^{3+}$ was in excess.

The plots of the absorbance at 450 nm versus the ratio of the reactants are presented in Figure II-5 and Figure II-6. The plots indicate the stoichiometry is 1:1 approximately under the condition where organochromium is titrated by the ruthenium complex. The stoichiometry of the reaction is approximately 2:1 (two $\text{Ru}(\text{bpy})_3^{3+}$ to one organochromium) for the reverse case--that is where $\text{Ru}(\text{bpy})_3^{3+}$ is titrated with organochromium. This is consistent with the idea that $\text{Ru}(\text{bpy})_3^{3+}$ oxidizes the organochromium and that this oxidation is then followed by homolysis of the organochromium. The homolysis produces $\text{L}'\text{Cr}^{3+}$ and R and so in the case of excess $\text{Ru}(\text{bpy})_3^{3+}$ (when $\text{Ru}(\text{bpy})_3^{3+}$ is titrated with $\text{L}'\text{CrR}^{2+}$) R can react with another $\text{Ru}(\text{bpy})_3^{3+}$. Of course in the case of limiting $\text{Ru}(\text{bpy})_3^{3+}$ only the direct reaction of $\text{Ru}(\text{bpy})_3^{3+}$ and $\text{L}'\text{CrR}^{2+}$ occurs; the R is left to dimerize and disproportionate.

Kinetics of the reaction between $\text{Ru}(\text{bpy})_3^{3+}$ and $\text{L}'\text{CrR}^{2+}$

The reactions were studied under conditions of excess organochromium concentration and the $\text{Ru}(\text{bpy})_3^{3+}$ was generated in situ by the quenching of the excited state of RuL_3^{2+} by either $\text{Co}(\text{NH}_3)_5\text{Br}^{2+}$, $\text{Co}(\text{NH}_3)_5\text{py}^{3+}$ or $\text{Co}(\text{NH}_3)_5\text{OH}_2^{3+}$. The individual runs were fit using a first order treatment and there was a linear dependence on $[\text{L}'\text{CrR}^{2+}]$, thus:

$$\text{Rate} = k[\text{RuL}_3^{3+}][\text{L}'\text{CrR}^{2+}] \quad (12)$$

In all cases the plots of k_{obs} versus $[\text{L}'\text{CrR}^{2+}]$ showed a negligible or slightly negative intercept and so the data were fit through the origin assuming no other pathways for loss of RuL_3^{3+} . Individual values of k_{obs} and their respective concentrations are presented in the Appendix in Tables A-17 to A-34. The rate constants (k) are presented in Table II-7 and a representative sample are plotted in Figure II-7.

The rate constants for the reaction of $\text{L}'\text{Cr}(\text{Ethyl})^{2+}$ with $\text{Ru}(\text{bpy})_3^{3+}$ in the presence of $\text{Co}(\text{NH}_3)_5\text{py}^{3+}$ and $\text{Co}(\text{NH}_3)_5\text{OH}_2^{3+}$ as well as the rate constant for the reaction of $\text{L}'\text{Cr}(1\text{-Propyl})^{2+}$ with $\text{Ru}(\text{bpy})_3^{3+}$ in the presence of $\text{Co}(\text{NH}_3)_5\text{py}^{3+}$ were also determined. The values of the observed rate constants and their respective $[\text{L}'\text{CrR}^{2+}]$ are presented in the Appendix Tables A-27 to A-29. As can be seen in Table II-7 the rate constants obtained for the ethyl chromium reaction are within experimental error no different than the result for the reaction in the presence of $\text{Co}(\text{NH}_3)_5\text{Br}^{2+}$. In the case of the

1-propyl chromium reaction the ratio of the rate constant where $\text{Co}(\text{NH}_3)_5\text{py}^{3+}$ was present to that where $\text{Co}(\text{NH}_3)_5\text{Br}^{2+}$ was present was approximately 1.4. These ratios will be used to determine an approximate lifetime for the proposed oxidized organochromium intermediate.

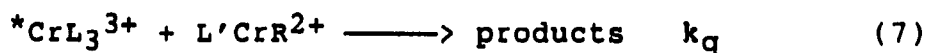
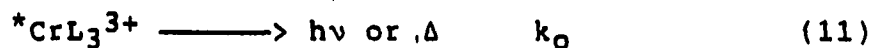
DISCUSSION

Kinetics of the quenching of $^*\text{CrL}_3^{3+}$ by $\text{L}'\text{CrR}^{2+}$

The quenching of the excited state of CrL_3^{3+} complexes by the organochromium complexes appears to obey the rate law:

$$-d[^*\text{CrL}_3^{3+}]/dt = k_q[^*\text{CrL}_3^{3+}][\text{L}'\text{CrR}^{2+}] + k_o[^*\text{CrL}_3^{3+}] \quad (13)$$

In the presence of excess organochromium, plots of the logarithm of the emission versus time are linear for at least three half lives. Plots of the observed rate constant versus the organochromium complex were linear indicating a first order dependence on the organochromium complex (see Figure II 1). The second order rate constants are presented in Table II-3. The plots of k_{obs} versus $[\text{L}'\text{CrR}^{2+}]$ had intercepts which indicates the presence of an organochromium independent pathway for the loss of the excited state. This organochromium independent pathway corresponds to the thermal and photochemical loss of the excited state. Thus the loss of the excited state can be summarized by the equations:



The products of the quenching of the excited state of $^*\text{CrL}_3^{3+}$ by the organochromium complexes shown in the second equation above will be discussed more fully later. That the intercepts of the plots of k_{obs} versus the $[\text{L}'\text{CrR}^{2+}]$ is k_o can be seen in Table II-8. The previously measured k_o 's are also listed in Table II-8. The values obtained for the k_o 's for the bipyridine and the dimethylbipyridine complexes match within

experimental error those previously determined for almost all the the $L'CrR^{2+}$ used with the exception of the aralkyls. In the case of the aralkyls there is a large variation in the k_0 's; the values range from a low of $5.9 \times 10^3 \text{ s}^{-1}$ for $L'Cr(CH_2C_6H_4Br)^{2+}$ to a high of $33.3 \times 10^3 \text{ s}^{-1}$ for $L'Cr(CH_2C_6H_5)^{2+}$. This variation may be due to the fact that the quenching rate constants (k_q) are largest for the aralkyls and the term $k_q[L'CrR^{2+}]$ may dominate the k_0 to the extent that more error is associated with the k_0 term. The substituted phenanthroline complexes have k_0 's significantly different from those of k_0 's previously measured. This is most likely the result of the sensitivity of the k_0 's which include the ground state quenching phenomena of the phenanthroline complexes to medium effects. This same effect was observed previously in the quenching of $^*CrL_3^{3+}$ ($L =$ bipyridine, phenanthroline and their substituted analogues) by $C_2O_4^{2-}$.⁵⁰

As mentioned earlier the observed rate constants measured for the quenching of $^*CrL_3^{3+}$ by a particular $L'CrR^{2+}$ were directly proportional to the $[L'CrR^{2+}]$ indicating a first order dependence on the organochromium concentration. Non-linear-least-squares analysis of the data was performed to determine the second order quenching rate constant from the k_{obs} dependence on $[L'CrR^{2+}]$ and these values are presented in Table II-3. The potentials for the $^*CrL_3^{3+}/CrL_3^{2+}$ couple are: bpy, 1.44 V; Clphen, 1.53 V; Mephen, 1.39 V; Me₂bpy, 1.25 V;

Me₂phen, 1.23 v.² There are two sets of quenching rate constants in which the organochromium used was the same (L'Cr(i-Propyl)²⁺ and L'Cr(Ethyl)²⁺) while the chromium polypyridyl complex was varied (thus varying the potential of the reaction). Figure II-8 is a graph of the logarithm of k_q versus the ${}^*\text{CrL}_3^3+/\text{CrL}_3^2+$ potential for the two series. From the graph it is apparent that the quenching of the excited states are electron transfer processes. Such dependences of the $\log(k_q)$ on the $E^{\circ}{}_{*3+/2+}$ has been observed before for the quenching of ${}^*\text{CrL}_3^3+$ by oxalate ions,⁵⁰ Ti^{3+} ,⁷ Fe^{2+} ⁸ and implies an electron transfer rate determining step. The slopes of the two lines shown in Figure II-8 are similar (L'Cr(Ethyl)²⁺: slope = 1.7; L'Cr(i-Propyl)²⁺; slope = 2.0) indicating that the quenching by the i-propyl chromium and the ethyl chromium are similar processes.

The reactivity trend when one varies the L'CrR²⁺ using the same ${}^*\text{CrL}_3^3+$ is also presented in Table II-3. The general trend is:

primary alkyl < secondary alkyl < aryl alkyl

This is also consistent with an electron transfer mechanism as seen before in the reactions of $(\text{H}_2\text{O})_5\text{CrR}^{2+}$ with $\text{Ru}(\text{bpy})_3^{3+}$, and $(\text{H}_2\text{O})_5\text{CrR}^{2+}$ with $\text{Ni}(\text{cyclam})^{3+}$. This trend is also that observed in the reaction of L'CrR²⁺ with $\text{Ru}(\text{bpy})_3^{3+}$ (vide infra). All of these reactions are believed to occur via a mechanism in which electron transfer is rate limiting. The similarity in the reactivity order between the reaction of

$^*\text{CrL}_3^{3+}$ with $\text{L}'\text{CrR}^{2+}$ and the reaction of $^*\text{CrL}_3^{3+}$ with $(\text{H}_2\text{O})_5\text{CrR}^{2+}$ is shown in Figure II-9 which is a plot of the $\log(k_q)$ versus the $\log(k_q')$ (where k_q' refers to the latter reaction). Figure II-10 is a similar plot showing the relationship between the quenching reaction of $^*\text{CrL}_3^{3+}$ by $\text{L}'\text{CrR}^{2+}$ and the reaction of $\text{Ru}(\text{bpy})_3^{3+}$ with $(\text{H}_2\text{O})_5\text{CrR}^{2+}$.

Quenching of $^*\text{CrL}_3^{3+}$ by the inorganic complex $\text{L}'\text{CrBr}^{2+}$

Presented in Table II-4 and Table II-5 are the results for the quenching of $^*\text{Cr}(\text{bpy})_3^{3+}$ and $^*\text{Cr}(\text{Clphen})_3^{3+}$ by $\text{L}'\text{CrBr}^{2+}$. It was found that varying the $[\text{L}'\text{CrBr}^{2+}]$ did not change the measured k_{obs} and also the k_{obs} obtained in the $\text{Cr}(\text{bpy})_3^{3+}$ case is similar to the known k_0 (see Table II-8) while as expected the k_{obs} for the $\text{Cr}(\text{Clphen})_3^{3+}$ is slightly higher than its known k_0 (vida supra). Thus $\text{L}'\text{CrBr}^{2+}$, if it does quench $^*\text{Cr}(\text{bpy})_3^{3+}$ does so with $k_q < 5 \times 10^5 \text{ M}^{-1}\text{s}^{-1}$ and so is unobservable at the concentrations used.

Previously, it has been postulated that the inorganic complexes tended to be the more efficient energy transfer quenchers of the excited states.⁶ If this is true then the lack of reactivity of $\text{L}'\text{CrBr}^{2+}$ toward the excited state of the chromium polypyridyl complexes implies that energy transfer if it occurs is a minor component in the quenching of $^*\text{CrL}_3^{3+}$ by the organochromiums.

Quantum yields and the spectrum of the initial product

A point-by-point absorbance spectrum of the product formed after the quenching of $^*\text{Cr}(\text{bpy})_3^{3+}$ by $\text{L}'\text{Cr}(2\text{-Butyl})^{2+}$

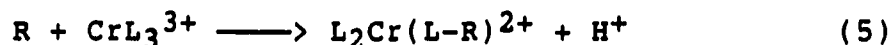
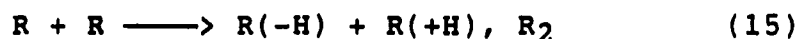
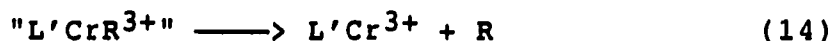
was taken and is shown in Figure II-4. The trend in absorbance with wavelength is that expected for $\text{Cr}(\text{bpy})_3^{2+}$ with peaks near 560 nm and 640 nm.⁶⁰ This indicates that electron transfer products are made somewhere in the course of the reaction--whether by direct rate limiting electron transfer or and electron transfer step following rate limiting energy transfer is not known.

The quantum yields for formation of $\text{Cr}(\text{bpy})_3^{2+}$ were determined for quenching $^*\text{Cr}(\text{bpy})_3^{3+}$ by $\text{L}'\text{Cr}(\text{1-Propyl})^{2+}$, $\text{L}'\text{Cr}(\text{Ethyl})^{2+}$, $\text{L}'\text{Cr}(\text{1-Butyl})^{2+}$, $\text{L}'\text{Cr}(\text{2-Propyl})^{2+}$ and $\text{L}'\text{Cr}(\text{2-Butyl})^{2+}$. The amounts of $\text{Cr}(\text{bpy})_3^{2+}$ follow the general trend:

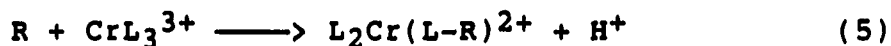
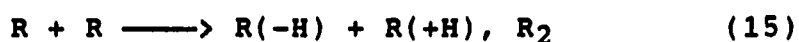
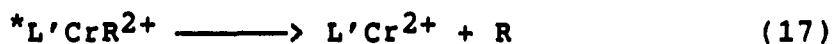
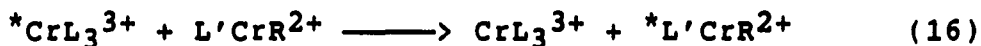
primary alkyl < secondary alkyl

This agrees qualitatively with what one would expect from the values of the k_q 's. The secondary alkyls quench more rapidly and so can produce more CrL_3^{2+} before the excited state becomes depleted via the deactivation pathway.

The maximum quantum yield (approximately 1) is obtained for the reaction of $^*\text{Cr}(\text{bpy})_3^{3+}$ with $\text{L}'\text{Cr}(\text{2-Butyl})^{2+}$; this is also the fastest of those used for the quantum yield studies. It was however, expected that the quantum yields would reach a limiting value of 2.0. This could come about if the following mechanism were operative:

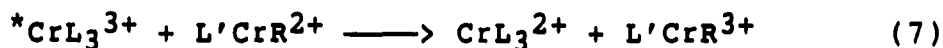


Thus for the mechanism above each time a quench occurs it produces directly a CrL_3^{2+} . Later after decomposition of the unstable $\text{L}'\text{CrR}^{3+}$ another mole of CrL_3^{2+} is formed. An alternative may be an energy transfer process as outlined below:



In this energy transfer scheme a quantum yield of 2.0 would also be expected as the maximum limit. It is known that CrL_3^{3+} reacts with radicals (R).⁶⁶ Also it has been observed that $\text{L}'\text{Cr}^{2+}$ reacts with CrL_3^{3+} on a stopped-flow time scale.

One possibility to explain the lack of ability to reach the theoretical quantum yield maximum concerns the possibility of back electron transfer. Many things which quench the excited state of CrL_3^{3+} produce species which react with each other to produce the ground states of the original species. For example both Fe^{2+} and $\text{Co}(\text{cyclam})^{2+}$ quench the excited state of $\text{Cr}(\text{bpy})_3^{3+}$ to make the electron transfer products $\text{Cr}(\text{bpy})_3^{2+}$ and either Fe^{2+} ⁸ or $\text{Co}(\text{cyclam})^{3+}$.⁹ This is then followed by the return electron transfer using up $\text{Cr}(\text{bpy})_3^{2+}$ to make $\text{Cr}(\text{bpy})_3^{3+}$ and either Fe^{2+} or $\text{Co}(\text{cyclam})^{2+}$. Thus the possibility may exist for:





Another possibility which exists is that the oxidized organochromium is somewhat stable. Thus after the initial quench CrL_3^{2+} and $\text{L}'\text{CrR}^{3+}$ are produced, a second mole of $\text{Cr}(\text{bpy})_3^{2+}$ is not observed.

It seems, however, more probable that both of the above processes are operating thus accounting for the low quantum yields (Et, 1-Pr, 1-Bu) as well as the maximum yield of 1.0 (2-Bu).

Reaction of $\text{Ru}(\text{bpy})_3^{3+}$ with $\text{L}'\text{CrR}^{2+}$

The reactions of $\text{Ru}(\text{bpy})_3^{3+}$ with $\text{L}'\text{CrR}^{2+}$ were studied for the most part by use of a photochemical method. The $\text{Ru}(\text{bpy})_3^{3+}$ was generated by quenching the excited state of $\text{Ru}(\text{bpy})_3^{2+}$ with $\text{Co}(\text{NH}_3)_5\text{Br}^{2+}$, $\text{Co}(\text{NH}_3)_5\text{OH}_2^{3+}$ or $\text{Co}(\text{NH}_3)_5\text{py}^{3+}$:

$$^*\text{Ru}(\text{bpy})_3^{2+} + \text{Co}(\text{NH}_3)_5\text{Br}^{2+} \longrightarrow \text{Ru}(\text{bpy})_3^{3+} + \text{Co}^{\text{II}} + 5\text{NH}_4^+ \quad (19)$$

The reaction between $\text{Ru}(\text{bpy})_3^{3+}$ and $\text{L}'\text{CrR}^{2+}$ was found to be first order in $[\text{L}'\text{CrR}^{2+}]$ and $[\text{Ru}(\text{bpy})_3^{3+}]$, so:

$$d[\text{Ru}(\text{bpy})_3^{2+}]/dt = k[\text{L}'\text{CrR}^{2+}][\text{Ru}(\text{bpy})_3^{3+}] \quad (20)$$

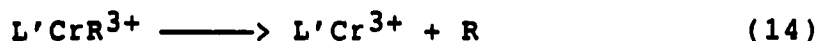
Plots of k_{obs} (determined from formation of $\text{Ru}(\text{bpy})_3^{2+}$ under conditions of excess $\text{L}'\text{CrR}^{2+}$) versus $[\text{L}'\text{CrR}^{2+}]$ were linear with practically zero intercepts. The second order rate constants are summarized in Table II-7. The kinetics as well as the fact that the electron transfer product $\text{Ru}(\text{bpy})_3^{2+}$ is observed suggests the following may happen as the rate determining step:



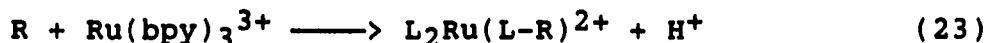
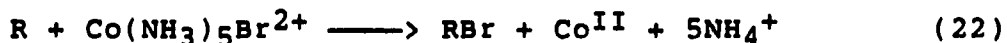
The reactivity trend as the organic group (R) is varied is similar to that for other reactions which are postulated to proceed via an electron transfer rate determining step such as in the reactions of $\text{Ni}(\text{cyclam})^{3+}$ ¹⁰ or $\text{Ru}(\text{bpy})_3^{3+}$ ¹¹ with $(\text{H}_2\text{O})_5\text{CrR}^{2+}$.

Effect of different quenchers

What is the fate of the oxidized organochromium produced by reaction of $\text{L}'\text{CrR}^{2+}$ with $\text{Ru}(\text{bpy})_3^{3+}$? The oxidized organochromium may dissociate to produce radicals:



The radicals may then participate in a variety of reactions including the dimerization/disproportionation of the radicals, reaction with the quencher, $\text{Co}(\text{NH}_3)_5\text{X}^{n+}$ or reaction with $\text{Ru}(\text{bpy})_3^{3+}$:



Radicals are known to react with $\text{Co}(\text{NH}_3)_5\text{Br}^{2+}$ as well as the other quenchers studied. Recently the rate constants for the reactions of ethyl radicals with $\text{Co}(\text{NH}_3)_5\text{Br}^{2+}$ and $\text{Co}(\text{NH}_3)_5\text{OH}_2^{3+}$ were determined to be $2.6 \times 10^6 \text{ M}^{-1}\text{s}^{-1}$ and $< 0.2 \times 10^6 \text{ M}^{-1}\text{s}^{-1}$ respectively.⁷⁰ Although few rate constants for the reactions of radicals with $\text{Co}(\text{NH}_3)_5\text{py}^{3+}$ have been measured they would be expected to be small like $\text{Co}(\text{NH}_3)_5\text{OH}_2^{3+}$ owing to the fact that pyridine is a poor bridging ligand unlike Br.¹¹ Rate constants for reaction of hydroxyalkyl radicals with

$\text{Ru}(\text{bpy})_3^{3+}$ have been determined as well; the radical $\text{CH}_2\text{C}(\text{CH}_3)_2\text{OH}$ reacts with $\text{Ru}(\text{bpy})_3^{3+}$ with $k = (1.3-1.9) \times 10^9 \text{ M}^{-1}\text{s}^{-1}$.^{71,72} $\text{Ru}(\text{bpy})_3^{2+}$ which is present in the reaction solutions here may not react with radicals; only lower limits for the rate constants of the reactions of $\text{CH}_2\text{C}(\text{CH}_3)_2\text{OH}$, CH_2OH , CH_3CHOH have been determined ($< 10^6 \text{ M}^{-1}\text{s}^{-1}$ for all three).⁷³ Self reaction rate constants for radicals generally tend to be near approximately 10^9 (CH_3 : $(1.24-1.6) \times 10^9$ ⁷⁴; Ethyl: $(0.96-1.2) \times 10^9$ ⁷⁵; cyclopentyl: 1×10^9 ⁷⁶).

Based on the above facts and the previous three equations one may predict the following. If $\text{Co}(\text{NH}_3)_5\text{Br}^{2+}$ is the quencher used to produce $\text{Ru}(\text{bpy})_3^{3+}$ then one would expect the rate law of the reaction of $\text{L}'\text{CrR}^{2+}$ with $\text{Ru}(\text{bpy})_3^{3+}$ to be:

$$\text{Rate} = k[\text{L}'\text{CrR}^{2+}][\text{Ru}(\text{bpy})_3^{3+}] \quad (24)$$

The radicals produced after decomposition of $\text{L}'\text{CrR}^{3+}$ are scavenged by the cobalt complex which is in large excess over the radicals and $\text{Ru}(\text{bpy})_3^{3+}$ and $\text{Ru}(\text{bpy})_3^{2+}$.

If, however, $\text{Co}(\text{NH}_3)_5\text{OH}_2^{3+}$ or $\text{Co}(\text{NH}_3)_5\text{py}^{3+}$ are the quenchers used, the rate law becomes for the reaction of $\text{L}'\text{CrR}^{2+}$ with $\text{Ru}(\text{bpy})_3^{3+}$:

$$\text{Rate} = 2k[\text{L}'\text{CrR}^{2+}][\text{Ru}(\text{bpy})_3^{3+}] \quad (25)$$

This occurs because the radicals produced would tend not to be reactive toward $\text{Ru}(\text{bpy})_3^{2+}$, $\text{Co}(\text{NH}_3)_5\text{py}^{3+}$ (or $\text{Co}(\text{NH}_3)_5\text{OH}_2^{3+}$) and so would react with $\text{Ru}(\text{bpy})_3^{3+}$. Thus for every $\text{L}'\text{CrR}^{2+}$ which reacts two $\text{Ru}(\text{bpy})_3^{3+}$ are used up.

This pattern has indeed been observed for the reaction of $(\text{H}_2\text{O})_5\text{CrR}^{2+}$ with $\text{Ru}(\text{bpy})_3^{3+}$ in the presence of $\text{Co}(\text{NH}_3)_5\text{Br}^{2+}$ and $\text{Co}(\text{NH}_3)_5\text{py}^{3+}$.¹¹ The slopes of the graph of k_{obs} versus $[(\text{H}_2\text{O})_5\text{Cr}(\text{Ethyl})^{2+}]$ for the reaction of $(\text{H}_2\text{O})_5\text{Cr}(\text{Ethyl})^{2+}$ with $\text{Ru}(\text{bpy})_3^{3+}$ were in the ratio of approximately 2:1 ($k_{\text{py}} : k_{\text{Br}}$).

In the present circumstances the ratios of the rate constants for the reaction of $\text{L}'\text{Cr}(\text{Ethyl})^{2+}$ with $\text{Ru}(\text{bpy})_3^{3+}$ are approximately 1:1 ($k_{\text{py}} : k_{\text{Br}} = 0.93:1$; $k_{\text{aqua}}:k_{\text{Br}} = 0.98:1$). The ratio is ($k_{\text{py}}:k_{\text{Br}}$) 1.4:1 for the reaction of $\text{L}'\text{Cr}(\text{1-Propyl})^{2+}$ with $\text{Ru}(\text{bpy})_3^{3+}$. This may indicate the possibility of a somewhat stable oxidized organochromium. If the $\text{L}'\text{Cr}(\text{Ethyl})^{3+}$ species has a lifetime longer than it takes for the direct reaction of $\text{L}'\text{Cr}(\text{Ethyl})^{2+}$ with $\text{Ru}(\text{bpy})_3^{3+}$, then by the time radicals are released via decomposition of $\text{L}'\text{CrR}^{2+}$ the $[\text{Ru}(\text{bpy})_3^{3+}]$ has been exhausted. This idea is also confirmed by the results for the 1-propyl complex. This complex reacts at a slower rate with $\text{Ru}(\text{bpy})_3^{3+}$ and thus it may be possible that some radical is released from $\text{L}'\text{Cr}(\text{1-Propyl})^{3+}$ before all the $\text{Ru}(\text{bpy})_3^{3+}$ is consumed, accounting for a ratio of rate constants of 1.4:1.

Lastly, it should be mentioned that R might possibly react with $\text{L}'\text{CrR}^{2+}$ such as is known for organocobalt complexes.⁷⁷ Recently this has been shown not to occur for the $\text{L}'\text{CrR}^{2+}$ complexes.⁷⁸

The reactivity trend

The reactivity of the various organochromiums with $\text{Ru}(\text{bpy})_3^{3+}$ (and $^*\text{Cr}(\text{bpy})_3^{3+}$) is primarily related to the electron withdrawing or donating power of the organic moiety on the chromium. This has been mentioned already and shown for a variety of reactions including the reaction of $\text{Ru}(\text{bpy})_3^{3+}$ with $(\text{H}_2\text{O})_5\text{CrR}^{2+}$.

The electron withdrawing or donating nature of the organic portion of an organochromium is obviously related to the ability of organochromium to be oxidized. Substituents which are electron donating should aid the oxidation of the organochromium while electron withdrawing substituents would be expected to hinder the oxidation of an organochromium. This trend can be shown by observing the correlation between the rate of reaction of $\text{Ru}(\text{bpy})_3^{3+}$ and the organochromiums and the ionization potential of the radicals which are known quantities. Ideally, one would consider the electrochemical oxidation potentials of the organochromiums as a better measure of their ability to be oxidized; however, these values are at present unknown.

The ionization potentials of the carbon centered radicals have been measured by photoelectron spectroscopy and the values are: methyl, 9.84;⁸² ethyl, 8.51;⁸² 1-propyl, 8.69;⁸¹ 1-butyl, 8.64;⁸¹ 2-propyl, 7.69;⁸² 2-butyl, 7.93;⁸⁰ cyclohexyl, 7.66;⁸¹ benzyl, 7.20.⁷⁹ The logarithm of the rate constants versus the

ionization potential are plotted in Figure II-11. As can be seen the trend in ionization potential is:

Me > 1-Pr > 1-Bu > Et > 2-Bu > 2-Pr > c-Hex > Benzyl
and is related to that for the $\text{Ru}(\text{bpy})_3^{3+}$ reaction:

Me < 1-Pr < 1-Bu < Et < 2-Bu < 2-Pr < c-Hex < Benzyl
This is as anticipated; the higher the ionization potential, the more difficult the radical is oxidized and so the less electron donating ability it has. Therefore, a radical with a high ionization energy is less electron donating and so it becomes more difficult to oxidize the chromium centre. The opposite is also true. A radical with a low ionization potential is easier to oxidize and so is more electron donating in the organochromium complex and thus makes the organochromium species easier to be oxidized. This trend represented in the figure is of paramount importance when considering the reactivity of the organochromium with $\text{Ru}(\text{bpy})_3^{3+}$.

The trend in the reactivity with $^*\text{Cr}(\text{bpy})_3^{3+}$ with the various organochromiums is similar. The trend is:

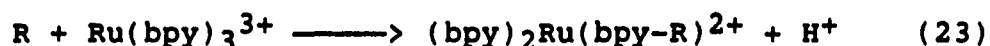
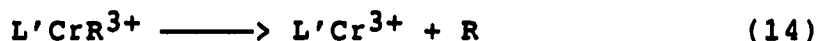
Me < Et < 1-Pr < 1-Bu < 2-Pr < c-Hex < 2-Bu < Benzyl
The general trend of primary alkyl < secondary alkyl < aryl alkyl still holds; however, some of the individual members in each of the subseries are out of order. For example, ethyl and 2-butyl are not in the right locations in terms of their reactivities. The reason for these inconsistencies is not known; however, there may be some relation to the fact that the rate constants for the $^*\text{Cr}(\text{bpy})_3^{3+}$ are so large (they vary

only over a range of 100-fold). Thus while there is a large reactivity range for the $\text{Ru}(\text{bpy})_3^{3+}$ (k : ~ 10 to $\sim 10^9$) the range is more compressed for the $^*\text{Cr}(\text{bpy})_3^{3+}$ (k : $\sim 10^6$ to $\sim 10^9$). The small reactivity range may then dilute the differences between individual members in a subseries (the primary alkyl, secondary alkyl or arylalkyl).

The reactivity trend in terms of the reactions of $\text{Ru}(\text{bpy})_3^{3+}$ with the para substituted benzyl chromium compounds also indicates that the reaction is dependent on the electron withdrawing nature of the organic group. The Hammett sigma values are: CF_3 , +0.54; Br, +0.23; Cl, +0.23; F, +0.06; H, 0.00; CH_3 , -0.17; OCH_3 , -0.27. A plot of the data is shown in Figure II-12. Again one sees that the rate constants for the oxidation of the organochromiums by $\text{Ru}(\text{bpy})_3^{3+}$ is influenced by the electron withdrawing or donating abilities of the organic moieties. The more electron donating (for example OCH_3) groups have larger rate constants while the more electron withdrawing one have smaller values of k (for example CF_3). The value of ρ , the Hammett reaction constant determined from the slope of Figure II-12 is -2.0. This value is very similar to that found (-2.5) from the data obtained for the oxidation of the organocobalt complexes ($\text{RCo}(\text{dmgH})_2$) by IrCl_6^{2-} .³⁰ In this series it would also be expected that the greater the electron donating ability of the organic part, the easier the complex is to be oxidized.

Lifetime of the oxidized organochromium intermediate, $L'CrR^{3+}$

The reaction of $Ru(bpy)_3^{3+}$ with the organochromium species $L'CrR^{2+}$ is thought to produce initially the one electron oxidized species $L'CrR^{3+}$. Indeed the scheme for the reaction is as outlined below:



It has been shown that if the above scheme holds true and if the decomposition reaction of $L'CrR^{3+}$ is a fast process then a factor of two should exist between the measured rate constant for the reaction when performed in the presence of $Co(NH_3)_5Br^{2+}$ and the result obtained in the presence of $Co(NH_3)_5py^{3+}$ or $Co(NH_3)_5OH_2^{3+}$. This was observed in the reaction of $Ru(bpy)_3^{3+}$ with $(H_2O)_5CrR^{2+}$.

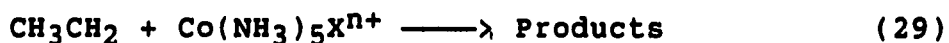
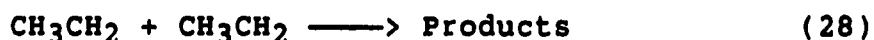
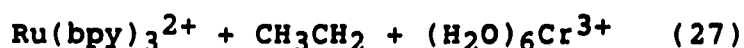
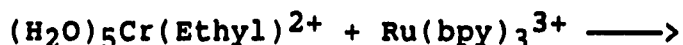
In the present situation, the reaction of $Ru(bpy)_3^{3+}$ with $L'CrR^{2+}$, this factor of two was not observed. The lack of this factor is believed to be due to the stability of the oxidized organochromium species $L'CrR^{3+}$. Previous studies have indicated the possible stability of this species, or alluded to the existence of $L'CrR^{3+}$. In the reaction of ABTS⁻ (ABTS²⁻ is 2,2'-azinobis-(3-ethylbenzthiazoline-6-sulphonate)) with $L'CrR^{2+}$ a kinetic inhibition by [ABTS²⁻] was observed implying an equilibrium process between reactants and the

products ABTS^{2-} and $\text{L}'\text{CrR}^{3+}$.¹³ The reaction of IrCl_6^{3-} with $\text{L}'\text{Cr}(\text{CH}_2\text{C}_6\text{H}_4\text{Br})^{2+}$ was found to be first order under all concentration conditions studied.¹³ If this is truly the case then the $\text{L}'\text{CrR}^{3+}$ must be stable enough such that a second stage ($\text{R} + \text{IrCl}_6^{2-}$) was not observed. In this study an upper limiting value of 57 s^{-1} was determined for the decomposition of $\text{L}'\text{Cr}(\text{CH}_2\text{C}_6\text{H}_4\text{Br})^{3+}$.

Kinetic simulations were performed in an attempt to determine a lifetime for $\text{L}'\text{Cr}(\text{Ethyl})^{3+}$. These simulations were performed on the scheme previously mentioned and assuming the lack of a kinetic factor of two (between the rate constant measured in the presence of $\text{Co}(\text{NH}_3)_5\text{Br}^{2+}$ and that measured in the presence of either $\text{Co}(\text{NH}_3)_5\text{py}^{3+}$ or $\text{Co}(\text{NH}_3)_5\text{OH}_2^{3+}$) was due to the stability of $\text{L}'\text{CrR}^{3+}$.

The rate constants used in the simulations were mostly those previously determined. The rate constant for the direct reaction of $\text{Ru}(\text{bpy})_3^{3+}$ with $\text{L}'\text{CrR}^{2+}$ was taken to be $2.13 \times 10^4 \text{ M}^{-1}\text{s}^{-1}$ which was that measured (see Table II-7). The rate constant for the reaction of ethyl radicals with $\text{Co}(\text{NH}_3)_5\text{Br}^{2+}$ has been recently measured to be $2.6 \times 10^6 \text{ M}^{-1}\text{s}^{-1}$,⁷⁰ and the rate constant for the dimerization/disproportionation of the ethyl radicals was taken to be $1 \times 10^9 \text{ M}^{-1}\text{s}^{-1}$.⁷⁵ The rate constants for the reaction of CH_3CH_2 with $\text{Co}(\text{NH}_3)_5\text{py}^{3+}$ and $\text{Co}(\text{NH}_3)_5\text{OH}_2^{3+}$ are not known but should be small. An upper limit of $2 \times 10^5 \text{ M}^{-1}\text{s}^{-1}$ was inferred from some laser flash photolysis experiments performed on the reaction of the ethyl

radical with $\text{Co}(\text{NH}_3)_5\text{OH}_2^{3+}$.⁷⁰ Indeed, the slowness of the reaction of radicals with $\text{Co}(\text{NH}_3)_5\text{py}^{3+}$ was the cause of the kinetic factor of two in the reaction of $(\text{H}_2\text{O})_5\text{Cr}(\text{Ethyl})^{2+}$ with $\text{Ru}(\text{bpy})_3^{3+}$. For the purposes of the kinetic simulations the rate constants for these reactions were taken to be $1 \times 10^4 \text{ M}^{-1}\text{s}^{-1}$. This number would afford no interference from this pathway in the reaction of $(\text{H}_2\text{O})_5\text{Cr}(\text{Ethyl})^{2+}$ with $\text{Ru}(\text{bpy})_3^{3+}$. The reaction of $\text{Ru}(\text{bpy})_3^{3+}$ with $\text{CH}_2\text{C}(\text{CH}_3)_2\text{OH}$ has been studied and its rate constant determined to be $(1.3 - 1.9) \times 10^8 \text{ M}^{-1}\text{s}^{-1}$.^{71,72} In an attempt to obtain a better estimate of this rate, data obtained from the reaction of $(\text{H}_2\text{O})_5\text{Cr}(\text{Ethyl})^{2+}$ with $\text{Ru}(\text{bpy})_3^{3+}$ was used along with kinetic simulations. The measured rate constant for this reaction is $2.0 \times 10^5 \text{ M}^{-1}\text{s}^{-1}$.¹¹ The scheme used for these simulations is as shown below:



The rate constant for the reaction of ethyl radicals with $\text{Ru}(\text{bpy})_3^{3+}$ was determined to be greater than or equal to $2 \times 10^8 \text{ M}^{-1}\text{s}^{-1}$ which is reasonable when considering the value known for the reaction with $\text{CH}_2\text{C}(\text{CH}_3)_2\text{OH}$. Based on some preliminary results⁸³ it is believed the rate constant should not exceed approximately $10^8 \text{ M}^{-1}\text{s}^{-1}$.

These rate constants along with the data for the $L'Cr(Ethyl)^{2+}$ reaction with $Ru(bpy)_3^{3+}$ (Appendix tables) were then used to determine the rate constant for the decomposition of $L'Cr(Ethyl)^{3+}$. A number on the order of $20\ s^{-1}$ seems appropriate from the simulations to account for the absence of the kinetic factor of two. This is slightly smaller than that determined for the $L'Cr(CH_2C_6H_4Br)^{3+}$; however, this may reflect the stability of the oxidized primary alkyl chromium over the oxidized aryl alkyl chromium.

Simulations were also performed for the reaction of the $L'Cr(1-Propyl)^{2+}$ with $Ru(bpy)_3^{3+}$ in the presence of $Co(NH_3)_5Br^{2+}$ and $Co(NH_3)_5py^{3+}$. The experimental ratio of rate constants was found to be equal to approximately 1.4 and the simulations confirm this result if the decomposition of the oxidized organochromium has a rate constant of approximately $20\ s^{-1}$. The values of the rate constants used in the simulations were the same (except for the $Ru(bpy)_3^{3+} + L'Cr(1-Propyl)^{2+}$ which the experimental value of $3.5 \times 10^3\ M^{-1}s^{-1}$ was used) as those used for the simulations performed above for the ethyl chromium complex. It is not entirely unusual for radicals such as ethyl, 1-propyl and even 1-butyl to react with similar rate constants; indeed, this is the case for the reaction of radicals with $Ni([14]aneN_4)^{2+}$.^{84,85} Simulations performed under these conditions imply that a ratio in the rate constants of 1.48 would be anticipated from the data for the two

different quenchers which is in agreement with the ratio observed.

One may ask why no difference was encountered for the reaction of the ethyl chromium complex in the presence in the different quenchers but was observed for the 1-propyl chromium complex. This is due to the difference in the rate constant for the direct reaction of the organochromium complex with $\text{Ru}(\text{bpy})_3^{3+}$; the ethyl complex reacts almost six times faster than the 1-propyl thus before radicals can be generated to any significant extent the $\text{Ru}(\text{bpy})_3^{3+}$ has been depleted. In the case of the 1-propyl, the reaction is slow enough that the oxidized organochromium can decompose producing radicals which react with $\text{Ru}(\text{bpy})_3^{3+}$ still present (when $\text{Co}(\text{NH}_3)_5\text{py}^{3+}$ is present).

Table II-1. Spectral Parameters for the Various
 $[15]aneN_4Cr(CH_2C_6H_4X)^{2+}$ Complexes^a

X	$\lambda(nm)$ $\epsilon(M^{-1}cm^{-1})$	$\lambda(nm)$ $\epsilon(M^{-1}cm^{-1})$	$\lambda(nm)$ $\epsilon(M^{-1}cm^{-1})$	$\lambda(nm)$ $\epsilon(M^{-1}cm^{-1})$
F	353 1830±140	296 6470±460	274 7540±520	285 -----
Cl	360 2010±280	302 8680±1380	283 9500±1350	246 8170±1060
CF ₃	353 1800±220	300 8330±850	284 8540±910	243 8280±840
OCH ₃	362 1920±340	295 9490±910	282 10110±1040	245 6980±400
CN	371 -----	310 -----	257 -----	210 -----

^aThese should not be regarded as absolute values but rather lower limits due to possible decomposition.

Table II-2. Observed Rate Constants for the Reaction of
 $^*\text{Cr}(\text{bpy})_3^{3+}$ and $\text{L}'\text{Cr}(\text{2-Pr})_2^{2+}$ ^a

$[\text{Fe}^{3+}]/\text{mM}$	$10^5 \times [\text{Cr}(\text{bpy})_3^{3+}]/\text{M}$	$10^{-4} \times k_{\text{obs}}/\text{s}^{-1}$
0.0	5.36	21.9
2.7	5.36	15.1
5.4	5.36	18.4
8.2	5.36	15.9
8.2	8.04	15.5
8.2	10.7	14.9
10.7	5.36	16.5

^a $[\text{L}'\text{Cr}(\text{2-Pr})_2^{2+}] = 1.18 \times 10^{-3} \text{ M}$ and at $(23 \pm 2)^\circ\text{C}$.

Table II-3. Rate Constants for the Quenching of $^*CrL_3^{3+}$
by $L'CrR^{2+}$ ^a

L	R	$10^{-7} \times k_q/M^{-1}s^{-1}$
bpy	Me	0.283 ± 0.050
bpy	Et	0.54 ± 0.06
Clphen	Et	1.28 ± 0.10
Mephen	Et	0.49 ± 0.11
Me ₂ bpy	Et	0.377 ± 0.010
bpy	1-Pr	0.89 ± 0.04
bpy	1-Bu	1.17 ± 0.06
bpy	2-Pr	10.8 ± 0.7
Clphen	2-Pr	19.3 ± 1.5
Mephen	2-Pr	7.4 ± 0.2
Me ₂ phen	2-Pr	4.5 ± 0.4
bpy	2-Bu	12.7 ± 0.5
bpy	c-hex	12.2 ± 0.1
bpy	benzyl	95.5 ± 2.1
bpy	bromobenzyl	141 ± 4
bpy	xylyl	155 ± 5

^aAt $(23 \pm 2)^\circ C$.

Table II-4. Observed Rate Constants for the Quenching of
 $^*\text{Cr}(\text{bpy})_3^{3+}$ by $\text{L}'\text{CrBr}_2^+$ ^a

$10^4 \times [\text{L}'\text{CrBr}_2^+]/\text{M}$	$10^{-3} \times k_{\text{obs}}/\text{s}^{-1}$
9.12	16.3
7.60	16.2
6.08	17.2
4.56	16.8
3.04	16.9 ₅

^a $[\text{Cr}(\text{bpy})_3^{3+}] = 3.16 \times 10^{-5} \text{ M}$ and at $(23 \pm 2)^\circ\text{C}$.

Table II-5. Observed Rate Constants for the Quenching of
 $^*\text{Cr}(\text{Clphen})_3^{3+}$ by $\text{L}'\text{CrBr}^{2+}$ ^a

$10^4 \times [\text{L}'\text{CrBr}^{2+}]/\text{M}$	$10^{-4} \times k_{\text{obs}}/\text{s}^{-1}$
9.12	21.3
7.60	21.8
6.08	23.2
4.56	23.7
3.04	24.0

^a $[\text{Cr}(\text{bpy})_3^{3+}] = 2.31 \times 10^{-5} \text{ M}$ and at $(23 \pm 2)^\circ\text{C}$.

Table II-6. Quantum Yields of Formation of $\text{Cr}(\text{bpy})_3^{2+}$

R	$10^4 \times [\text{L}'\text{CrR}^{2+}]/\text{M}$	$10^5 \times [\text{Cr}(\text{bpy})_3^{3+}]/\text{M}$	Φ
1-Pr	14.0	12.2	0.10
1-Pr	10.5	12.2	0.067
1-Pr	7.00	12.2	0.091
2-Pr	11.5	12.2	0.55
2-Pr	8.65	12.2	0.44
2-Pr	5.77	12.2	0.39
2-Pr	11.5	8.11	0.49
2-Pr	11.5	4.05	0.63
1-Bu	14.7	12.2	0.072
1-Bu	11.0	12.2	0.020
1-Bu	7.35	12.2	0.045
2-Bu	15.5	12.2	0.85
2-Bu	11.6	12.2	1.06
2-Bu	7.75	12.2	1.00
Et	12.8	12.2	0.16
Et	9.63	12.2	0.054

Table II-7. Second Order Rate Constants for the Reaction of $\text{Ru}(\text{bpy})_3^{3+}$ with $\text{L}'\text{CrR}^{2+}$ ^a

R	$k_2/\text{M}^{-1}\text{s}^{-1}$
Me	$(1.4 \pm 0.05) \times 10$
Et	$(2.13 \pm 0.04) \times 10^4$
Et ^b	$(2.04 \pm 0.03) \times 10^4$
Et ^c	$(2.14 \pm 0.12) \times 10^4$
1-Pr	$(3.5 \pm 0.09) \times 10^3$
1-Pr ^b	$(5.10 \pm 0.27) \times 10^3$
1-Bu	$(3.8 \pm 0.09) \times 10^3$
2-Pr	$(4.74 \pm 0.25) \times 10^6$
2-Bu	$(1.42 \pm 0.08) \times 10^6$
c-hex	$(1.18 \pm 0.03) \times 10^7$
p-trifluoromethylbenzyl	$(2.72 \pm 0.11) \times 10^7$
p-fluorobenzyl	$(2.95 \pm 0.03) \times 10^8$
p-chlorobenzyl	$(3.84 \pm 0.21) \times 10^8$
p-bromobenzyl	$(4.27 \pm 0.08) \times 10^8$
p-bromobenzyl ^c	$(4.10 \pm 0.22) \times 10^8$
benzyl	$(5.51 \pm 0.21) \times 10^8$
p-xylyl	$(1.05 \pm 0.02) \times 10^9$
p-methoxybenzyl	$(1.23 \pm 0.04) \times 10^9$

^aAll rate constants measured at $(23 \pm 2)^\circ\text{C}$ and with $\text{Co}(\text{NH}_3)_5\text{Br}^{2+}$ as the quencher unless stated otherwise.

^bQuencher used to produce RuL_3^{3+} was $\text{Co}(\text{NH}_3)_5\text{py}^{3+}$.

^cQuencher used to produce RuL_3^{3+} was $\text{Co}(\text{NH}_3)_5\text{OH}_2^{3+}$.

Table II-8. Rate Constants for the Organochromium
Independent Loss of Excited State (k_0)

CrL_3^{3+}	$\text{L}'\text{CrR}^{2+}$	$10^{-3} \times k_0/\text{s}^{-1}$	$10^{-3} \times k_0^{\text{act}}/\text{s}^{-1}$ a
bpy	Me	15.1	14.3 - 19.6 ^b
bpy	Et	13.3	
Clphen	Et	19.8	5.55 - 7.69 ^c
Mephen	Et	13.0	2.38 - 3.70 ^d
Me_2bpy	Et	5.84	3.23 - 4.76 ^e
bpy	1-Pr	14.9	
bpy	1-Bu	11.1	
bpy	2-Pr	20.5	
Clphen	2-Pr	66.5	
Mephen	2-Pr	24.5	
Me_2phen	2-Pr	32.4	1.75 - 2.94
bpy	2-Bu	12.6	
bpy	c-hexyl	15.1	
bpy	benzyl	33.3	
bpy	Brbenzyl	5.89	
bpy	xylyl	11.9	

^a k_0^{act} refers to literature values.

^bSee reference 5b and 5c.

^cSee reference 3 and 8b.

^dSee reference 3.

^eSee reference 3 and 2.

^fSee reference 3 and 8b.

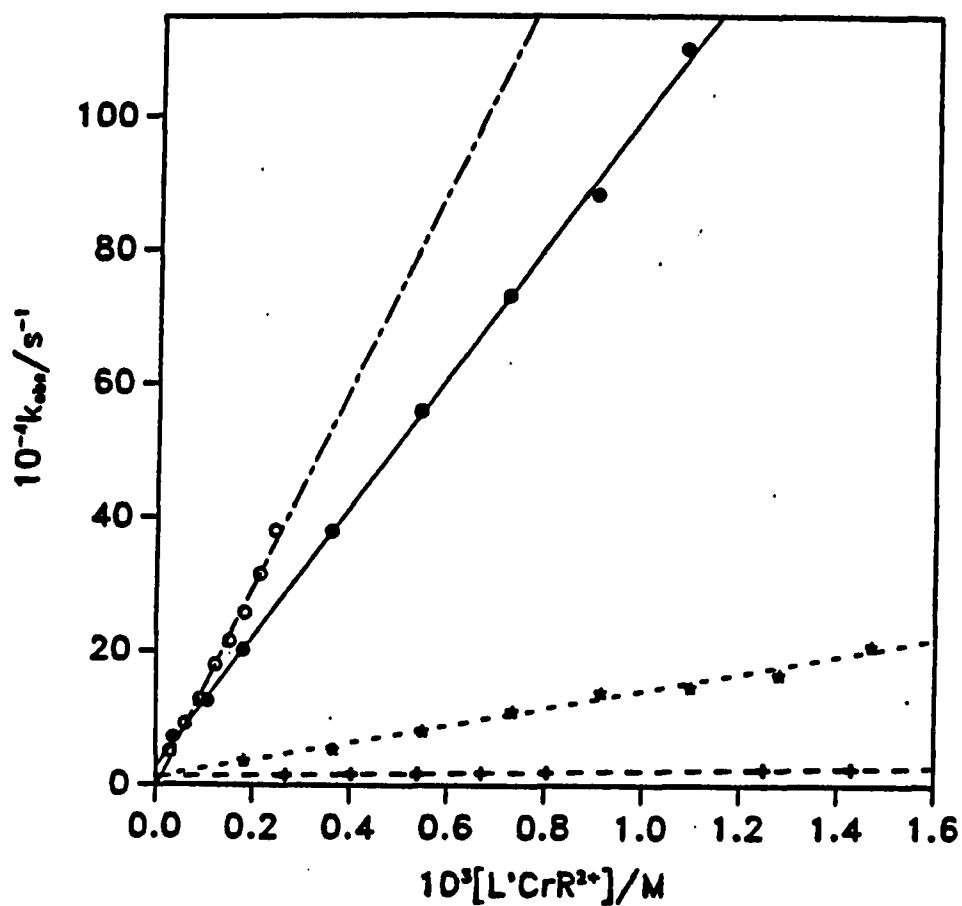


Figure II-1. Quenching of $^*Cr(bpy)_3^{3+}$ by the organochromiums $L'Cr(1-Pr)^{2+}$ (+), $L'Cr(CH_2C_6H_4Br)^{2+}$ (o) and $L'Cr(CH_2C_6H_5)^{2+}$ (●) and $L'Cr(2-Bu)^{2+}$ (*) at $(23 \pm 2)^\circ C$

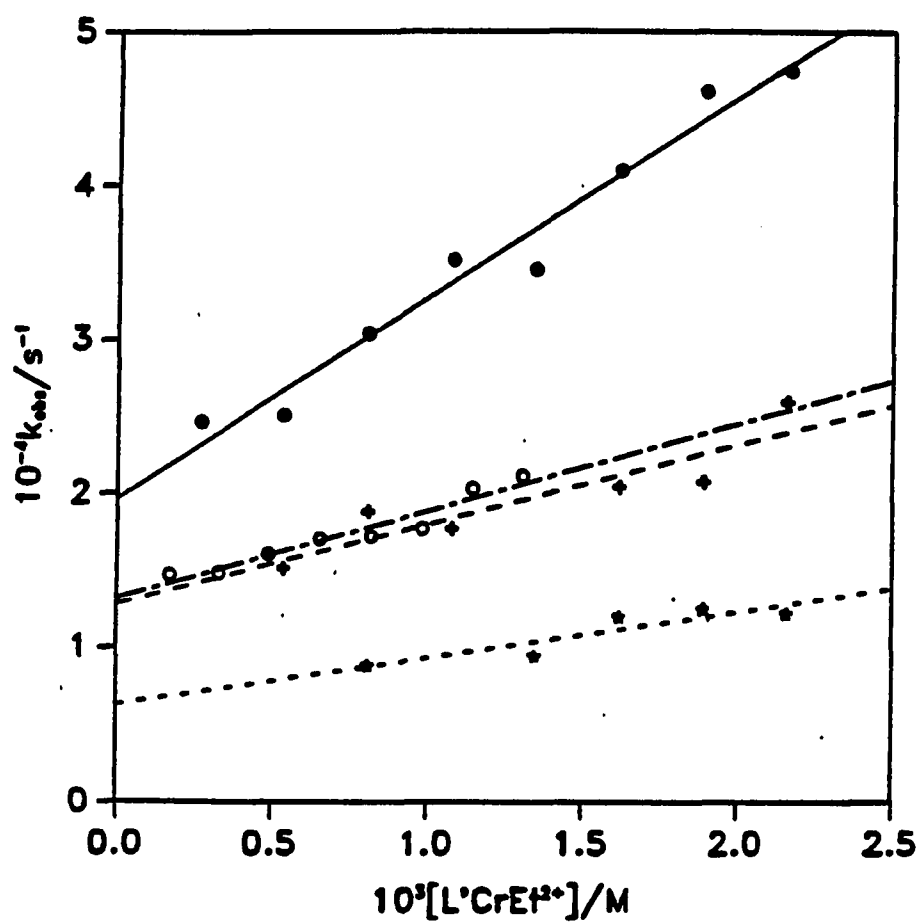


Figure II-2. Quenching of $*CrL_3^{3+}$ by $L'Cr(Et)_2^{2+}$, where L is Clphen (●), bpy (○), Mephen (+) and Me₂bpy (*) at $(23 \pm 2)^\circ C$

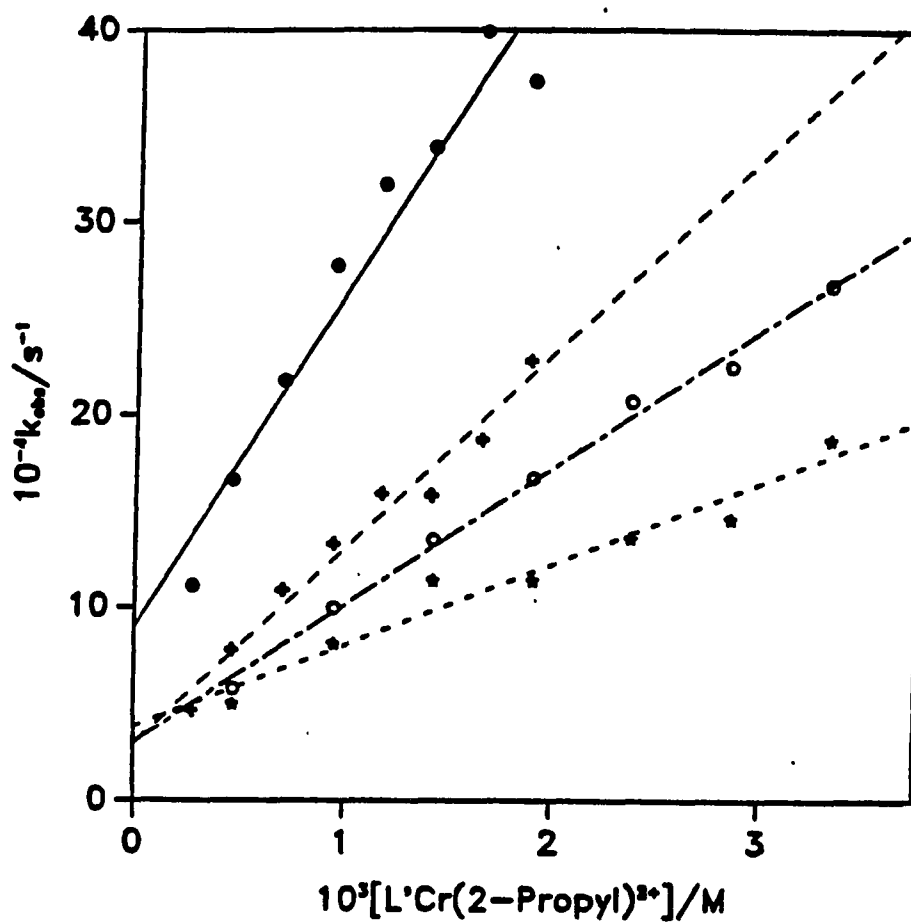


Figure II-3. Quenching of $^*CrL_3^{3+}$ by $L'Cr(2-Pr)_2^{2+}$, where L is Clphen (●), bpy (+), Mephen (○) and Me₂phen (*) at $(23 \pm 2)^\circ C$

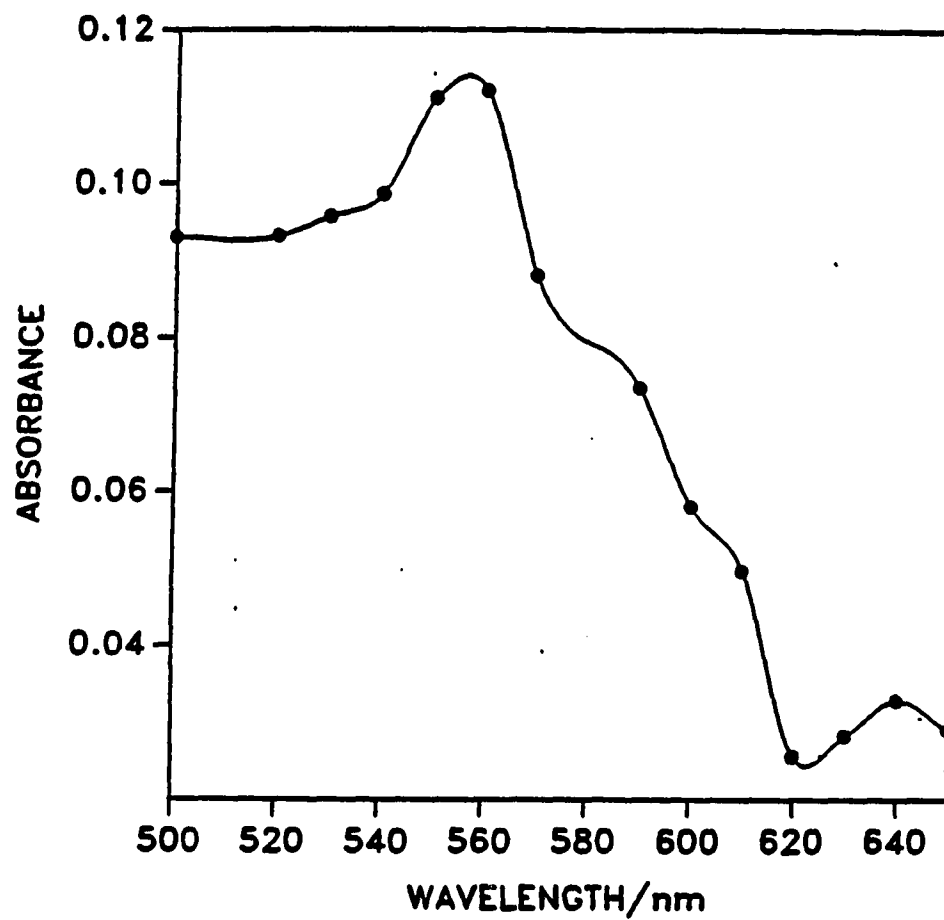


Figure II-4. Final product spectrum for the quenching of $^*\text{Cr}(\text{bpy})_3^{3+}$ by $\text{L}'\text{Cr}(2\text{-Bu})^{2+}$

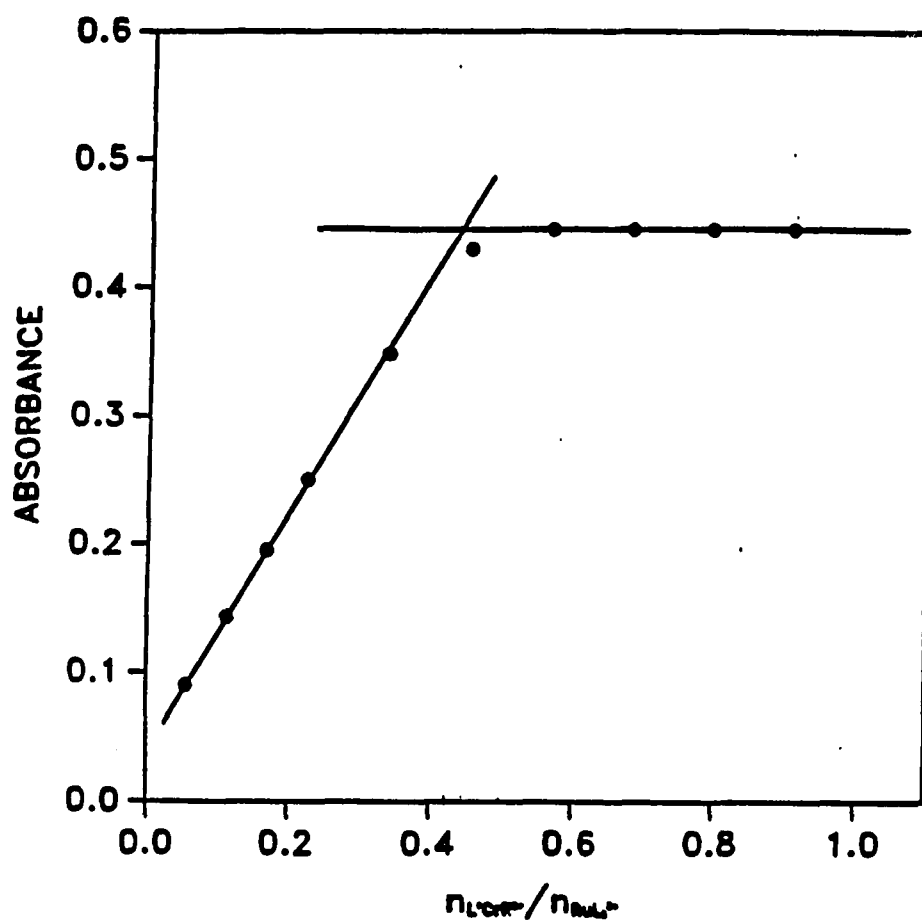


Figure II-5. Plot of the absorbance at 450 nm versus the ratio of reactants for the titration of $\text{Ru}(\text{bpy})_3^{3+}$ by $[\text{15}] \text{aneN}_4\text{Cr}(\text{CH}_2\text{C}_6\text{H}_4\text{Br})^{2+}$

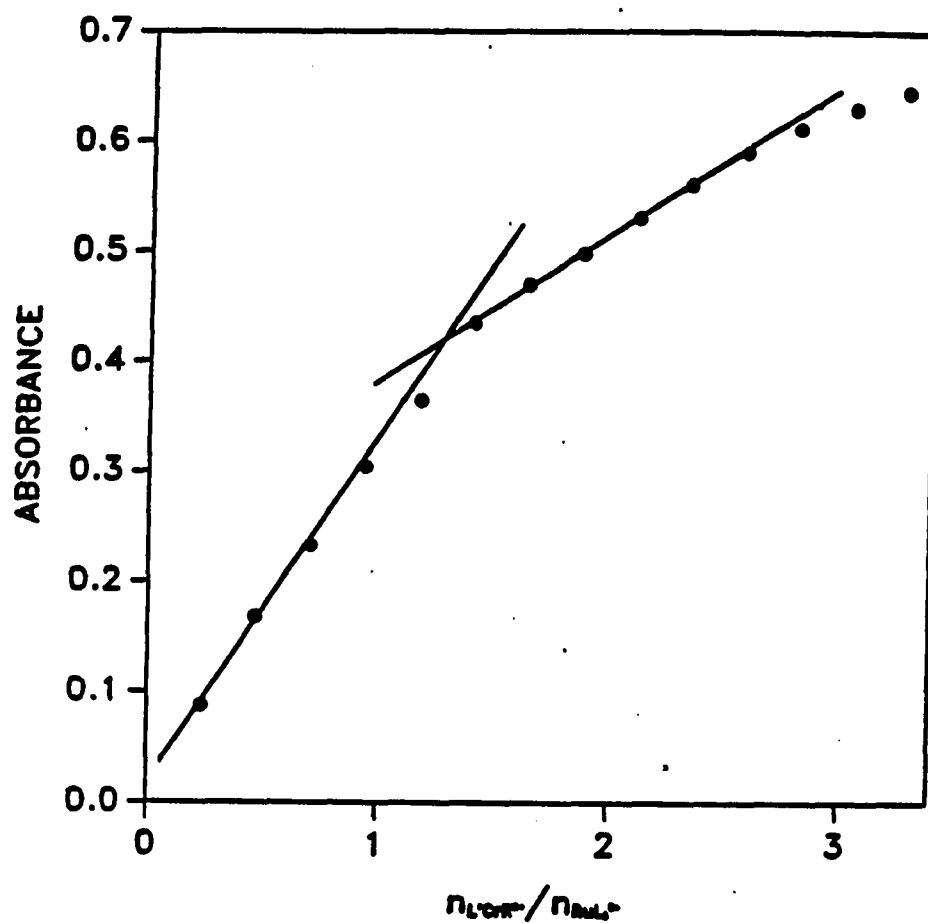


Figure II-6. Plot of the absorbance at 450 nm versus the ratio of reactants for the titration of $[15]aneN_4Cr(CH_2C_6H_4Br)^{2+}$ by $Ru(bpy)_3^{3+}$

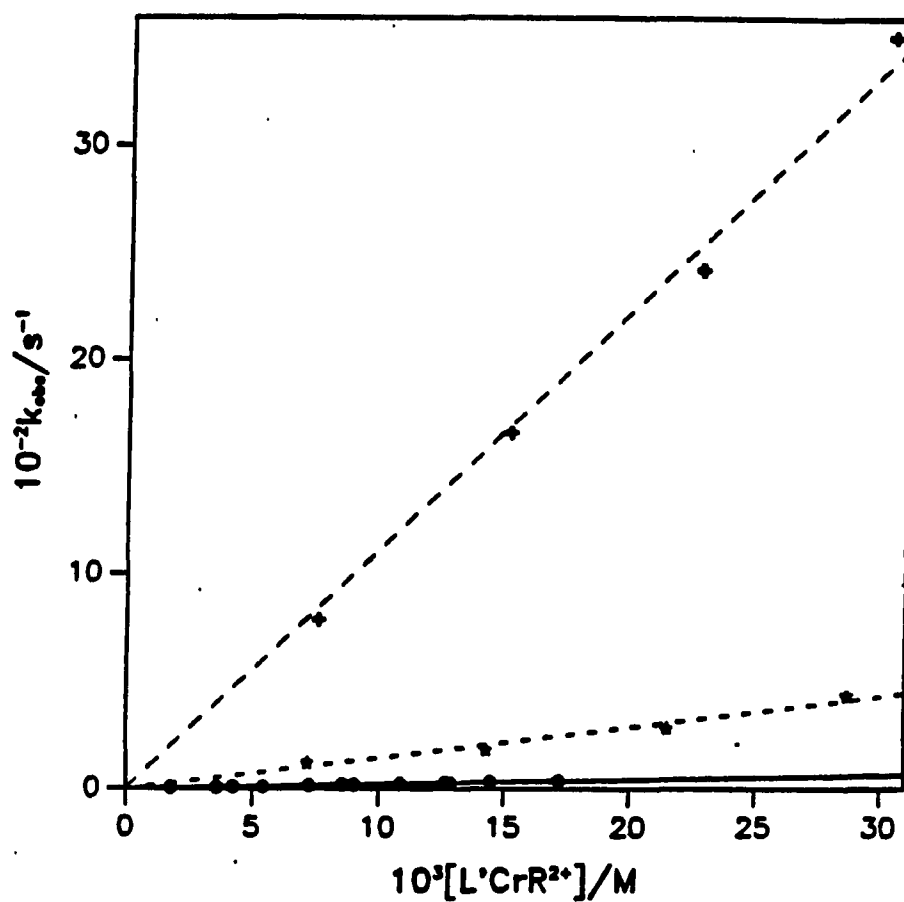


Figure II-7. Plot of k_{obs} versus the organochromium concentration for the reaction of $Ru(bpy)_3^{3+}$ with the organochromiums, $L'Cr(Et)^{2+}$ (\bullet), $L'Cr(2-Bu)^{2+}$ ($*$), $L'Cr(c-Hex)^{2+}$ ($+$) at $(23 \pm 2)^\circ C$

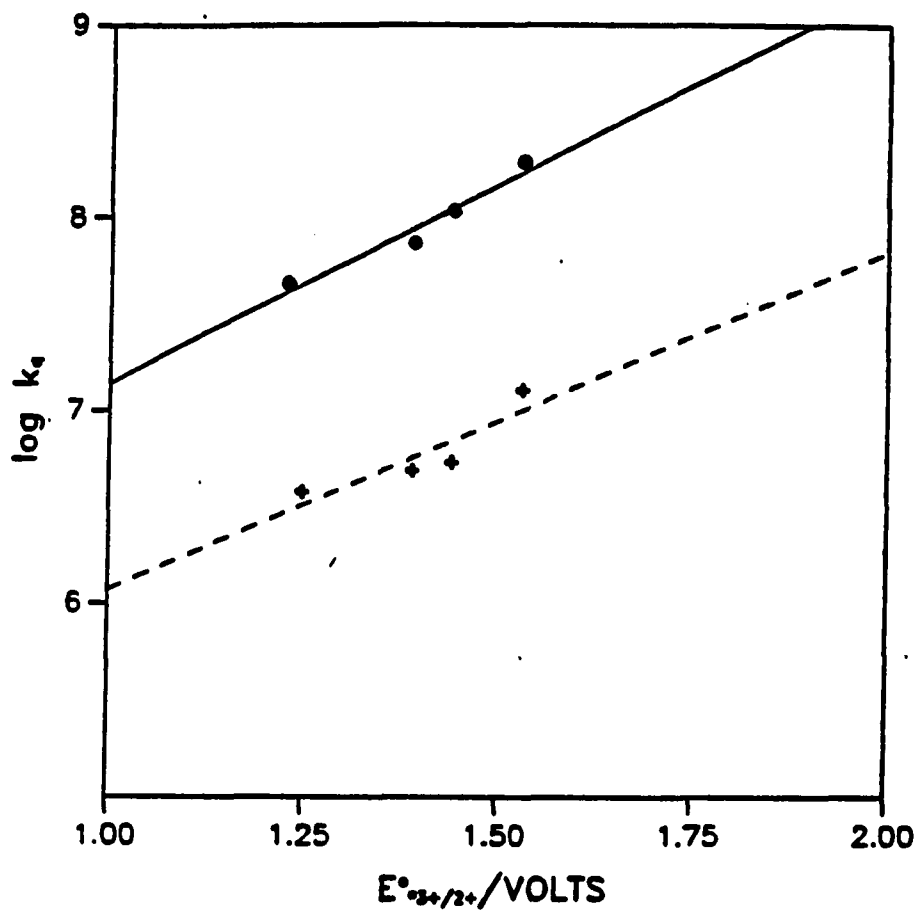


Figure II-8. Plot of $\log(k_q)$ versus $E^\circ_{3+/2+}$ for the reaction of $^*\text{CrL}_3^{3+}$ with $\text{L}'\text{Cr}(\text{Ethyl})^{2+}$ (+) and with $\text{L}'\text{Cr}(2\text{-Propyl})^{2+}$ (●)

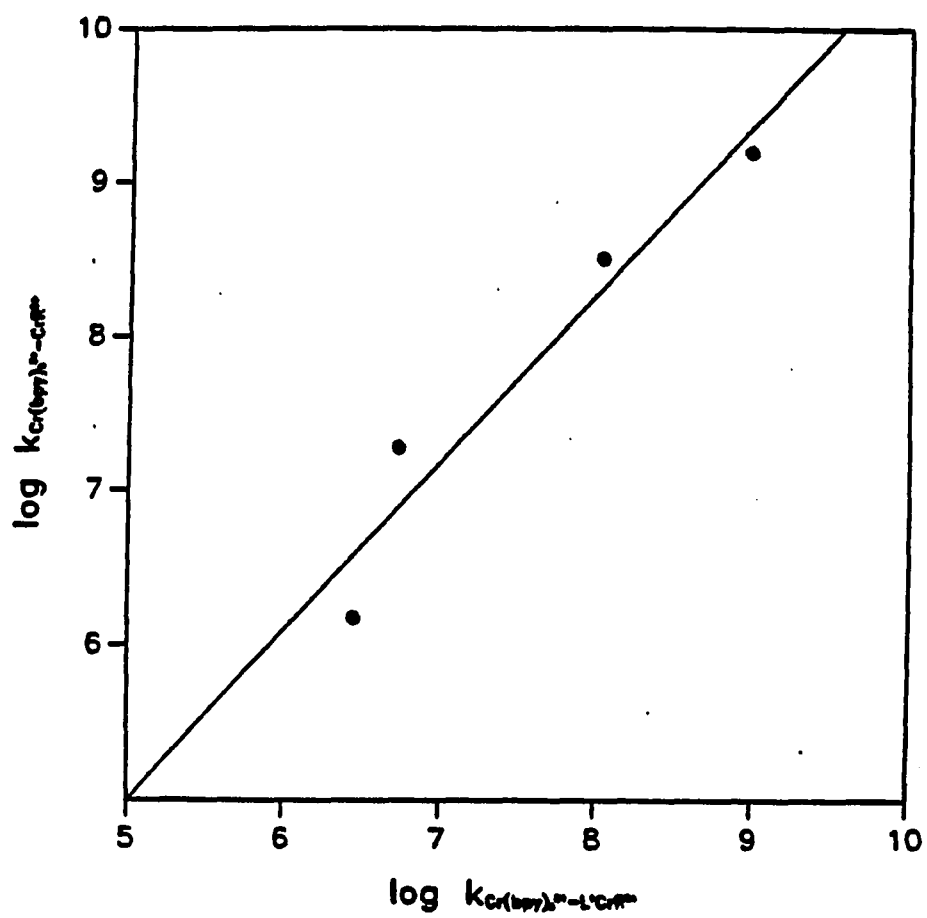


Figure II-9 Plot of $\log(k_q)$ for the reaction of $^*Cr(bpy)_3^{3+}$ with $L'CrR^{2+}$ versus $\log(k_q)$ for the reaction of $^*Cr(bpy)_3^{3+}$ with $(H_2O)_5CrR^{2+}$

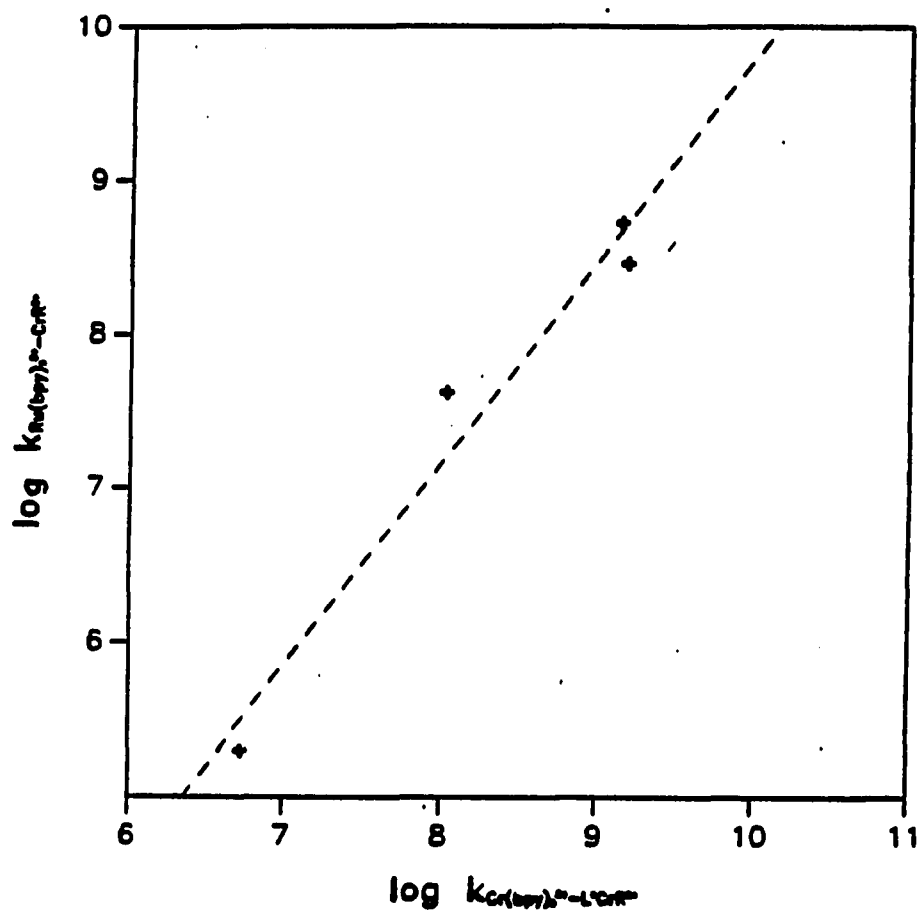


Figure II-10 Plot of $\log(k_q)$ for the reaction of $^*Cr(bpy)_3^{3+}$ with $L'CrR^{2+}$ versus $\log(k)$ for the reaction of $Ru(bpy)_3^{3+}$ with $(H_2O)_5CrR^{2+}$

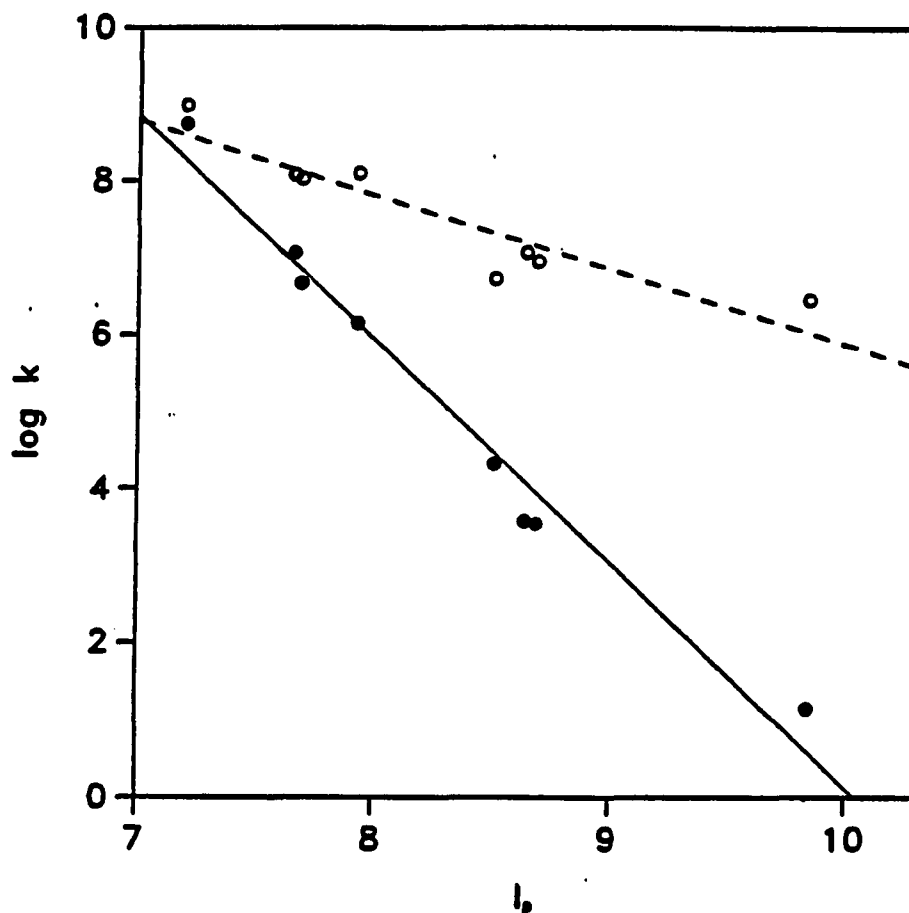


Figure II-11. Plot of the logarithm of the rate constants for the reaction of $\text{Ru}(\text{bpy})_3^{3+}$ (●) and $^*\text{Cr}(\text{bpy})_3^{3+}$ (○) with the organochromiums versus the ionization potential of the radicals (I_p).

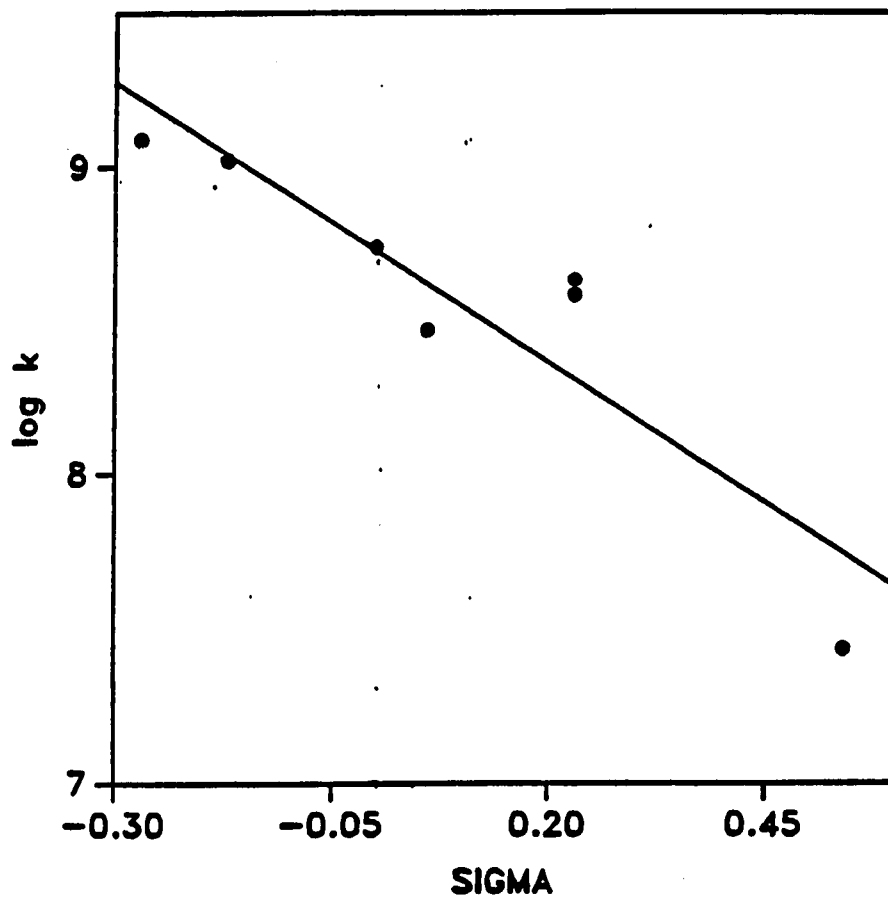


Figure II-12. Plot of the logarithm of the rate constants for the reaction of $\text{Ru}(\text{bpy})_3^{3+}$ with the organochromiums versus the Hammett σ values

REFERENCES

- 1 (a) Balzani, V.; Moggi, V.; Manfrin, M. F.; Bolletta, F.; Lawrence, G. S. Coord. Chem. Rev. 1975, 15, 321; (b) Balzani, V.; Bolletta, F.; Gandolfi, M. T.; Maestri, M. Top. Curr. Chem. 1978, 75, 1.
- 2 Brunschwig, B.; Sutin, N. J. Am. Chem. Soc. 1978, 100, 7568.
- 3 Jamieson, M. A.; Serpone, N.; Hoffman, M. Z.; Bolletta, F. Inorg. Chim. Acta 1983, 72, 247.
- 4 Bolletta, F.; Maestri, M.; Moggi, L.; Jamieson, M. A.; Serpone, N.; Henry, M. S.; Hoffman, M. Z. Inorg. Chem. 1981, 22, 2502.
- 5 (a) Serpone, N.; Jamieson, M. A.; Sriram, R.; Hoffman, M. Z. Inorg. Chem. 1981, 20, 3983; (b) Juris, A.; Manfrin, M. F.; Maestri, M.; Serponi, N. Inorg. Chem. 1978, 17, 2258; (c) Endicott, J. F.; Ramasami, T.; Gaswick, D. C.; Tamilarasan, R.; Heeg, M. J.; Brubaker, G. R.; Pyke, S. C. J. Am. Chem. Soc. 1983, 105, 5301.
- 6 Bakac, A.; Espenson, J. H. J. Am. Chem. Soc. 1988, 110, 3453.
- 7 Huston, P. L.; Bakac, A.; Espenson, J. H., to be in Inorg. Chem.
- 8 (a) Bakac, A.; Zahir, K.; Espenson, J. H. Inorg. Chem. 1988, 27, 315; (b) Serpone, N.; Jamieson, M. A.; Henry, M. S.; Hoffman, M. Z.; Bolletta, F.; Maestri, M. J.

- Am. Chem. Soc. 1979, 101, 2907; (c) Endicott, J. F.; Ferraudi, G. J. J. Am. Chem. Soc. 1977, 99, 5812.
- 9 Simmons, C. A.; Bakac, A.; Espenson, J. H., to be in Inorg. Chem.
- 10 Katsuyama, T.; Bakac, A.; Espenson, J. H. Inorg. Chem. 1989, 28, 339.
- 11 Melton, J. D.; Espenson, J. H.; Bakac, A. Inorg. Chem. 1986, 25, 4104.
- 12 Melton, J. D.; Bakac, A.; Espenson, J. H. Inorg. Chem. 1986, 25, 3360.
- 13 Shi, S.; Bakac, A.; Espenson, J. H., to be in Inorg. Chem.
- 14 Gardner, H. C.; Kochi, J. K. J. Am. Chem. Soc. 1974, 96, 1982.
- 15 Gardner, H. C.; Kochi, J. K. J. Am. Chem. Soc. 1975, 97, 1855.
- 16 Chen, J. Y.; Gardner, H. C.; Kochi, J. K. J. Am. Chem. Soc. 1976, 98, 6150.
- 17 Tsou, T. T.; Kochi, J. K. J. Am. Chem. Soc. 1978, 100, 1634.
- 18 Lau, W.; Huffman, J. C.; Kochi, J. K. Organometallics 1982, 1, 155.
- 19 Fukuzumi, S.; Kuroda, S.; Tanaka, T. J. Chem. Soc. Perkin Trans. II 1986, 25.
- 20 Wong, C. L.; Mochida, K.; Gin, A.; Weiner, M. A.; Kochi, J. K. J. Org. Chem. 1979, 44, 3979.

- 21 Wong, C. L.; Kochi, J. K. J. Am. Chem. Soc. 1979, 101, 5593.
- 22 Chen, J. Y.; Kochi, J. K. J. Am. Chem. Soc. 1977, 99, 1450.
- 23 Byrne, E. K.; Theopold, K. H. J. Am. Chem. Soc. 1987, 109, 1282.
- 24 Bower, B. K.; Tennent, H. G. J. Am. Chem. Soc. 1972, 94, 2512.
- 25 Byrne, E. K.; Richeson, D. S.; Theopold, K. H. J. Chem. Soc. Chem. Commun. 1986, 1491.
- 26 Vol'pin, M. E.; Levitin, I. Ya.; Sigan, A. L.; Nikitaev, A. T. J. Organometallic Chem. 1985, 279, 263.
- 27 Levitin, I. Ya.; Sigan, A. L.; Vol'pin, M. E. J. Organometallic Chem. 1976, 114, C53.
- 28 Tambllyn, W. H.; Klinger, R. J.; Hwang, W. S.; Kochi, J. K. J. Am. Chem. Soc. 1981, 103, 3161.
- 29 Abley, P.; Dockal, E. R.; Halpern, J. J. Am. Chem. Soc. 1972, 94, 659.
- 30 Halpern, J.; Chan, M. S.; Roche, T. S.; Tom, G. M. Acta Chem. Scand. A 1979, A33, 141.
- 31 Levitin, Ilya; Sigan, A. L.; Vol'pin, M. E. J. Chem. Soc. Chem. Commun. 1975, 469.
- 32 Halpern, J.; Chan, M. S.; Hanson, J.; Roche, T. S.; Topich, J. A. J. Am. Chem. Soc. 1975, 97, 1606.
- 33 Topich, J.; Halpern, J. Inorganic Chem. 1979, 18, 1339.

- 34 Halpern, J.; Topich, J.; Zamaraev, K. I. Inorg. Chim. Acta 1976, 20, L21.
- 35 Anderson, S. N.; Ballard, D. H.; Chrzastowski, J. Z.; Dodd, D.; Johnson, M. D. J. Chem. Soc. Chem. Commun. 1972, 685.
- 36 Magnuson, R. H.; Halpern, J. J. Chem. Soc. Chem. Commun. 1978, 44.
- 37 Vol'pin, M. E.; Levitin, I. Ya.; Sigan, A. L. Inorg. Chim. Acta 1980, 41, 271.
- 38 Roy, M.; Kumar, M.; Gupta, B. D. Inorg. Chim. Acta 1986, 114, 87.
- 39 Gupta, B. D.; Kumar, M. Inorg. Chim. Acta 1988, 149, 223.
- 40 Dreos, R.; Tauzher, G.; Marsich, N.; Costa, G. J. Organometallic Chem. 1976, 108, 235.
- 41 Dreos, R.; Tauzher, G.; Marsich, N.; Costa, G. J. Organometallic Chem. 1975, 92, 227.
- 42 Gupta, B. D.; Kumar, M. Inorg. Chim. Acta 1986, 113, 9.
- 43 Gupta, B. D.; Roy, S. Tetrahedron Lett. 1984, 25, 3255.
- 44 Okamoto, T.; Goto, M.; Oka, S. Inorg. Chem. 1981, 20, 899.
- 45 Costa, G.; Puxeddu, A.; Tavagnacco, C.; Dreos-Garlatti, R. Inorg. Chim. Acta 1984, 89, 65.
- 46 Reisenhofer, E.; Costa, G. Inorg. Chim. Acta
-

- 1981, 49, 121.
- 47 Samuels, G. J. Ph.D. Dissertation, Iowa State University, Ames, IA, 1979.
- 48 Holah, D. G.; Fackler, J. P. Inorg. Synth. 1969, 10, 26.
- 49 Samuels, G. J.; Espenson, J. H. Inorg. Chem. 1979, 18, 2587.
- 50 Steffan, C. R.; Bakac, A.; Espenson, J. H. Inorg. Chem. 1989, 28, 2992.
- 51 (a) Bakac, A.; Butkovic, V.; Espenson, J. H.; Marcec, R.; Orhanovic, M. Inorg. Chem. 1986, 25, 341; (b) Nordmeyer, F.; Taube, H. J. Am. Chem. Soc. 1968, 90, 1162.
- 52 DeSimone, R.; Drago, R. J. Am. Chem. Soc. 1970, 92, 2343.
- 53 Bryant, G. M.; Fergusson, J. E. Aust. J. Chem. 1971, 24, 275.
- 54 Kane-Maguire, N. A. P.; Conway, J.; Langford, C. H. J. Chem. Soc., Chem. Commun. 1974, 801.
- 55 (a) Connolly, P. Ph.D. Dissertation, Iowa State University, Ames, IA, 1985; (b) Hoselton, M. A.; Lin, C.-T.; Schwartz, H. A.; Sutin, N. J. Am. Chem. Soc. 1978, 100, 2383.
- 56 Navon, G.; Sutin, N. Inorg. Chem. 1974, 13, 2159.
- 57 (a) Leopold, K. R.; Haim, A. Inorg. Chem. 1978, 17, 1753; (b) Boettcher, W.; Haim, A. J. Am. Chem.

- Soc. 1980, 102, 1564.
- 58 Sutin, N.; Creutz, C. Pure Appl. Chem. 1980, 52, 2717.
- 59 (a) Ueno, F. B.; Sasaki, Y.; Ito, T.; Saito, K.
J. Chem. Soc. Chem. Commun. 1982, 329, (b) Sandrini,
D.; Gandolfi, M. T.; Maestri, M.; Bolletta, F.;
Balzani, V. Inorg. Chem. 1984, 23, 3017.
- 60 Serponi, N.; Jamieson, M. A.; Emmi, S. S.; Fuochi,
P. G.; Mulazzani, Q. G.; Hoffman, M. Z. J. Am. Chem.
Soc. 1981, 103, 1091.
- 61 Maestri, M.; Bolletta, F.; Moggi, L.; Balzani, V.;
Henry, M. S.; Hoffman, M. Z. J. Am. Chem. Soc.
1978, 100, 2694.
- 62 Ballardini, R.; Verani, G.; Scandola, F.; Balzani, V.
J. Am. Chem. Soc. 1976, 98, 7432.
- 63 Berdnikov, G. V.; Zhiravleva, O. S.; Terent'eva, L. A.
Bull. Acad. Sci. USSR, Div. Chem. Sci. 1977, 26, 2050.
- 64 Buxton, G. V.; Green, J. C. J. Chem. Soc., Faraday
Trans. I 1978, 74, 697.
- 65 Butler, J.; Jayson, G. G.; Swallow, A. J. J. Chem. Soc.,
Faraday Trans. I 1974, 70, 1394.
- 66 Venturi, M.; Emmi, S.; Fuochi, P. G.; Mulazzani, Q. G.
J. Phys. Chem. 1980, 84, 2160
- 67 Serpone, N.; Jamieson, M. A.; Henry, M. S.; Hoffman, M.
Z.; Bolletta, F.; Maestri, M. J. Am. Chem. Soc. 1979,
101, 1979.
- 68 Jamieson, M. A.; Serpone, N. Coord. Chem. Rev. 1981,

- 39, 121.
- 69 Sriram, R.; Hoffman, M. Z.; Jamieson, M. A.; Serpone, N. J. Am. Chem. Soc. 1980, 102, 1754.
- 70 Kelley, D.; Espenson, J. H.; Bakac, A., to be published in Inorg. Chem.
- 71 Martin, J. E.; Hart, E. J.; Adamson, A. W.; Gafney, H.; Halpern, J. J. Am. Chem. Soc. 1972, 94, 9238.
- 72 Jonah, C. D.; Matheson, M. S.; Meisel, D. J. Am. Chem. Soc. 1978, 100, 1449.
- 73 Mulazzani, Q. G.; Emmi, S.; Fuochi, P. G.; Hoffman, M. Z.; Venturi, M. J. Am. Chem. Soc. 1978, 100, 981.
- 74 Stevens, G. C.; Clarke, R. M.; Hart, E. J. J. Phys. Chem. 1972, 76, 3863.
- 75 Hickel, B. J. Phys. Chem. 1975, 79, 1054.
- 76 Rabani, J.; Pick, M.; Simic, M. J. Phys. Chem. 1974, 78, 1049.
- 77 (a.) Lee, S.; Espenson, J. H.; Bakac, A., to be published in Inorg. Chem. (b.) McHatton, R. C.; Espenson, J. H.; Bakac, A. J. Am. Chem. Soc. 1986, 108, 5885.
- 78 Huston, P.; Espenson, J. H.; Bakac, A., to be published in Inorg. Chem.
- 79 Houle, F. A.; Beauchamp, J. L. J. Am. Chem. Soc. 1978, 100, 3290.
- 80 Taubert, R.; Lossing, F. P. J. Am. Chem. Soc.

- 1962, 84, 1523.
- 81 Lossing, F. P.; DeSousa, J. B. J. Am. Chem. Soc.
1959, 81, 281.
- 82 Houle, F. A.; Beauchamp, J. L. J. Am. Chem. Soc.
1979, 101, 4067.
- 83 Bakac, A.; unpublished results, Ames Lab, Ames, IA.
- 84 Kelley, D.; Espenson, J. H.; Bakac, A., in progress
at Iowa State University, Ames, IA.
- 85 Marchaj, A.; Espenson, J. H.; Bakac, A., in progress
at Ames Lab, Ames, IA.

APPENDIX

Table A-1. Rate Constants for the Quenching of the
Excited State of $\text{Cr}(\text{bpy})_3^{3+}$ by the
 $\text{L}'\text{CrCH}_3^{2+}$ Ion^a

$10^3 \times [\text{L}'\text{CrCH}_3^{2+}]/\text{M}$	$10^{-4} \times k_{\text{obs}}/\text{s}^{-1}$
1.56	1.95
1.42	1.94
1.28	1.87
1.14	1.81
0.994	1.79
0.852	1.70
0.710	1.76

^a $[\text{Cr}(\text{bpy})_3^{3+}] = 5.47 \times 10^{-5} \text{ M}$. In 0.2 M NaClO_4 and
10 mM HClO_4 .

Table A-2. Rate Constants for the Quenching of the
Excited State of $\text{Cr}(\text{bpy})_3^{3+}$ by the
 $\text{L}'\text{Cr}(\text{CH}_2\text{CH}_3)^{2+}$ Ion^a

$10^4 \times [\text{L}'\text{CrCH}_2\text{CH}_3^{2+}]/\text{M}$	$10^{-4} \times k_{\text{obs}}/\text{s}^{-1}$
13.1	2.11
11.5	2.03
9.85	1.77
8.20	1.72
6.55	1.70
4.92	1.60
3.28	1.48
1.69	1.47

^a $[\text{Cr}(\text{bpy})_3^{3+}] = 2.94 \times 10^{-5} \text{ M}$. In 0.2 M NaClO_4 and
10 mM HClO_4 .

Table A-3. Rate Constants for the Quenching of the
Excited State of $\text{Cr}(\text{bpy})_3^{3+}$ by the
 $\text{L}'\text{Cr}(\text{1-Propyl})^{2+}$ Ion^a

$10^4 \times [\text{L}'\text{Cr}(\text{1-Propyl})^{2+}]/\text{M}$	$10^{-4} \times k_{\text{obs}}/\text{s}^{-1}$
14.3	2.55
12.5	2.49
8.05	2.01
6.70	1.87
5.40	1.77
4.03 ₅	1.72
2.69	1.54

^a $[\text{Cr}(\text{bpy})_3^{3+}] = 2.94 \times 10^{-5} \text{ M}$. In 0.2 M NaClO_4 and
10 mM HClO_4 .

Table A-4. Rate Constants for the Quenching of the
Excited State of $\text{Cr}(\text{bpy})_3^{3+}$ by the
 $\text{L}'\text{Cr}(\text{l-Butyl})^{2+}$ Ion^a

$10^4 \times [\text{L}'\text{Cr}(\text{l-Butyl})^{2+}]/\text{M}$	$10^{-4} \times k_{\text{obs}}/\text{s}^{-1}$
15.0	2.91
13.1	2.70
11.2	2.45
9.35	2.06
7.48	1.95
5.61	1.77 ₅
3.74	1.59
1.87	1.32

^a $[\text{Cr}(\text{bpy})_3^{3+}] = 2.94 \times 10^{-5} \text{ M}$. In 0.2 M NaClO_4 and
10 mM HClO_4 .

Table A-5. Rate Constants for the Quenching of the
Excited State of $\text{Cr}(\text{bpy})_3^{3+}$ by the
 $\text{L}'\text{Cr}(2\text{-Propyl})^{2+}$ Ions^a

$10^3 \times [\text{L}'\text{Cr}(2\text{-Propyl})^{2+}]/\text{M}$	$10^{-4} \times k_{\text{obs}}/\text{s}^{-1}$
1.89 ⁵	22.8
1.66	18.7
1.42	15.8
1.18 ⁹	21.9
1.18 ^d	15.1
1.18 ^e	18.4
1.18	15.9
1.18 ^f	16.5
1.18 ^b	15.5
1.18 ^c	14.9
0.95	13.3
0.71	10.9
0.47	7.79
0.28	4.67

^aAll 0.2 M NaClO_4 , 10 mM HClO_4 , $[\text{Cr}(\text{bpy})_3^{3+}] = 5.36 \times 10^{-5}\text{M}$ and $[\text{Fe}^{3+}] = 8.2\text{ mM}$.

^b $[\text{Cr}(\text{bpy})_3^{3+}] = 8.04 \times 10^{-5}\text{ M}$.

^c $[\text{Cr}(\text{bpy})_3^{3+}] = 10.7 \times 10^{-5}\text{ M}$.

^d $[\text{Fe}^{3+}] = 2.7\text{ mM}$.

^e $[\text{Fe}^{3+}] = 5.4\text{ mM}$.

^f $[\text{Fe}^{3+}] = 10.9\text{ mM}$.

⁹No iron.

Table A-6. Rate Constants for the Quenching of the
Excited State of $\text{Cr}(\text{bpy})_3^{3+}$ by the
 $\text{L}'\text{Cr}(\text{2-Butyl})^{2+}$ ion^a

$10^3 \times [\text{L}'\text{Cr}(\text{2-Butyl})^{2+}]/\text{M}$	$10^{-4} \times k_{\text{obs}}/\text{s}^{-1}$
1.47	20.8
1.28	16.6
1.10	14.7
0.916	13.9
0.733	11.1
0.550	8.23
0.367	5.47
0.183	3.72

^a $[\text{Cr}(\text{bpy})_3^{3+}] = 5.47 \times 10^{-5} \text{ M}$. In 0.2 M NaClO_4 and
10 mM HClO_4 . $[\text{Fe}^{3+}] = 8.2 \text{ mM}$.

Table A-7 . Rate Constants for the Quenching of the
Excited State of $\text{Cr}(\text{bpy})_3^{3+}$ by the
 $\text{L}'\text{CrC}_6\text{H}_{11}^{2+}$ Ions^a

$10^3 \times [\text{L}'\text{CrC}_6\text{H}_{11}^{2+}]/\text{M}$	$10^{-4} \times k_{\text{obs}}/\text{s}^{-1}$
1.02	14.4
0.891	13.0
0.764	10.7
0.637	10.4
0.509	7.46
0.382	5.56
0.255	4.36
0.127	3.34

^a $[\text{Cr}(\text{bpy})_3^{3+}] = 3.73 \times 10^{-5} \text{ M}$. $[\text{Fe}^{3+}] = 6.71 \text{ mM}$. In
0.2 M NaClO_4 , 10 mM HClO_4 .

Table A-8. Rate Constants for the Quenching of the
Excited State of $\text{Cr}(\text{bpy})_3^{3+}$ by the
 $\text{L}'\text{CrCH}_2\text{C}_6\text{H}_5^{2+}$ Ion^a

$10^3 \times [\text{L}'\text{CrCH}_2\text{C}_6\text{H}_5^{2+}]/\text{M}$	$10^{-4} \times k_{\text{obs}}/\text{s}^{-1}$
1.08	110.
0.899	88.2
0.719	73.1
0.540	55.9
0.360	37.9
0.180	20.2
0.108	12.6
0.036	7.09

^a $[\text{Cr}(\text{bpy})_3^{3+}] = 4.02 \times 10^{-5} \text{ M}$. In 0.2 M NaClO_4 and
10 mM HClO_4 .

Table A-9. Rate Constants for the Quenching of the
Excited State of $\text{Cr}(\text{bpy})_3^{3+}$ by the
 $\text{L}'\text{CrCH}_2\text{C}_6\text{H}_4\text{CH}_3^{2+}$ Iona

$10^4 \times [\text{L}'\text{CrCH}_2\text{C}_6\text{H}_4\text{CH}_3^{2+}]/\text{M}$	$10^{-4} \times k_{\text{obs}}/\text{s}^{-1}$
4.32	71.7
3.80	59.1
3.28	55.7
2.76	45.9
2.25	38.5
1.73	27.4
1.21	18.3
0.691	10.7
0.173	4.06

$a[\text{Cr}(\text{bpy})_3^{3+}] = 3.73 \times 10^{-5} \text{ M}$. In 0.2 M NaClO_4 and 10 mM HClO_4 .

Table A-10. Rate Constants for the Quenching of the
Excited State of $\text{Cr}(\text{bpy})_3^{3+}$ by the
 $\text{L}'\text{Cr}(\text{CH}_2\text{C}_6\text{H}_4\text{Br})^{2+}$ Ion^a

$10^4 \times [\text{L}'\text{Cr}(\text{CH}_2\text{C}_6\text{H}_4\text{Br})^{2+}]/\text{M}$	$10^{-4} \times k_{\text{obs}}/\text{s}^{-1}$
2.44	38.0
2.13	31.5
1.83	25.7
1.52	21.5
1.22	17.9
0.914	12.8
0.609	9.11
0.305	5.01

^a $[\text{Cr}(\text{bpy})_3^{3+}] = 3.73 \times 10^{-5} \text{ M}$. In 0.2 M NaClO_4 and 10 mM HClO_4 .

Table A-11. Rate Constants for the Quenching of the
Excited State of $\text{Cr(5-Clphen)}_3^{3+}$ by the
 $\text{L'Cr(2-Propyl)}^{2+}$ Ion^a

$10^3 \times [\text{L'Cr(2-Propyl)}^{2+}]/\text{M}$	$10^{-4} \times k_{\text{obs}}/\text{s}^{-1}$
1.89 ₅	37.3
1.66	39.9
1.42	33.8
1.18	31.9
0.95	27.7
0.71	21.7
0.47	16.6
0.28	11.1

^a $[\text{Cr(5-Clphen)}_3^{3+}] = 3.56 \times 10^{-5} \text{ M}$. In 0.2 M NaClO_4
and 10 mM HClO_4 . $[\text{Fe}^{3+}] = 8.2 \text{ mM}$.

Table A-12. Rate Constants for the Quenching of the
Excited State of $\text{Cr}(4,7\text{-diMephen})_3^{3+}$ by the
 $\text{L}'\text{Cr}(2\text{-Propyl})^{2+}$ Ion^a

$10^3 \times [\text{L}'\text{Cr}(2\text{-Propyl})^{2+}]/\text{M}$	$10^{-4} \times k_{\text{obs}}/\text{s}^{-1}$
3.34	18.7
2.86	14.6
2.38	13.6
1.91	11.4
1.43	11.4
0.953	8.13
0.476	5.01

^a $[\text{Cr}(4,7\text{-diMephen})_3^{3+}] = 3.14 \times 10^{-5} \text{ M}$. In 0.2 M
 NaClO_4 and 10 mM HClO_4 .

Table A-13. Rate Constants for the Quenching of the
Excited State of $\text{Cr(5-Mephen)}_3^{3+}$ by the
 $\text{L'Cr(2-Propyl)}^{2+}$ Ion^a

$10^3 \times [\text{L'Cr(2-Propyl)}^{2+}]/\text{M}$	$10^{-4} \times k_{\text{obs}}/\text{s}^{-1}$
3.34	26.7
2.86	22.5
2.38	20.7
1.91	16.7
1.43	13.5
0.953	9.97
0.476	5.79

^a $[\text{Cr(5-Mephen)}_3^{3+}] = 2.95 \times 10^{-5} \text{ M}$. In 0.2 M NaClO_4
and 10 mM HClO_4 .

Table A-14. Rate Constants for the Quenching of the
Excited State of $\text{Cr}(4,4'\text{-diMebpy})_3^{3+}$ by the
 $\text{L}'\text{CrCH}_2\text{CH}_3^{2+}$ Ion^a

$10^3 \times [\text{L}'\text{CrCH}_2\text{CH}_3^{2+}]/\text{M}$	$10^{-4} \times k_{\text{obs}}/\text{s}^{-1}$
2.16	1.22
1.89	1.25
1.62	1.20
1.35	0.946
0.810	0.883

^a $[\text{Cr}(4,4'\text{-diMebpy})_3^{3+}] = 2.90 \times 10^{-5} \text{ M}$. In 0.2 M
 NaClO_4 and 10 mM HClO_4 .

Table A-15. Rate Constants for the Quenching of the
Excited State of $\text{Cr(5-Mephen)}_3^{3+}$ by the
 $\text{L'CrCH}_2\text{CH}_3^{2+}$ Ion^a

$10^3 \times [\text{L'CrCH}_2\text{CH}_3^{2+}]/\text{M}$	$10^{-4} \times k_{\text{obs}}/\text{s}^{-1}$
2.16	2.59
1.89	2.07
1.62	2.04
1.08	1.77
0.810	1.88
0.540	1.51

^a $[\text{Cr(5-Mephen)}_3^{3+}] = 2.95 \times 10^{-5} \text{ M}$. In 0.2 M NaClO_4
and 10 mM HClO_4 .

Table A-16. Rate Constants for the Quenching of the
Excited State of $\text{Cr(5-Clphen)}_3^{3+}$ by the
 $\text{L'CrCH}_3\text{CH}_3^{2+}$ Ion^a

$10^3 \times [\text{L'CrCH}_2\text{CH}_3^{2+}]/\text{M}$	$10^{-4} \times k_{\text{obs}}/\text{s}^{-1}$
2.16	4.74
1.89	4.60
1.62	4.09
1.35	3.45
1.08	3.51
0.810	3.03
0.540	2.50
0.270	2.46

^a $[\text{Cr(5-Clphen)}_3^{3+}] = 3.95 \times 10^{-5} \text{ M}$. In 0.2 M NaClO_4
and 10 mM HClO_4 .

Table A-17. Rate Constants for the Reaction of $\text{Ru}(\text{bpy})_3^{3+}$ with $\text{L}'\text{Cr}(\text{CH}_3)_2^+$ ^a

$10^3 \times [\text{L}'\text{Cr}(\text{CH}_3)_2^+]/\text{M}$	$10^2 k_{\text{obs}}/\text{s}^{-1}$
1.54	2.46
1.23	1.68
0.924	1.22
0.616	0.840
0.308	0.478

^a $[\text{RuL}_3^{3+}] = 3.83 \times 10^{-6} \text{ M}$. In 0.2 M NaClO_4 and 10 mM HClO_4 .

Table A-18. Rate Constants for the Reaction of $\text{Ru}(\text{bpy})_3^{3+}$ with $\text{L}'\text{Cr}(\text{Ethyl})_2^+$ ^a

$10^4 \times [\text{L}'\text{Cr}(\text{Ethyl})_2^+]/\text{M}$	$k_{\text{obs}}/\text{s}^{-1}$
1.72	36.0
1.45	32.1
1.29	27.1
1.27	27.5
1.09	22.7
0.908	18.5
0.859	18.2
0.727	14.4
0.545	10.9
0.429	9.88
0.363	8.22
0.182	5.54

^a $[\text{RuL}_3^{3+}] = 5 \times 10^{-6} \text{ M}$. $[\text{Co}(\text{NH}_3)_5\text{Br}^{2+}] = 0.883 - 1.4 \text{ mM}$. In 0.2 M NaClO_4 and 10 mM HClO_4 .

Table A-19. Rate Constants for the Reaction of $\text{Ru}(\text{bpy})_3^{3+}$ with $\text{L}'\text{Cr}(\text{1-Propyl})^{2+}$ ^a

$10^4 \times [\text{L}'\text{Cr}(\text{1-Propyl})^{2+}]/\text{M}$	$k_{\text{obs}}/\text{s}^{-1}$
7.94	2.68
5.96	1.96
3.97	1.48
1.99	0.56

^a $[\text{RuL}_3^{3+}] = 5 \times 10^{-6} \text{ M}$. $[\text{Co}(\text{NH}_3)_5\text{Br}^{2+}] = 1.01 \text{ mM}$.
In 0.2 M NaClO_4 and 10 mM HClO_4 .

Table A-20. Rate Constants for the Reaction of $\text{Ru}(\text{bpy})_3^{3+}$ with $\text{L}'\text{Cr}(\text{1-Butyl})^{2+}$ ^a

$10^4 \times [\text{L}'\text{Cr}(\text{1-Butyl})^{2+}]/\text{M}$	$k_{\text{obs}}/\text{s}^{-1}$
8.92	3.39
6.69	2.35
4.46	1.74
2.23	0.79

^a $[\text{RuL}_3^{3+}] = 5 \times 10^{-6} \text{ M}$. $[\text{Co}(\text{NH}_3)_5\text{Br}^{2+}] = 1.10 \text{ mM}$.
In 0.2 M NaClO_4 and 10 mM HClO_4 .

Table A-21. Rate Constants for the Reaction of $\text{Ru}(\text{bpy})_3^{3+}$ with $\text{L}'\text{Cr}(\text{2-Propyl})^{2+}$ ^a

$10^4 \times [\text{L}'\text{Cr}(\text{2-Propyl})^{2+}]/\text{M}$	$10^{-2} \times k_{\text{obs}}/\text{s}^{-1}$
6.14	19.6
5.37	17.7
4.61	13.5
3.84	10.4
3.07	8.07
2.30	7.11
1.54	3.75
0.768	1.94

^a $[\text{RuL}_3^{3+}] = 5 \times 10^{-6} \text{ M}$. $[\text{Co}(\text{NH}_3)_5\text{Br}^{2+}] = 5.30 \text{ mM}$.
In 0.2 M NaClO_4 and 10 mM HClO_4 .

Table A-22. Rate Constants for the Reaction of $\text{Ru}(\text{bpy})_3^{3+}$ with $\text{L}'\text{Cr}(\text{2-Butyl})_2^+$ ^a

$10^4 \times [\text{L}'\text{Cr}(\text{2-Butyl})_2^+]/\text{M}$	$10^{-2} \times k_{\text{obs}}/\text{s}^{-1}$
5.73	9.20
5.02	7.38
4.30	6.18
3.58	5.21
2.87	4.35
2.15	2.84
1.43	1.83
0.717	1.20

$a[\text{RuL}_3^{3+}] = 5 \times 10^{-6} \text{ M. } [\text{Co}(\text{NH}_3)_5\text{Br}^{2+}] = 0.922 \text{ mM.}$

In 0.2 M NaClO_4 and 10 mM MClO_4 .

Table A-23. Rate Constants for the Reaction of $\text{Ru}(\text{bpy})_3^{3+}$ with $\text{L}'\text{Cr}(\text{c-Hex})^{2+}$ ^a

$10^4 \times [\text{L}'\text{Cr}(\text{c-Hex})^{2+}]/\text{M}$	$10^{-3} \times k_{\text{obs}}/\text{s}^{-1}$
6.08	7.09
5.32	6.41
4.56	5.68
3.80	4.72
3.04	3.51
2.28	2.42
1.52	1.66
0.760	0.787

^a $[\text{RuL}_3^{3+}] = 5 \times 10^{-6} \text{ M}$. $[\text{Co}(\text{NH}_3)_5\text{Br}^{2+}] = 5.30 \text{ mM}$.
In 0.2 M NaClO_4 and 10 mM HClO_4 .

Table A-24. Rate Constants for the Reaction of $\text{Ru}(\text{bpy})_3^{3+}$ with $\text{L}'\text{Cr}(\text{CH}_2\text{C}_6\text{H}_5)_2^+$ ^a

$10^4 \times [\text{L}'\text{Cr}(\text{CH}_2\text{C}_6\text{H}_5)_2^+]/\text{M}$	$10^{-4} \times k_{\text{obs}}/\text{s}^{-1}$
3.98	20.25
3.48	19.7
2.98	16.1
2.49	11.9
1.99	11.5
1.49	7.85
0.994	5.27
0.497	2.19

^a $[\text{RuL}_3^{3+}] = 5 \times 10^{-6} \text{ M}$. $[\text{Co}(\text{NH}_3)_5\text{Br}^{2+}] = 0.782 \text{ mM}$.
In 0.2 M NaClO_4 and 10 mM HClO_4 .

Table A-25. Rate Constants for the Reaction of $\text{Ru}(\text{bpy})_3^{3+}$ with $\text{L}'\text{Cr}(\text{CH}_2\text{C}_6\text{H}_4\text{Br})^{2+}$ ^a

$10^4 \times [\text{L}'\text{Cr}(\text{CH}_2\text{C}_6\text{H}_4\text{Br})^{2+}]/\text{M}$	$10^{-4} \times k_{\text{obs}}/\text{s}^{-1}$
4.95	23.1
4.33	20.9
3.71	17.1
3.10	13.5
2.48	11.8
1.86	7.99
1.24	5.04
0.619	2.12

^a $[\text{RuL}_3^{3+}] = 5 \times 10^{-6} \text{ M}$. $[\text{Co}(\text{NH}_3)_5\text{Br}^{2+}] = 1.04 \text{ mM}$.
In 0.2 M NaClO_4 and 10 mM HClO_4 .

Table A-26. Rate Constants for the Reaction of $\text{Ru}(\text{bpy})_3^{3+}$ with $\text{L}'\text{Cr}(\text{CH}_2\text{C}_6\text{H}_4\text{CH}_3)^{2+}$ ^a

$10^4 \times [\text{L}'\text{Cr}(\text{CH}_2\text{C}_6\text{H}_4\text{CH}_3)^{2+}]/\text{M}$	$10^{-4} \times k_{\text{obs}}/\text{s}^{-1}$
5.80	63.6
5.80	64.4
5.08	56.0
4.35	43.3
3.63	35.6
2.90	28.5
2.90	26.7
2.18	19.2
1.45	12.6
0.725	5.61
0.290	2.57

^a $[\text{RuL}_3^{3+}] = 5 \times 10^{-6} \text{ M}$. $[\text{Co}(\text{NH}_3)_5\text{Br}^{2+}] = 1.15 \text{ mM}$.
In 0.2 M NaClO_4 and 10 mM HClO_4 .

Table A-27. Rate Constants for the Reaction of $\text{Ru}(\text{bpy})_3^{3+}$ with $\text{L}'\text{Cr}(\text{Ethyl})_2^+$ ^a

$10^3 \times [\text{L}'\text{Cr}(\text{Ethyl})_2^+]/\text{M}$	$k_{\text{obs}}/\text{s}^{-1}$
1.27	25.5
1.11	23.0
0.950	19.0
0.633	13.6

$^a[\text{RuL}_3^{3+}] = 5 \times 10^{-6} \text{ M. } [\text{Co}(\text{NH}_3)_5\text{py}^{3+}] = 5.19 \text{ mM.}$
In 0.2 M NaClO_4 and 10 mM HClO_4 .

Table A-28. Rate Constants for the Reaction of $\text{Ru}(\text{bpy})_3^{3+}$ with $\text{L}'\text{Cr}(\text{l-Propyl})^{2+}$ ^a

$10^3 \times [\text{L}'\text{Cr}(\text{l-Propyl})^{2+}]/\text{M}$	$k_{\text{obs}}/\text{s}^{-1}$
1.66	7.93
1.45	7.49
1.25	5.95
0.831	5.44
0.415	2.56

^a $[\text{RuL}_3^{3+}] = 5 \times 10^{-6} \text{ M}$. $[\text{Co}(\text{NH}_3)_5\text{py}^{3+}] = 5.19 \text{ mM}$.
In 0.2 M NaClO_4 and 10 mM HClO_4 .

Table A-29. Rate Constants for the Reaction of $\text{Ru}(\text{bpy})_3^{3+}$ with $\text{L}'\text{Cr}(\text{Ethyl})_2^+$ ^a

$10^3 \times [\text{L}'\text{Cr}(\text{Ethyl})_2^+]/\text{M}$	$k_{\text{obs}}/\text{s}^{-1}$
1.165	22.25
1.02	19.35
0.874	17.1
0.728	15.0
0.583	13.95
0.437	11.1
0.291	8.33

^a $[\text{RuL}_3^{3+}] = 5 \times 10^{-6} \text{ M}$. $[\text{Co}(\text{NH}_3)_5\text{OH}_2^{3+}] = 6.33 \text{ mM}$.
In 0.2 M NaClO_4 and 10 mM HClO_4 .

Table A-30. Rate Constants for the Reaction of $\text{Ru}(\text{bpy})_3^{3+}$
with $\text{L}'\text{Cr}(\text{CH}_2\text{C}_6\text{H}_4\text{F})_2^{2+}$ ^a

$10^4 \times [\text{L}'\text{Cr}(\text{CH}_2\text{C}_6\text{H}_4\text{F})_2^{2+}]/\text{M}$	$10^{-4} \times k_{\text{obs}}/\text{s}^{-1}$
6.03	18.6
5.28	13.9
4.53	13.4
3.77	11.05
3.02	8.76
2.26	6.60
1.57	4.37

$a[\text{RuL}_3^{3+}] = 8.0 \times 10^{-6} \text{ M}$. $[\text{Co}(\text{NH}_3)_5\text{Br}^{2+}] = 5.8 \text{ mM}$.
In 0.2 M NaClO_4 and 10 mM HClO_4 .

Table A-31. Rate Constants for the Reaction of $\text{Ru}(\text{bpy})_3^{3+}$ with $\text{L}'\text{Cr}(\text{CH}_2\text{C}_6\text{H}_4\text{Cl})_2^+$ ^a

$10^4 \times [\text{L}'\text{Cr}(\text{CH}_2\text{C}_6\text{H}_4\text{Cl})_2^+]/\text{M}$	$10^{-4} \times k_{\text{obs}}/\text{s}^{-1}$
2.90	9.92
2.58	8.70
2.20	7.22
1.93	6.53
1.61	4.95
1.29	3.55
0.967	2.92
0.645	1.26

^a $[\text{RuL}_3^{3+}] = 2.6 \times 10^{-6} \text{ M}$. $[\text{Co}(\text{NH}_3)_5\text{Br}^{2+}] = 3.8 \text{ mM}$.
In 0.2 M NaClO_4 and 10 mM HClO_4 .

Table A-32. Rate Constants for the Reaction of $\text{Ru}(\text{bpy})_3^{3+}$ with $\text{L}'\text{Cr}(\text{CH}_2\text{C}_6\text{H}_4\text{CF}_3)_2^{2+}$ ^a

$10^4 \times [\text{L}'\text{Cr}(\text{CH}_2\text{C}_6\text{H}_4\text{CF}_3)_2^{2+}]/\text{M}$	$10^{-3} \times k_{\text{obs}}/\text{s}^{-1}$
3.82	9.14
3.39	8.75
2.97	6.54
2.54	5.74
2.12	4.14
1.70	3.14
1.27	2.26

$a[\text{RuL}_3^{3+}] = 2.6 \times 10^{-6} \text{ M}$. $[\text{Co}(\text{NH}_3)_5\text{Br}^{2+}] = 3.8 \text{ mM}$.
In 0.2 M NaClO_4 and 10 mM HClO_4 .

Table A-33. Rate Constants for the Reaction of $\text{Ru}(\text{bpy})_3^{3+}$ with $\text{L}'\text{Cr}(\text{CH}_2\text{C}_6\text{H}_4\text{OCH}_3)_2^+$ ^a

$10^4 \times [\text{L}'\text{Cr}(\text{CH}_2\text{C}_6\text{H}_4\text{OCH}_3)_2^+]/\text{M}$	$10^{-4} \times k_{\text{obs}}/\text{s}^{-1}$
2.37	28.4
2.11	24.1
1.85	20.3
1.58	17.6
1.31	14.7
1.05	10.9
0.791	7.23
0.527	4.82

^a $[\text{RuL}_3^{3+}] = 2.6 \times 10^{-6} \text{ M}$. $[\text{Co}(\text{NH}_3)_5\text{Br}^{2+}] = 4.3 \text{ mM}$.
In 0.2 M NaClO_4 and 10 mM HClO_4 .

Table A-34. Rate Constants for the Reaction of $\text{Ru}(\text{bpy})_3^{3+}$ with $\text{L}'\text{Cr}(\text{CH}_2\text{C}_6\text{H}_4\text{Br})^{2+}$ ^a

$10^4 \times [\text{L}'\text{Cr}(\text{CH}_2\text{C}_6\text{H}_4\text{Br})^{2+}]/\text{M}$	$10^{-4} \times k_{\text{obs}}/\text{s}^{-1}$
2.34	11.05
2.08	10.3
1.82	8.71
1.56	7.37
1.30	5.53
1.04	4.41
0.78	3.08
0.52	2.01
0.26	0.795

^a $[\text{RuL}_3^{3+}] = 8.3 \times 10^{-6} \text{ M}$. $[\text{Co}(\text{NH}_3)_5\text{OH}_2^{3+}] = 7.22 \text{ mM}$.
In 0.2 M NaClO_4 and 10 mM HClO_4 .

GENERAL SUMMARY

It has been determined in Part I that the reaction of $^*\text{Cr}(\text{bpy})_3^{3+}$ with oxalate ions occurs via a rate determining irreversible electron transfer. The mechanism of the reaction includes a prior ion-pairing equilibrium. The oxalate ions are oxidized to possibly CO_2 and the unstable CO_2^- ion. This last species reacts with ground state $\text{Cr}(\text{bpy})_3^{3+}$ to produce more of the reduced chromium polypyridyl complex.

Part II concerned the reaction of $[\text{15}] \text{aneN}_4 \text{CrR}^{2+}$ with the excited state of $\text{Cr}(\text{bpy})_3^{3+}$ and with the $\text{Ru}(\text{bpy})_3^{3+}$ ion. The reaction with $^*\text{Cr}(\text{bpy})_3^{3+}$ has been determined to proceed via an electron transfer mechanism as opposed to an energy transfer mechanism. The reaction between $\text{Ru}(\text{bpy})_3^{3+}$ and $[\text{15}] \text{aneN}_4 \text{CrR}^{2+}$ proceeds via a rate determining electron transfer to produce the $\text{Ru}(\text{bpy})_3^{2+}$ ion and the unstable $[\text{15}] \text{aneN}_4 \text{CrR}^{3+}$ which probably decomposes by homolysis.

ACKNOWLEDGEMENT

I would like to thank Dr. Espenson for his assistance and patience over the years. Also I would like to thank Dr. Bakac for many helpful suggestions. Much thanks also go to my family for their encouragement; Mrs. Jane Steffan and the late Mr. Edward Steffan; Dr. Mike Steffan; Miss Susan Steffan. Last, but not least thanks go to the many Espenson group members who have been of much assistance through their helpful discussions, suggestions and ideas.